

# Implementation of an IEC 61850 Sampled Values Based Line Protection IED with a New Transients-Based Hybrid Protection Algorithm

By

Kapuge Kariyawasam Mudalige Sachintha Kariyawasam

A thesis submitted to the Faculty of Graduate Studies of  
The University of Manitoba  
in partial fulfilment of the requirements of the degree of

**MASTER OF SCIENCE**

Department of Electrical and Computer Engineering  
University of Manitoba  
Winnipeg, MB, Canada.

Copyright © April 2016 by Kapuge Kariyawasam Mudalige Sachintha  
Kariyawasam

## Abstract

Over the course of the last decade, IEC 61850 has become the leading standard for electrical substation automation the world over. This thesis presents the work done towards implementing an IEC 61850 sampled values based line protection Intelligent Electronics Device (IED) on a desktop computer. This IED is capable of subscribing, decoding and processing the sampled values published by a source to be used in line protection algorithms.

The novel hybrid line protection algorithm implemented in the IED combines a distance protection scheme with a transients-based unit protection method that uses sampled values complying with IEC 61850-9-2-LE. Application of the line protection relay for protecting a series compensated transmission line was examined using hardware-in-the-loop simulations. Results indicate that (i) the implemented algorithms are robust and reliable, and (ii) the class of transients based protection algorithms examined in this thesis can be successfully implemented with IEC 61850 sampled values.

# Acknowledgments

During my stay at University of Manitoba over the last two years, I have had the luxury of finding the support of many, without whom the successful completion of this thesis would not have been possible. Therefore, it is only decent to mention a few of them at least.

First and foremost, I owe my sincerest gratitude to my advisor, Dr. Athula Rajapakse, who guided me all the way and supported me in every possible aspect in completing this work. I'm also grateful to the Faculty of Graduate Studies, University of Manitoba and Natural Sciences and Engineering Research Council of Canada for supporting me financially throughout. Further, I would like to convey my heartiest thanks to the examining committee for accepting this thesis for review.

I would also like to acknowledge the financial, equipment, and technical assistance provided by Pauley Family Foundation, USA, RTDS Technologies Inc., Canada, Schweitzer Engineering Laboratories, USA, ERL Phase Power Technologies, Canada and Kalkitech Pvt. Ltd, India.

The ever-supportive academic and technical staffs of the Department of Electrical and Computer Engineering should be specially mentioned for their extended support. My loving family and caring friends must not go without a mention, for they were the ones who made my life in Winnipeg enjoyable.

Finally, I would like to pay my tribute to each and everyone, who shared their thoughts of wisdom and knowledge under difficult circumstances to make this endeavor a success.

Sachintha Kariyawasam

# Dedication

To my loving parents.

# Contents

Abstract.....	ii
Acknowledgments.....	iii
Dedication .....	iv
Contents .....	v
List of Tables.....	ix
List of Figures.....	x
List of Abbreviations .....	xiv
List of Appendices.....	xvi
<b>1 Introduction</b> .....	<b>1</b>
1.1 Background.....	1
1.1.1 Substation Automation.....	1
1.1.2 Substation Architecture of IEC 61850 .....	3
1.1.3 GOOSE and SV .....	4
1.1.4 Present Status of the Standard IEC 61850 .....	5
1.2 Motivation.....	6
1.3 Objectives of the Thesis.....	7
1.4 Thesis Outline.....	8
<b>2 Literature Review</b> .....	<b>9</b>
2.1 Introduction to the Standard IEC 61850.....	9
2.1.1 Inception.....	9
2.1.2 Structure and Scope of IEC 61850 .....	11

2.1.3	Terms and Definitions .....	12
2.1.4	Key Advantages and Features of IEC 61850.....	13
2.1.5	System Configuration description Language (SCL).....	16
2.1.6	Logical Interfaces.....	18
2.1.7	Generic Object Oriented Substation Event .....	22
2.1.8	Sampled Values.....	24
2.1.9	IEC 61850-9-2 LE .....	25
2.1.10	Merging Unit.....	26
2.1.11	Inter-Substation Communication as per IEC 61850-90-5.....	28
2.2	Transmission Line Protection Schemes.....	29
2.2.1	Distance Protection.....	29
2.2.2	Challenges in Protecting Series Compensated Transmission Lines	30
2.2.3	Current Transients Based Line Protection.....	32
2.3	Chapter Summary .....	36
<b>3</b>	<b>Implementation of a Process Bus Compatible IED Using Generic Hardware</b>	<b>37</b>
3.1	Experimental Setup.....	37
3.2	Line Protection IED Application.....	40
3.2.1	Implementation of IEC 61850 Services .....	42
3.2.2	Digital Mimic Filter .....	43
3.2.3	Phasor Extraction using Discrete Fourier Transform .....	46
3.3	IEC 61850 Communication Configurations.....	50
3.3.1	Publication and Subscription of Information in IEC 61850....	50
3.3.2	Network Interface Card of the RTDS .....	53
3.3.3	SV Publication from the RTDS.....	55
3.3.4	SV Subscription by the Line Protection IED .....	57
3.3.5	GOOSE Publication from the Line Protection IED .....	59
3.3.6	GOOSE Subscription by the RTDS .....	59

3.4	Time Delays in the Setup .....	61
3.5	Chapter Summary .....	62
<b>4</b>	<b>Distance Protection Scheme</b>	<b>63</b>
4.1	Distance Estimation Units .....	63
4.2	Impedance Characteristics .....	65
4.2.1	Mho Characteristic .....	65
4.2.2	Quadrilateral Characteristics .....	67
4.3	Fault Identification .....	69
4.4	Validation of the Implemented Distance Protection Scheme .....	70
4.5	Results Comparison for Impedance Estimations .....	72
4.6	Estimated Impedance Trajectories .....	74
4.7	Fault Detection Time .....	76
4.8	Results for Series Compensated Transmission Lines .....	79
4.9	Chapter Summary .....	81
<b>5</b>	<b>Transients Based Protection Scheme</b>	<b>82</b>
5.1	Concept of the Proposed Method of Line Protection .....	83
5.2	Implementation of the Transient Protection Scheme .....	85
5.2.1	Clarke Transformation of the Line Currents .....	85
5.2.2	Performing the Discrete Wavelet Transform .....	86
5.2.3	Fault Identification .....	92
5.3	Hybrid Protection Algorithm .....	93
5.4	Validation of the Hybrid Protection Scheme .....	97
5.5	Performance Evaluation of the Hybrid Protection Scheme .....	110
5.5.1	Behaviour for Non-faulty Conditions .....	111
5.6	Effect of the Bit Resolution of the A/D Converter .....	113
5.7	Chapter Summary .....	117
<b>6</b>	<b>Conclusions</b>	<b>118</b>

6.1 Contributions and Conclusions .....	118
6.2 Future Work .....	122
<b>7 References</b>	<b>124</b>
<b>8 Appendix A</b>	<b>131</b>
<b>9 Appendix B</b>	<b>147</b>
<b>10 Appendix C</b>	<b>150</b>
<b>11 Appendix D</b>	<b>151</b>



# List of Tables

Table 1: Comparison of phase unit impedance calculations .....	72
Table 2: Comparison of ground unit impedance calculations .....	73
Table 3: Fault detection time in terms of number of samples for distance protection algorithm .....	78
Table 4: Performance of the proposed protection scheme under different fault conditions .....	110

# List of Figures

Figure 1: Typical substation architecture of IEC 61850 .....	3
Figure 2: Flow of information in the configuration process .....	17
Figure 3: Logical interfaces for substation communication in IEC 61850 [6]	19
Figure 4: Typical substation topology of IEC 61850.....	20
Figure 5: A representation of IEC 61850 sampled values protocol.....	24
Figure 6: Function of a merging unit [15].....	27
Figure 7: Impedance seen by a distance protection relay .....	29
Figure 8: Distance characteristics on R-X (resistance-reactance) plane for three zones; (a) Mho, (b) Quadrilateral (line impedance is plotted in dashed line).	30
Figure 9: Voltage and current inversion in a series compensated transmission line .....	31
Figure 10: Wavelet function of (a) ‘db4’ mother Wavelet, (b) ‘Symlets 2’ mother wavelet.....	34
Figure 11: Multi-level filter bank implementation of DWT; (2↓) denotes down-sampling by 2 .....	35
Figure 12: Schematic of the apparatus for the distance protection scheme...	38
Figure 13: Implementation structure of the line protection IED; only the distance protection function is illustrated .....	41
Figure 14: (a) Unfiltered current waveform, (b) Filtered current waveform .	45
Figure 15: Magnitude and phase of the extracted current phasor plotted against the sample number .....	49
Figure 16: Physical connections in the LAN.....	54

Figure 17: Anti-aliasing filters (left) and the sampled values component (right), residing in the RTDS simulation case.....	56
Figure 18: Signal mapping for SV subscription.....	58
Figure 19: An example signal mappings for GOOSE subscription in; (a) Distance Protection scheme (b) Transients based protection scheme .....	60
Figure 20: Illustration of the implementation of a breaker IED in the RTDS simulation.....	61
Figure 21: Implementation of zone 1 Mho characteristic.....	65
Figure 22: Implementation of zone 1 quadrilateral characteristic .....	67
Figure 23: Fault Identification algorithm of the distance protection scheme	69
Figure 24: SLD of the simulated power system using which the implemented distance protection scheme is validated.....	70
Figure 25: Schematic of the setup for testing the distance protection scheme .....	71
Figure 26: Trajectory of the estimated impedance of the line protection IED for a zone 1, AB fault, plotted on a R-X plane; Zone 1 Mho characteristics and impedance line are shown.....	75
Figure 27: Fault detection in the distance protection scheme for a 10 % fault .....	76
Figure 28: Fault detection in the distance protection scheme for a 90 % fault .....	77
Figure 29: Estimated impedance trajectories for a bus 1 fault (a) with, and (b) without series compensation. Zone 1 Mho characteristic is also shown.....	80
Figure 30: Estimated impedance trajectories for a bus 1 fault (a) with, and (b) without series compensation. Zones 1 and 2 Mho characteristic are also shown. ....	81
Figure 31: Origination of high frequency wave-fronts due to a fault .....	83
Figure 32: Implementation of the DWT .....	87
Figure 33: Extracted high frequency transient from $I_a$ (for a sampling frequency 80 samples per cycle) .....	87

Figure 34: Extracted high frequency transient from $I_a$ (for a sampling frequency 256 samples per cycle) .....	88
Figure 35: Detail wavelet coefficients at the near end for the same fault with a sampling rate of (a) 256 samples per cycle (b) 80 samples per cycle .....	89
Figure 36: Detail wavelet coefficients at near end for (a) a 10% fault with fault inception angle at $0^\circ$ , (b) a 10% fault with fault inception angle at $180^\circ$ , (c) a 50% fault with fault inception angle at $0^\circ$ and (d) a 90% fault with fault inception angle at $0^\circ$ .....	90
Figure 37: Detail wavelet coefficients at either end for a 50% fault.....	91
Figure 38: Absolute values of the detail wavelet coefficients at either end for a 50% fault.....	91
Figure 39: Sending of GOOSE messages corresponding to wave-front polarity .....	93
Figure 40: Illustration of the transfer-trip scheme .....	94
Figure 41: Modified Mho characteristics for the proposed protection method.....	95
Figure 42: Combined algorithm of fault detection for the proposed hybrid protection scheme.....	96
Figure 43: SLD of the simulated power system using which the implemented transient protection scheme is validated .....	97
Figure 44: Schematic of the developed system for the hybrid protection scheme .....	98
Figure 45: Three phase currents, voltages, model current component ( $I_a$ ), detail WTCs, trajectories of the estimated impedance and the fault detection at either end for a 50%, ABC fault. ....	100
Figure 46: Voltage measurements at the bus side and the line side .....	101
Figure 47: Trajectories of the estimated impedance and detail wavelet coefficients at either end for a bus 1, ABC fault, with the effect of voltage inversion .....	102
Figure 48: Trajectory of the estimated impedance for a 5% three phase fault with series capacitor in service, (with the effect of voltage inversion) .....	103

Figure 49: Detail wavelet coefficients at either end for a 5% three phase fault with series capacitor in service, (with the effect of voltage inversion) .....	103
Figure 50: Detail wavelet coefficients at either end for a 10% AB fault .....	104
Figure 51: Detail wavelet coefficients at either end for a 50% AB fault .....	105
Figure 52: Detail wavelet coefficients at either end for a 90% AB fault .....	105
Figure 53: Detail wavelet coefficients at either end for an external fault (a bus 1 fault) .....	106
Figure 54: Detail wavelet coefficients at either end for a 5% AB fault with 40% series compensation .....	108
Figure 55: Detail wavelet coefficients at either end for a 95% AG fault with a 50 $\Omega$ fault impedance .....	108
Figure 56: Fault detection in the proposed protection scheme for a solid AB fault, 5% away from bus-1. ....	109
Figure 57: Detail wavelet coefficients at either end for a closing operation of the circuit breaker at the near end .....	111
Figure 58: Detail wavelet coefficients at either end for a closing operation of the bypass switch of the series capacitor. ....	112
Figure 59: Detail wavelet coefficients at the near end for a 50% fault, with an assumed A/D converter bit resolution of (a) 24 bits, (b) 18 bits (c) 16 bits and (d) 12 bits .....	115
Figure 60: Modelling the effect of a 24 bit A to D converter .....	116

# List of Abbreviations

BIED	Breaker Intelligent Electronic Device
CID	Configured IED Description
CT	Current Transformer
DB4	Daubechies 4
DFT	Discrete Fourier Transform
DNP3	Distributed Network Protocol
DWT	Discrete Wavelet Transform
EMT	Electromagnetic Transient
FCDA	Functionally Constrained Data Attributes
Gbps	Gigabits per Second
GPS	Global Positioning System
GOOSE	Generic Object Oriented Substation Event
HMI	Human Machine Interface
ICD	IED Capability Description
IEC	International Electro-Technical Commission
IED	Intelligent Electronic Device
IID	Instantiated IED Description
LAN	Local Area Network

LN	Logical Node
MAC	Media Access Control
Mbps	Megabits per Second
MU	Merging Unit
NIC	Network Interface Card
PMU	Phasor Measurement Unit
PPS	Pulse per Second
RTDS	Real Time Digital Simulator
SA	Substation Automation
SAS	Substation Automation System
SCD	Substation Configuration Description
SCL	System Configuration description Language
SCSM	Specific Communication Service Mapping
SED	System Exchange Description
SLD	Single Line Diagram
SSD	System Specification Description
SV	Sampled Values
VLAN	Virtual Local Area Network
VT	Voltage Transformer
WAN	Wide Area Network
XML	Extensible Markup Language
WT	Wavelet Transform

# List of Appendices

## Appendix A:

- I. IEC 61850 Service Modules
- II. CID file of the RTDS™ for SV publication
- III. CID file of the Line Protection IED

## Appendix B:

- I. Transmission Line Parameters
- II. Series Capacitor Parameters

## Appendix C: Filter coefficients for the mother wavelet “Daubechies 4 (db4)”

## Appendix D:

- I. Behaviour of traveling waves at a junction on a transmission line
- II. Analysis of Wave-front polarities for a R-L circuit



# Chapter 1

## Introduction

### 1.1 Background

IEC 61850 is a relatively new standard for electrical substation automation. It was introduced in early 2000s by the International Electrotechnical Commission responding to the long existed necessity to standardize substation automation practices. In recent years, many power utilities around the world have implemented IEC 61850, often partially or on trial basis, in their grids. However, IEC 61850 is fast becoming the leading standard for substation automation [1].

#### 1.1.1 Substation Automation

Substation Automation (SA), on the subject of electrical engineering, refers to the automatic real-time operation and control of a power system. Main tasks of substation automation include data acquisition, power system monitoring, power system control and communication among, intelligent

electronic devices (IED). These SA functions should be implemented in such a way that the necessary operational efficiency is maintained with minimal human intervention and engineering resources. Substation automation has been an integral part of power system operation for decades. Among the key components of an automated electrical substation are meters, sensors, actuators, control equipment, human-machine interface equipment, and the communication network [2], [3].

The communication network plays a crucial role in a substation automation system, and the communication protocols enable various devices connected to the communication network to properly decode the information received [4]. Over the years, vendor specific proprietary protocols as well as a number of standard protocols such as Modbus, DNP3 and IEC 60870-5-104 have been utilized for implementation of substation automation systems. Numerous flaws in these standards, such as the lack of interoperability among equipment from different vendors, prompted the inception of the standard IEC 61850 [1]. It unifies all substation automation practices into one single standard [4], [5]. IEC 61850 provides explicit procedures for design, modelling, data representation, and IED configurations, covering all aspects of a SA system. As a result, the degree of interoperability among IEC 61850 compliant IEDs is far superior to that of their non-compliant counterparts, a fact that is often cited as a major advantage of the standard [4].

### 1.1.2 Substation Architecture of IEC 61850

IEC 61850 introduces a distinctive substation architecture for communication within the SA system. In its most commonly encountered form, the IEC 61850 substation architecture contains three levels and two communication bus systems as shown in Figure 1. The three levels are referred to as process level, bay level and station level, whereas the two buses are referred to as process bus and station bus [6].

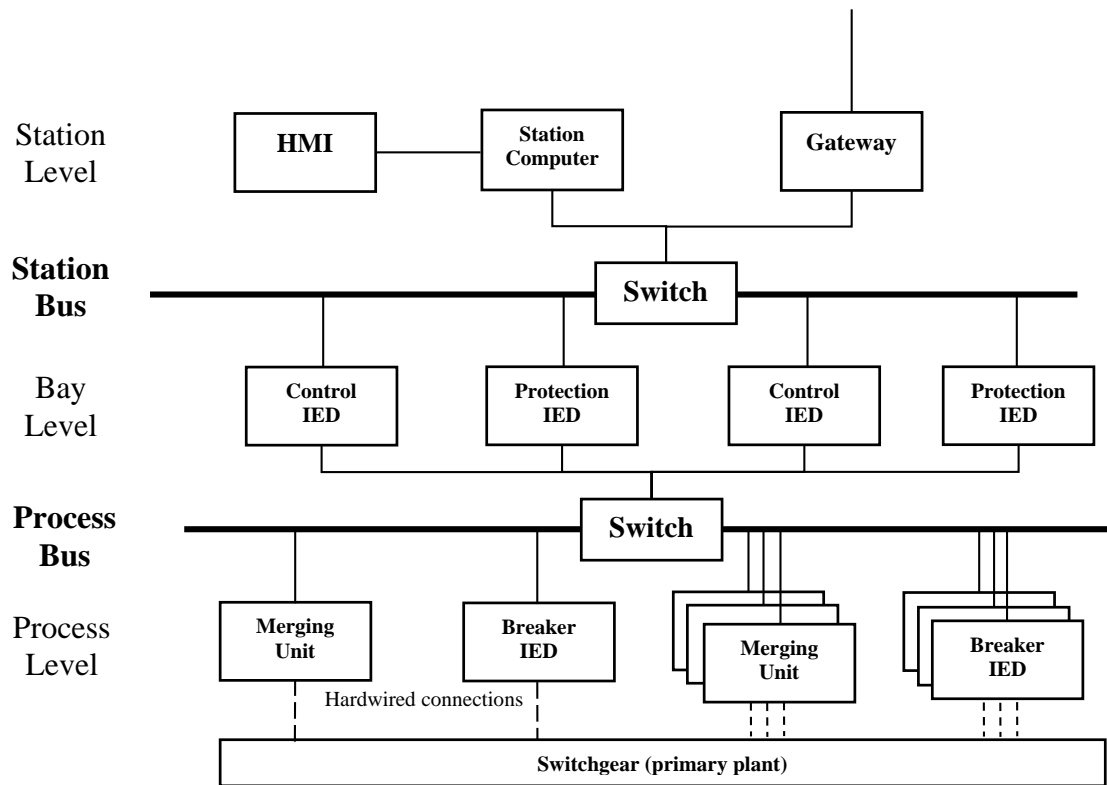


Figure 1: Typical substation architecture of IEC 61850

The process level comprises of devices, which interface with the primary plant (switchgear and instrument transformers) such as merging units (MU), breaker IEDs (BIED), sensors, and actuators.

The bay level comprises of all the protection, control and monitoring IEDs. And the station level typically consists of a Human Machine Interface (HMI), station computers, a database and remote communication interfaces.

The station bus enables communication between the station level and the bay level, along with inter-IED communication within the station/bay levels. The process bus facilitates the communication between the process level and the bay level. This includes the exchange of instantaneous raw data (such as current and voltage transformer measurements) as well as control information between process and bay levels [6].

### 1.1.3 GOOSE and SV

GOOSE (Generic Object Oriented Substation Event) and SV (Sampled Values) are two of the main specific communication services mappings (SCSM) defined in IEC 61850, in parts 8-1 and 9-2, respectively [7], [8]. Generally, GOOSE messages are employed for exchange of fast control information between IEDs. Moreover, GOOSE messages are time critical, uni-directional, multicast messages with no acknowledgements. Even though GOOSE messages are primarily used to indicate changes in the state of substation parameters, they can carry both binary and analog values.

SV, in contrast, is the protocol for acquisition of raw information particularly that is measured by instrument transformers. SV streams carry digitized samples of the analog measurements at a defined sampling rate. These messages are also time critical. The special IED that converts the analog readings from the instrument transformers into SV packets is called a Merging Unit (MU). A majority of vendors follow the UCA International Users Group Implementation Guidelines, better known as IEC 61850-9-2 LE, for the implementation of SV protocol. According to 9-2 LE, a SV packet carries 8 instantaneous values; three phase and neutral values for both voltage and current at a specified sampling rate of either 80 or 256 samples per cycle. Further details on the IEC 61850 substation architecture and the sampled values will be provided in subsequent chapters of the thesis.

#### 1.1.4 Present Status of the Standard IEC 61850

The standard IEC 61850 comprises of ten parts. There are two editions of the standard; edition 2 being is the latest. With the integration of modern communication technologies into substation automation systems, implementation of IEC 61850 is becoming an inevitable eventuality; many utilities around the world have already shifted towards IEC 61850 [1]. It is widely accepted and implemented in Europe and Asia. Implementation of IEC 61850 is making a relatively slow progress in North America.

## 1.2 Motivation

Majority of the IEC 61850 implementations in real-world operational SAS system are restricted to the station bus. Many utilities around the world have incorporated IEC 61850 station bus communication into their grids; at least to a certain extent. Application of GOOSE messages in SA functions including event recording, status updating and interlocking is widespread, while its use in more critical tasks such as breaker tripping is less common.

On the other hand, many of the SV implementations still remain at testing and research levels, even-though SV based digital process bus communication is an integral part of IEC 61850. This is due to many reasons including lack of SV compatible IEDs (at both process and bay levels), unreliability caused by extensive network traffic and high bandwidth demand.

Although many of the commercially available protection IEDs are IEC 61850 station bus compliant, commercial protection IEDs that use SV (process bus compatible IEDs) are not very common. In addition, many aspects of SV communication remains unexplored and much of its potential is unexploited. SV presents an opportunity of innovation of protection philosophies: for example it allows development of distributed applications based on current and voltage values communicated between devices connected to the process bus. Also, the high sampling rates associated with IEC 61850-9-2 LE implementation allows development of protection algorithms based on high

frequency transient signals. These prospects are the factors that motivated this research.

### 1.3 Objectives of the Thesis

An SV compatible IED prototype developed in-house, not only presents the opportunity to study various practical aspects of SV communication but also allows exploring the potential for implementing innovative protection algorithms. A test setup fully compatible with IEC 61850, including the digital process bus, is needed for testing SV compatible protection IEDs and SV communication. Development of such a test setup has additional long lasting usages for future research, teaching and training. Thus, the primary objectives of this thesis are:

1. Developing a line protection IED that is compatible with Sampled Values protocol as per IEC 61850-9-2. This IED implements the basic functionality of a distance protection relay.
2. Incorporating a transient based protection algorithm that is not normally used in traditional line protection relays into the developed IED to improve the reliability when protecting series compensated transmission lines.
3. Integrate the developed SV compatible prototype IED to a test setup developed in [9] to complete a fully IEC 61850 compliant laboratory.

## 1.4 Thesis Outline

The subsequent sections of this thesis are organized as follows. Chapter 2 presents a comprehensive introduction to the IEC 61850 standard, emphasizing on SV protocol and process bus communication. Further, brief reviews on distance protection and current transients based line protection are also provided. In Chapter 3, development of the line protection IED is extensively explained, providing details on its structure, internal algorithms and communication configurations.

In Chapters 4 and 5, implementations of the two protection schemes; distance protection and transient based line protection schemes, are presented, respectively, with corresponding results for validation. The protection algorithms are tested for a variety of faults and for varied system parameters. Moreover, the power system simulated in a Real Time Digital Simulator (on which the developed IED is tested), is also described in this chapter. Finally, Chapter 6 presents the conclusions and the future work of the research.



# Chapter 2

## Literature Review

### 2.1 Introduction to the Standard IEC 61850

#### 2.1.1 Inception

Communication between IEDs is of paramount importance to substation automation and therefore, to the overall operation and control of the power system. Few of the fundamental requirements of a communication system of an electrical substation include,

- Fast inter-IED communication
- Multi-vendor interoperability
- High availability
- Sufficient security
- Assured delivery times

With the internet and other communication technologies in rapid progression, the need for standardization of substation automation practices became essential [4].

Prior to IEC 61850, SA systems were often developed using vendor-specific protocols, which essentially lacked interoperability as well as were inherently inflexible and limited. Development of SA systems based on these protocols consumed countless hours of tedious work for designing, testing and troubleshooting. Therefore, the need for standardized, interoperable means of substation automation was ever present among the electrical automation engineers the world over [1], [3]. The standard IEC 61850 came into existence in early 2000s, owing to the work done in the IEC (International Electrotechnical Commission) Technical Committee Number 57 (TC57), Working Group 10 (WG10) [4].

The initial objectives, which the standard was intended to serve included, unification of all substation automation disciplines into one standard, enhancement of multi-vendor interoperability, standardization of data representation and introduction of necessary procedures for equipment testing [4], [5].

## 2.1.2 Structure and Scope of IEC 61850

IEC 61850 standard comprises 10 main parts, which are as listed below [5],

- IEC 61850-1:** Introduction and overview
- IEC 61850-2:** Glossary
- IEC 61850-3:** General requirements
- IEC 61850-4:** System and project management
- IEC 61850-5:** Communication requirements for functions and device models
- IEC 61850-6:** Configuration language for communication in electrical substations related to IEDs
- IEC 61850-7:** Basic communication structure for substation and feeder equipment
  - IEC 61850-7-1: Principles and models
  - IEC 61850-7-2: Abstract communication service interface (ACSI)
  - IEC 61850-7-3: Common Data Classes
  - IEC 61850-7-4: Compatible logical node classes and data classes
  - IEC 61850-7-10: Communication networks and systems in power utility automation - Requirements for web-based and structured access to the IEC 61850 information models [Approved new work]
- IEC 61850-8:** Specific communication service mapping (SCSM)
  - IEC 61850-8-1: Mappings to MMS (ISO/IEC9506-1 and ISO/IEC 9506-2)
- IEC 61850-9:** Specific communication service mapping (SCSM)
  - IEC 61850-9-1: Sampled values over serial unidirectional multi-drop point to point link
  - IEC 61850-9-2: Sampled values over ISO/IEC 8802-3
- IEC 61850-10:** Conformance testing

### 2.1.3 Terms and Definitions

IEC 61850 provides many terms and definitions related to its scope. Following are few of the most important among them, which are used frequently in the following sub-sections of this thesis [6].

#### 2.1.3.1 *Primary System*

Primary system or primary plant refers to all the power system equipment and switchgear contained in an electrical substation [6].

#### 2.1.3.2 *Substation Automation System (SAS)*

Substation automation system operates, controls, protects and monitors the primary system using the substation communication system [6].

#### 2.1.3.3 *Function*

With reference to IEC 61850, a function is simply a task executed by the SA systems. These functions oversee the control, protection, monitoring and maintenance of the SA systems. Logical nodes exist as subsets of functions (this is further explained under logical nodes). Some functions are performed by more than one logical node, which might be placed in different IEDs. These functions are referred to as distributed functions [6].

#### 2.1.3.4 *Logical Node (LN)*

A logical node is the smallest part in a function that can exchange data. By definition, only LNs can exchange data (consequently, the only data that can

be exchanged is that resides within a LN). A LN of a power system equipment represents the intelligent body of that device in the SA system (such as a circuit breaker) and it contains its own data. Additionally, within an IED, it represents and implements a function (such as a distance protection scheme). Communication links between LNs are called logical connections [6].

#### *2.1.3.5 Intelligent Electronic Device (IED)*

An intelligent electronic device or an IED is a device that possesses one or more electronic processors that are capable of receiving/sending information from/to an external device. It can implement the functionalities of the logical nodes above specified in a specific context. IEDs contain internal clocks to provide necessary time tags. Protection and control (digital) relays are classic examples of IEDs. The term “physical device” has the same meaning as “intelligent electronic device” in the context of IEC 61850 [6].

### **2.1.4 Key Advantages and Features of IEC 61850**

IEC 61850 has several unique features and advantages that set it apart from legacy SA protocols. Few of the most important among them are briefly explained below.

#### *2.1.4.1 Enhancement of Multi-Vendor Interoperability*

The word interoperability, in the context of IEC 61850, refers to the capability of IEDs of the same or different manufacturers to exchange

information among each other and to apply that information to acquire the desired coordination. Manufactures can achieve this by adhering to the explicit definitions, specifications and procedures provided in the standard.

Substation automation protocols prior to IEC 61850 have had several issues regarding interoperability. Manufactures sometimes have their own proprietary protocols for substation automation functions. This makes the configurations between devices of different vendors a tedious exercise. Usually, utilities either have to stick with one vendor or use protocol convertors [1]. In contrast, all IEC 61850 compliant devices, once configured, are capable of working in tandem with each other regardless of their make. This essentially simplifies the engineering tasks involved, and also enables the selection of devices based on performance rather than compatibility.

#### *2.1.4.2 Simplification of Hardwired Implementations*

The next vital advantage IEC 61850 offers is the simplification of hardwired engineering implementations. Older SASs require a huge number of physical connections, both for communication between devices and for raw data acquisition. Significant amounts of time and money must be consumed in designing, configuring and troubleshooting these connections. With IEC 61850, the number of connections and associated configurations are considerably reduced, as all communication is done digitally. As a result, IEC 61850 based SASs are more or less copper-free, which reduces the overall costs [10].

Moreover, addition or modification of equipment in legacy substations requires physical reconfiguration of the system, whereas in IEC 61850 SASs, all the required new configurations can be performed on software and sent to IEDs via the communication network.

#### *2.1.4.3 Organized Substation Modelling and Data Representation*

Object oriented data representation and object modelling IEC 61850 offers, makes it far more intuitive and user friendly than its counterparts. Data representation (data models) in IEC 61850 emulates the structure (topology) of the substation it's intended for [4], [11]. This concept is referred to in the standard as virtualization. Data representation in other substation automation protocols do not specifically represent the physical substation entity that it represents. This again makes design and configuration with IEC 61850 easier, which in a SA system with hundreds of IEDs could make a substantial difference.

IEC 61850 put forth meticulous engineering procedures, naming conventions and equipment models for the design and configuration of an entire substation. IEC 61850 follows a unified approach in developing the SAS. This starts from the specification of requirements and gradually evolves into a descriptive virtual model of the actual substation. Another unique feature of IEC 61850 is its relative independence from the prevailing communication technology. In IEC 61850, the basic modelling parts are decoupled from the

methods of information exchange (i.e. it uses abstract modelling). In that way, the core of the standard will remain intact, while its implementations can adopt the state-of-the-art communication technologies [4].

### 2.1.5 System Configuration description Language (SCL)

The XML based Substation Configuration description Language (SCL) is introduced in IEC 61850-6, for the purpose of formal documentation of the configuration flow in a SAS. This is used for the description of configurations of IEDs, communication systems as well as for defining the connection between the SAS and the physical substation itself [12]. It further facilitates the exchange of engineering configurations back and forth between different stages of the design process of the SAS in correct coordination, thus, ensuring interoperability.

In part 6 of the standard, two conceptual tools are introduced for the purpose of configuring the SAS, which are, IED configurator and system configurator. IED configurators are mostly vendor-specific. They are capable of generating IED template files, setting-up IED specific configurations and loading files into the IEDs. In contrast, a system configurator is independent of the IEDs (and the vendors) and used for higher level system engineering. It imports configuration files from different IEDs and creates a substation-related configuration file with shared system information. This file is then taken into the IED configuration tools for final IED related configurations. For



the purpose of abovementioned configuration information exchange, SCL defines six file types with the extensions ICD, IID, SSD, SCD, CID, and SED [12]. The basic flow of information in the configuration process is depicted in Figure 2 [12].

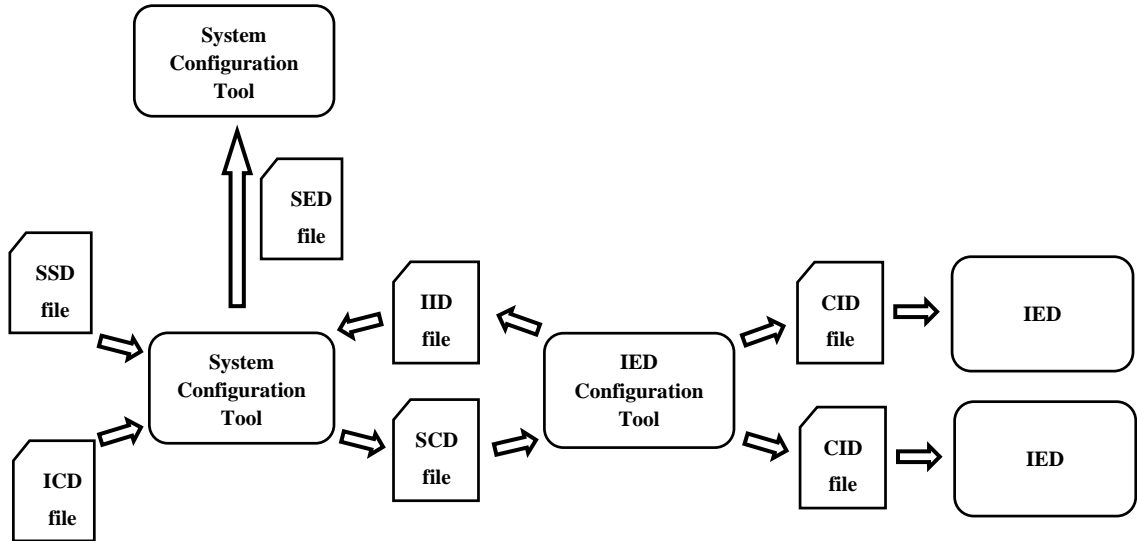


Figure 2: Flow of information in the configuration process

Two types of SCL files mentioned above are used exclusively for setting up the IEC 61850 configurations in IEDs. They are the ICD (IED Capability Description) files and the CID (Configured IED Description) file. An ICD file can be considered as a template file of a certain IED, describing the functionality (related to IEC 61850) of that IED. It contains data type definitions, logical nodes type definitions and sometimes substation templates as well. All commercially available IEDs come with an ICD file provided by the manufacturer. A CID file, on the other hand, is describing the IEC 61850

communication configurations of an instantiated IED. It is created by the IED configurator from a larger, overall substation based file called SCD (System Configuration Description) file.

The object model in IEC 61850 consists of three parts, namely, substation model, product model and Communication model. The substation model is a hierarchy of virtual objects (data models) reproducing the physical substation. It defines the topology of switchyard equipment and their functional designations. The product model (or the IED model) is also a hierarchy of data models, which represent the functional aspects of the IEDs that form the SAS. The communication model is not a hierarchy and it describes the possible communication connections between IEDs. It comprises of communication-specific data objects [12].

#### 2.1.6 Logical Interfaces

Different logical interfaces in a SAS as defined in IEC 61850-5, are illustrated in Figure 3 [6]. The corresponding logical structure of the SAS is reproduced in Figure 4 for convenience. The interfaces (**IFs**) illustrated in Figure 3 (as numbers) are [6],

**IF 1:** Communication between bay level and station level to exchange protection data

**IF 2:** Communication between bay level and remote protection schemes

**IF 3:** Communication within bay level

**IF 4:** Communication between process and bay level to exchange CT and VT instantaneous data (especially samples)

**IF 5:** Communication between process and bay level to exchange control data

**IF 6:** Communication between bay and station level to exchange control data

**IF 7:** Communication between substation (level) and a remote engineer's workplace

**IF 8:** Communication between bays (for fast functions such as interlocking)

**IF 9:** Communication within station level

**IF 10:** Communication between substation and a remote control centre to exchange control data

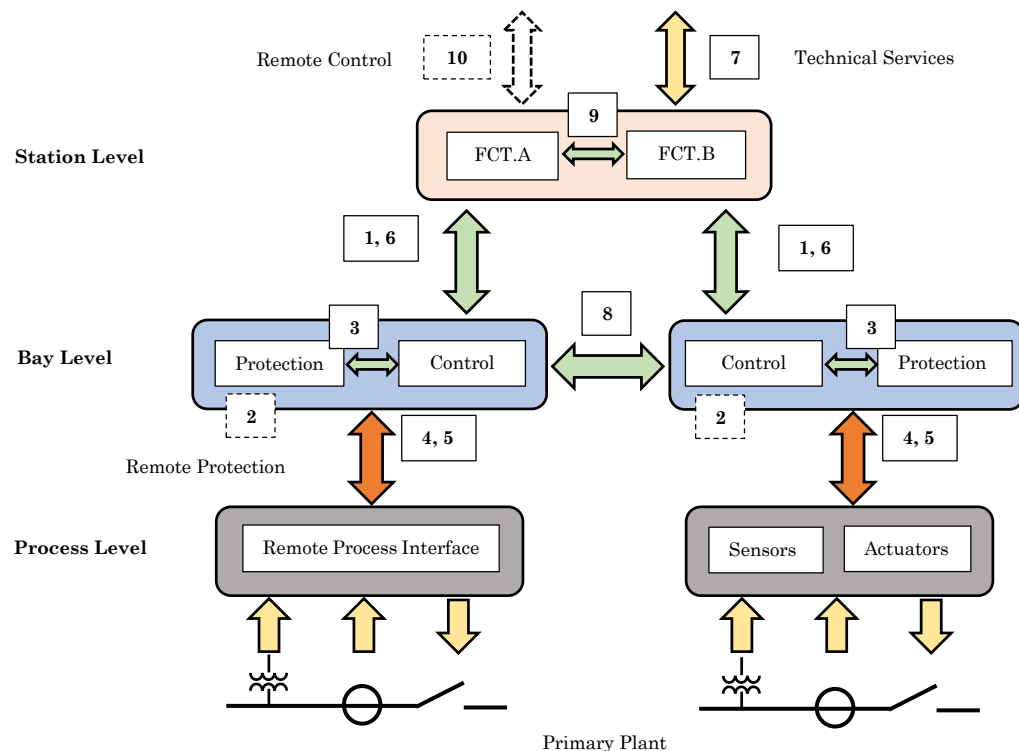


Figure 3: Logical interfaces for substation communication in IEC 61850 [6]

As shown in Figure 4, equipment that interface with the primary plant (switchgear) such as merging units (MU), breaker IEDs (BIED), sensors and actuators are contained in the process level. The bay level contains all protection, control and monitoring IEDs, while the station level usually consists of a Human Machine Interface (HMI), a station computer, a database etc.

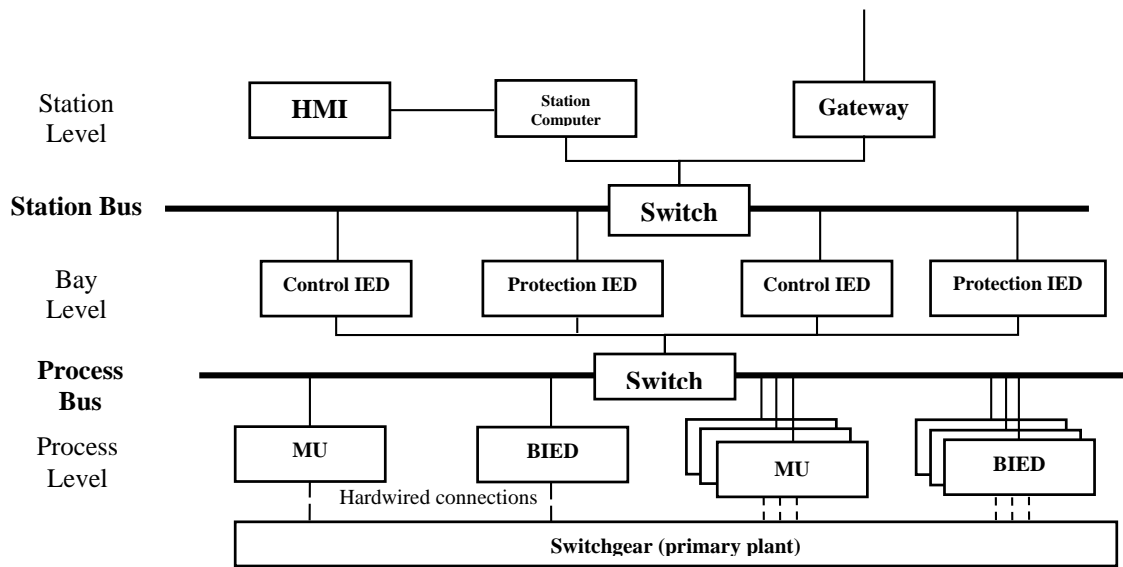


Figure 4: Typical substation topology of IEC 61850

The structure shown in Figure 3 refers to the logical structure of the SAS given in Figure 4. The physical devices, however, may be installed in a different structure. There is no definite connection between this logical architecture and the physical arrangement of devices. These logical interfaces can be implemented as separate physical interfaces or a couple of logical interfaces can be integrated into one physical interface. For instance, some process and bay level functions might be found inside the same physical device.

Moreover, one or more of these physical interfaces can be combined into a single LAN. This physical architecture depends on factors like availability of devices, performance requirements, cost, geography and other constraints. It is also important to understand that not all of the logical interfaces are compulsory in a SAS [6].

Using the logical interfaces given in Figure 3, two important LANs (or bus systems) can be identified. According to IEC 61850-5, the combination of the interfaces 1, 6, 3, 9 and 8 can be identified as the **Station Bus**, whereas interfaces 4 and 5, together can be identified as the **Process Bus** [6].

#### *2.1.6.1 Station Bus*

The station bus facilitates communication between the station level and the bay level as well as inter-IED communication within the station/bay levels. It is usually used for SA functions such as interlocking, reporting and event recording.

#### *2.1.6.2 Process Bus*

In an electrical substation, high voltage equipment and switchgear such as power transformers, instrument transformers, busbars and circuit breakers are referred to as the “primary plant”, while the protection, control and monitoring equipment including relays, event recorders and other IEDs are called the substation automation system (SAS). The process bus facilitates the communication between IEDs that govern the primary plant and the main

protection and control devices of the SAS. The links in the process bus in a traditional SAS usually are dedicated, function specific and hardwired copper connections, connecting the primary plant to the IEDs at bay level.

A digital process bus as proposed in IEC 61850, however, only comprises a single Ethernet network that carries digitized information of the measured analog signals. It may also carry command signals, alarms and indicator information like status updates from the relays to the primary plant as well. A process bus is typically confined to a single bay only [6]. Occasions in which process bus extends to more than one bay, it might govern the data exchange between bay level IEDs as well.

### 2.1.7 Generic Object Oriented Substation Event

Generic Object Oriented Substation Event (GOOSE) is one of the two main specific communication services mappings (SCSM) used in IEC 61850. Defined in IEC 61850-8-1 [7], GOOSE is a method of exchanging messages between IEDs over a local Ethernet network. It is both fast and reliable and therefore, well suited for time-critical applications such as protection functions in a substation.

Since GOOSE messages are involved with time-critical functions, acknowledgements are not sent. Instead, to increase redundancy, the same GOOSE message is retransmitted in a predefined pattern. Moreover, GOOSE is a type of multicast messaging that can carry both binary and analog values

in their messages. However, in practice, GOOSE messages mainly carry changes of state of substation parameters. GOOSE messages are suitable for the exchange data involving SA functions such as breaker tripping, status update, interlocking and event recording.

GOOSE messages are based on a publisher/subscriber model and since there are usually multiple receivers involved, multicasting is required (i.e. multicasting refers to sending information to a selected group of destinations, simultaneously). Since, GOOSE are time critical messages, application layer is directly mapped to data link layer, skipping the intermediate layers including transport and network layers. Due to this, GOOSE messages involve no IP, no addressing, and can be transmitted via a LAN only (are not routable through a WAN).

From the above discussion, the following can be viewed as features of IEC 61850 GOOSE messaging [13],

- Uni-directional communication
- Multicast messaging
- Subscriber receives only the required (mapped) information; the rest is neglected
- Very fast communication
- No acknowledgements sent upon reception of the message
- Can be used only for intra-substation communication

### 2.1.8 Sampled Values

Sampled Values (SV) or Sampled Measured Values (SMV) is a protocol defined in IEC 61850-9-2 for the acquisition of raw data [8]. In particular, it facilitates the transfer of digitized samples of analog measurements. Similar to GOOSE, SV are also time critical messages and can be streamed as either unicast or multicast. The following can be viewed as the key features of SV,

- SV are time critical messages, hence no acknowledgements are sent. And as in GOOSE, link and application layers are directly mapped, improving the time performance of data transfer. However, unlike in GOOSE, the same message is not retransmitted in SV.
- SV protocol continuously publishes data packets at a specific rate(s) defined by the user (as depicted in Figure 5).

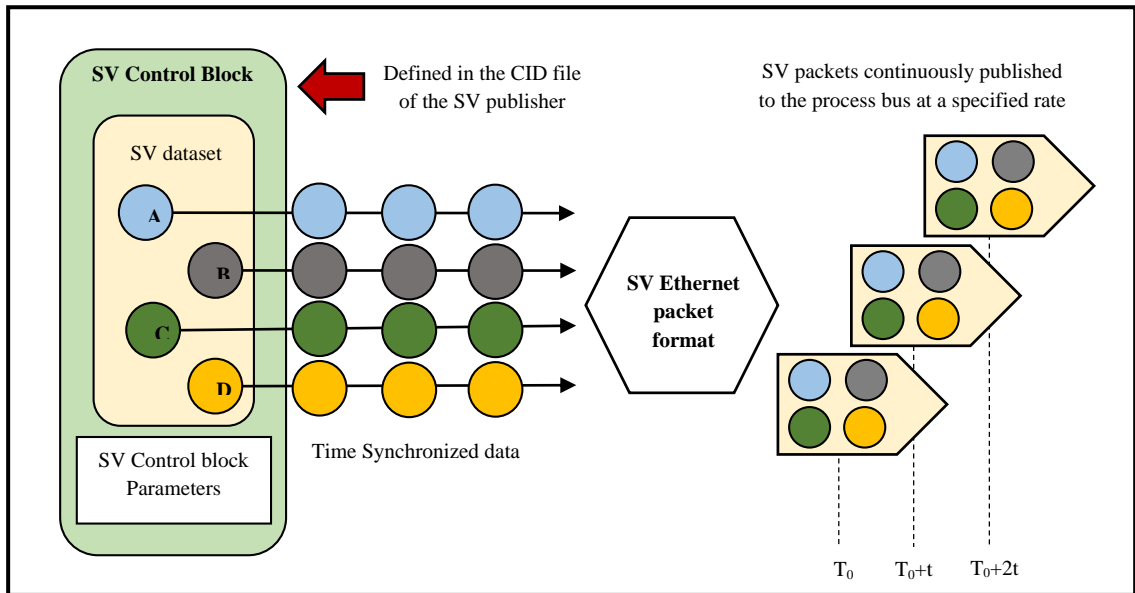


Figure 5: A representation of IEC 61850 sampled values protocol



### 2.1.9 IEC 61850-9-2 LE

The UCAIug implementation guideline, often referred to as “9-2 Light Edition” (9-2 LE) [14], specifies simplified guidelines for implementing IEC 61850-9-2 based process bus communication using SVs. With 9-2 LE, dataset size, sampling rate, time synchronization requirements and the physical interfaces to be used are predefined. An IEC 61850-9-2 LE compliant device would publish eight simultaneous, digitalized data streams, four voltages and four currents (three phases and neutral for each), at a sampling rate of 80 or 256 samples per cycle.

The function of an instrument transformer (i.e. measuring and publishing of a particular parameter), is represented by a corresponding logical node inside the ICD file of merging unit. For instance, the current transformer attached to phase A is represented by an instance of current transformer logical node class “TCTR”. Similarly, the voltage transformer function is represented by voltage transformer logical node class “TVTR”. Therefore, an ICD file of a MU compliant with 9-2 LE, comprises of four logical node instances each, of classes TCTR and TVTR, in order to accommodate eight SV streams published.

Further, MUs in SAS can be synchronized to an external time reference (often to a GPS clock) and the synchronization signal must be a 1PPS input, which shall have an accuracy of  $\pm 1 \mu\text{s}$ , according to the specification in IEC 60044-8. According to the standard, there can be a maximum propagation

delay of  $\pm 2 \mu\text{s}$  between the synchronization signal output and the MU clock input, which otherwise ought to be compensated by the MU [14].

Moreover, if the neutral current/ voltage are not measured by the MU, they should be calculated using phase measurements inside the MU. Also, this should be informed to the receiver using the respective quality field. The attribute “SmpSynch” indicates the state of the synchronization signal of the MU. The attribute “SmpCnt” designates the sample number taken. It is incremented at every new sample and is reset to zero with every synchronizing pulse (i.e. at the start of each second) [14]. Therefore, for 60 Hz systems, this variable moves from 0 to 4799 or 15359 depending on the sampling rate used. This sample count can be used for the time synchronizing purposes in IEDs.

#### 2.1.10 Merging Unit

A Merging unit (MU) is an IED that digitizes the analog measurements, taken mainly by conventional current and voltage transformers. It then publishes those data as a stream into the process bus at a predefined rate, to be captured by protection and control relays at the bay level. MUs merge (or combine) and perform time correlation of voltages and currents of the three phases (of a line) as shown in Figure 6 and hence, given its name [15]. These devices operate as per part 9 of the standard IEC 61850. Further, it is important to notice that the connections from the instrument transformers to merging units are usually hardwired.

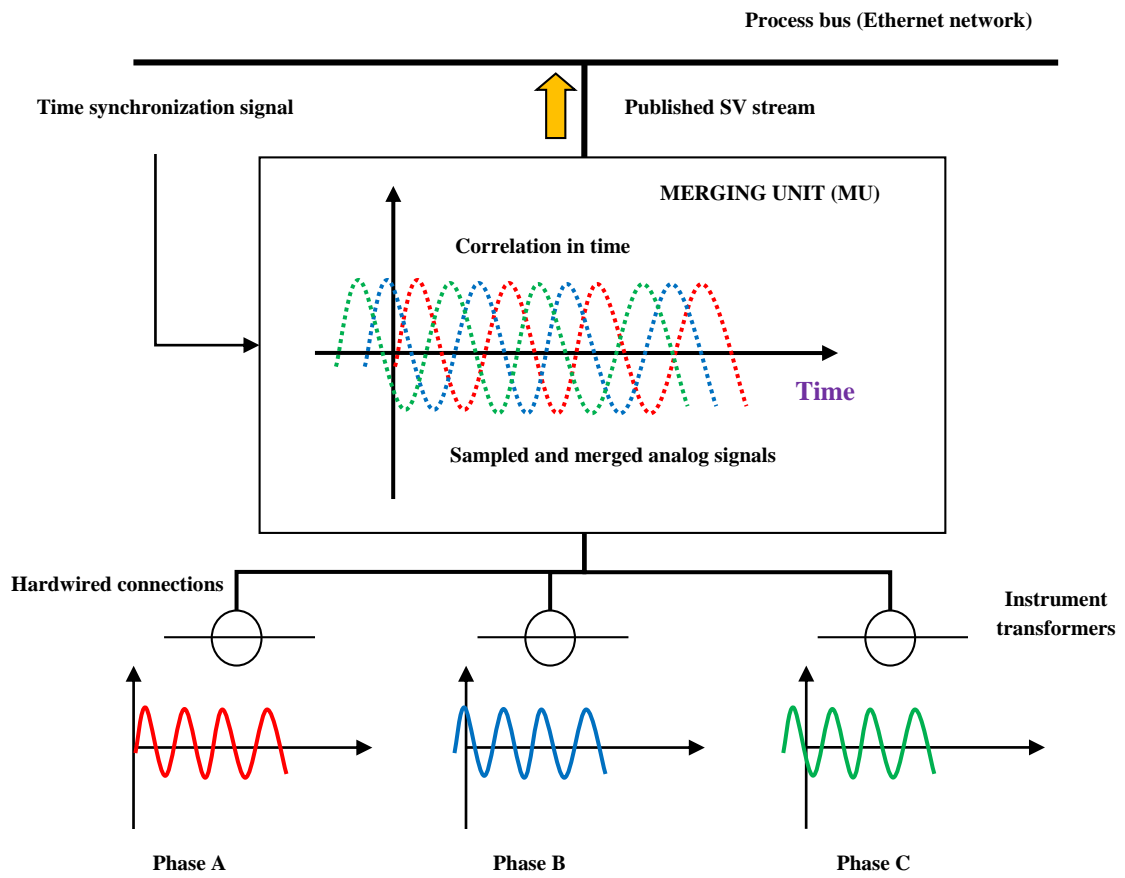


Figure 6: Function of a merging unit [15]

### 2.1.11 Inter-Substation Communication as per IEC 61850-90-5

All communication mechanisms discussed thus far in this thesis with reference to IEC 61850 are confined within a particular substation (In other words, IEC 61850 is basically for intra-substation communication). However, a newly introduced part of the standard, IEC/TR 61850-90-5, stretches its boundaries in an attempt to incorporate information exchange among substations over a WAN as well [16].

This new part of the standard basically focuses on the transmission of synchrophasor information according to IEEE C37.118, using IEC 61850. In addition, this enables regular IEC 61850-8-1 GOOSE and IEC 61850-9-2 SV packets to be routed over a WAN [17]. This new routable GOOSE messaging is envisioned to be used in order to accomplish the transfer trip scheme proposed in a later stage of this thesis.

## 2.2 Transmission Line Protection Schemes

### 2.2.1 Distance Protection

Distance protection is one of the most established practices in power system protection. It is a non-unit type protection method and widely used for transmission line protection. A distance protection relay estimates the impedance down the line to a fault using currents and voltage measurements at the relay point [18].

As illustrated in Figure 7, the impedance seen by the distance protection relay at point A for a fault occurring at point B would be  $Z_{AB}$ , irrespective of the magnitudes of voltage and current during the fault. Owing to this, distance protection has the capability to discriminate faults in different parts of the power system. It is also fast operating and simple to implement [18].

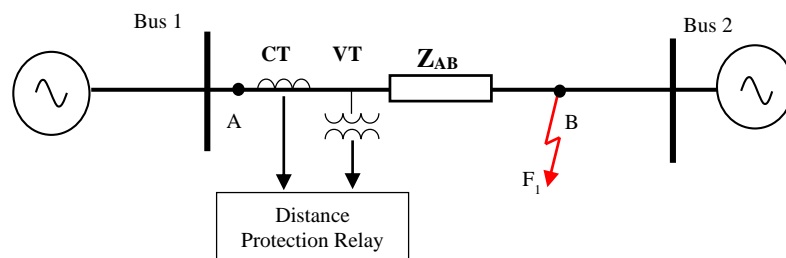


Figure 7: Impedance seen by a distance protection relay

In general, a distance protection relay has two types of settings; reach settings and operating time settings. The reach settings are applied as zones,

usually 3 or 4 in number. Zone 1 reach setting is often set at 80% of the protected line and that of zone 2 is at 100% of the protected line, plus 50% of the shortest next line. Zone 3 setting is set to cover 100% of the protected line, and 100% of the second longest line, plus 25% of the shortest remote line. Zone 1 operation very often is instantaneous and operating times for Zones 2 and 3 are typical in the ranges of 0.25-0.4 s and 0.6-1.0 s, respectively. Distance protection relays have characteristics to define its protected region. Mho and quadrilateral are two of the most commonly employed distance characteristics. In some instances, reverse looking zones are also defined.

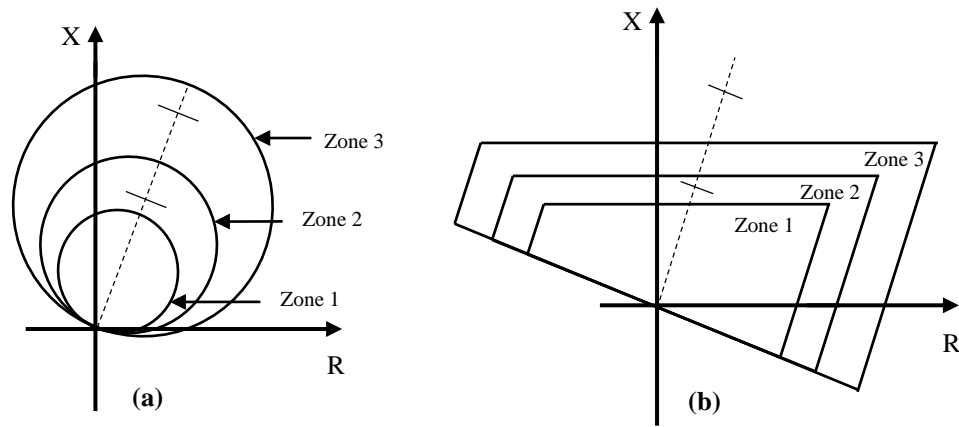


Figure 8: Distance characteristics on R-X (resistance-reactance) plane for three zones; (a) Mho, (b) Quadrilateral (line impedance is plotted in dashed line)

### 2.2.2 Challenges in Protecting Series Compensated Transmission Lines

Capacitor banks are often connected in series with transmission lines in order to increase their power transfer capabilities. Protection of these series compensated transmission lines is one of the long prevailing challenges in

power system protection [19]. The occurrence of voltage and current inversions in a series compensated transmission line is explained below with the help of Figure 9.

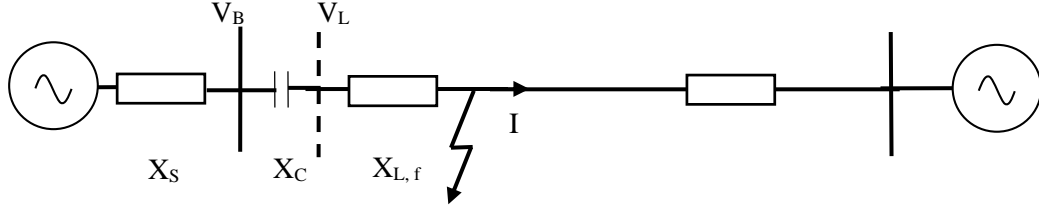


Figure 9: Voltage and current inversion in a series compensated transmission line

Voltage and current inversions across the series capacitor can provide complications to conventional protection algorithms and make traditional distance relays to mal-operate. When the series capacitor is in service, the bus side voltage,  $V_B$ , is equal to  $I \cdot (X_{L,f} - X_C) \cdot j$  and the line side voltage,  $V_L$  is equal to  $I \cdot X_{L,f} \cdot j$ . For certain faults, where the inductive reactance of the faulty line section is smaller than the capacitive reactance of the series capacitor ( $X_{L,f} < X_C$ ),  $V_B$  gets inverted by  $180^\circ$  [19]. A distance relay, fed with  $V_B$ , sees such a fault (which should be a zone 1 fault in most cases) as a reverse fault and will restrain itself from operating. This can be avoided by feeding the relay with the line side voltage,  $V_L$ . However, then voltage inversion happens for reverse faults. The relay will consequently see certain reverse faults as forward and could mal-operate.

Current inversion happens when the impedance between the power system source and fault point is capacitive ( $X_S + X_{L,f} < X_C$ ). In this case, the

current at bus 1 would be capacitive, while current at bus 2 is still inductive. This causes a complication in protection algorithms as the phase relationship of the two currents in this scenario is similar to that of an external fault [19]. Furthermore, sub-harmonic frequency transients in series compensated lines can induce oscillations in impedance estimations of the relays, causing them to overreach.

### 2.2.3 Current Transients Based Line Protection

Analysis of high frequency electromagnetic transients caused by various power system events is a well-known strategy in power system protection. High frequency transients, particularly those superimposed in line currents, are commonly analysed in modern protection algorithms [20]-[25]. These protection schemes usually employ time-frequency-transformations to extract the high frequency transients generated by a power system abnormality such as an occurrence of a fault or a switching operation. The extracted waveforms are further examined to gain information about the event including its location and magnitude.

#### 2.2.3.1 *Filtering methods used for transient extraction*

There exist several means of digital signal processing for the extraction of high frequency transients superimposed in line currents and voltages. The main methods are conventional filtering, short-time Fourier transform (STFT)



and wavelet transform (WT). The use of the wavelet transform in power system studies is relatively newer than the other two techniques.

Regular band-pass filters can be employed for the study of high frequency transients. However, WT has several advantages over conventional filtering, including better performance in signal de-noising [21]. In addition, the selection of the optimum threshold frequencies for the filters can be a complication, when using conventional filters.

Conventional Fourier Transform cannot be used to analyze momentary high frequency components in line currents, as it does not provide any time localization. However, both STFT and WT deliver frequency decomposition of a signal and provide means of two dimensional localization of time-frequency. The main difference between the two techniques is the window size of STFT is fixed, in contrast to that of WT, which is scalable (as a result, the frequency resolution of STFT is uniform and, on the other hand, WT has multi-resolution properties) [20].

The transients based algorithm proposed in this work depends on the capability of the signal processing unit to deliver the polarity of the wave-front of a high frequency transient. With STFT, all information about the high frequency transient (contained within the considered time window) is available in the frequency domain. Hence, obtaining information related to the wave-front polarity is not straightforward. In contrast, WT extracts the required frequency band in time domain, and as a result, the polarity of the wave-front

is readily available. The WT is, therefore, better suited for the application considered in thesis and a brief explanation about WT and its implementation methods are provided below.

### 2.2.3.2 Wavelet Transform

The wavelet transform of a continuous signal  $x(t)$  is given by [20],[26],

$$WT(a, b) = \frac{1}{\sqrt{a}} \int_{-\infty}^{\infty} x(t) \cdot g\left(\frac{t-b}{a}\right) dt \quad \text{-----(1)}$$

; Where,  $g(t)$  is referred to as the “mother wavelet” and “a” and “b” are scaling and translation constants, respectively. For a function to be considered as a mother wavelet, it must have zero average and be quickly decaying at each end. By definition, an infinite number of mother wavelets can exist, but there exist several commonly used families of mother wavelets. The selection of the mother wavelet for a certain study is governed by the requirements and the nature of the study. Two example mother wavelets are given in Figure 10.

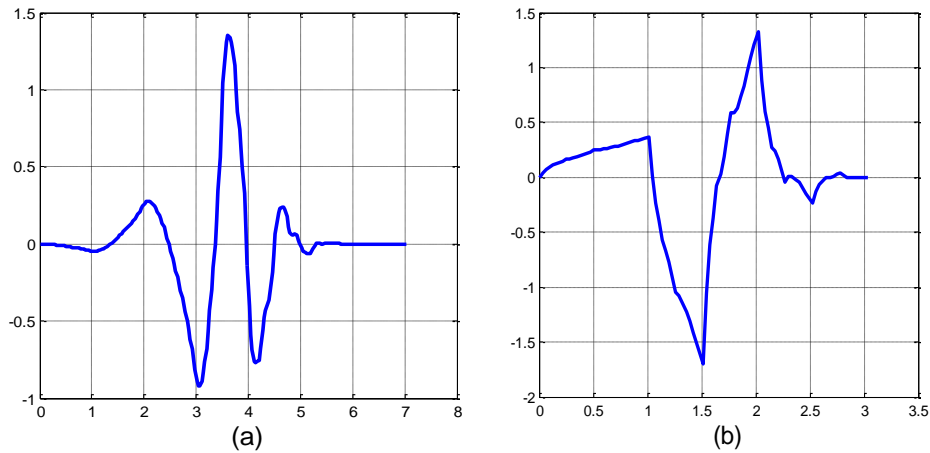


Figure 10: Wavelet function of (a) ‘db4’ mother Wavelet, (b) ‘Symlets 2’ mother wavelet

Moreover, the discrete form of the wavelet transform is referred to as the discrete wavelet transform (DWT) and can be given as [20],

$$DWT(m, n) = \frac{1}{\sqrt{a_0^m}} \sum_k x[n] \cdot g \left[ \frac{k - na_0^m}{a_0^m} \right] \quad \text{-----}(2)$$

It has been mathematically proven that the DWT can be implemented using a series of low and high pass filters as shown in Figure 11 [20], [26].

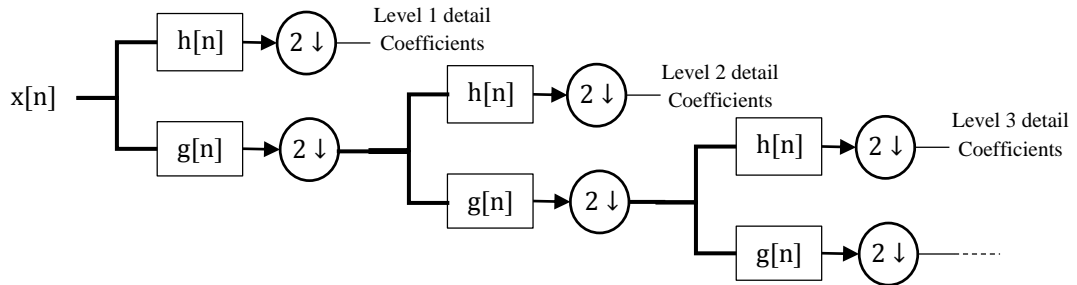


Figure 11: Multi-level filter bank implementation of DWT; (2↓) denotes down-sampling by 2

Here, the signal  $x[n]$  is decomposed using a low pass filter,  $g[n]$  and its high pass dual,  $h[n]$ . They are known as quadrature mirror filters and their filter coefficients are the reverse of each other, with every other coefficient negated [20]. Further, the outputs of the high pass filter are called “detail coefficients”, whereas those of the low pass filter are called “approximation coefficients”.

These filters are designed in such a way that their output has half the frequency band of that of the input. Since the top half of the frequencies are removed by  $h[n]$ , one half of the samples can be dispensed with before the next

level, as per Nyquist–Shannon sampling theorem. The effect of down-sampling the filter output by 2 is equivalent to the scaling of the wavelet function by a scaling factor of 2 in the subsequent level [20]. This scheme can be implemented using any wavelet after determining the corresponding filter coefficients. Filter coefficients for commonly used wavelets are found in [27].

## 2.3 Chapter Summary

In this chapter, a comprehensive introduction to the standard IEC 61850 was provided with its advantages, definitions, architectures and protocols. The emphasis was given on sampled values (SV) protocol. Further, an overview of transmission line protection using impedance based methods was provided. Basics of transients based protection were also briefly explained.

## Chapter 3

# Implementation of a Process Bus Compatible IED Using Generic Hardware

### 3.1 Experimental Setup

At the beginning of this section, the basic arrangement of the experimental setup, including the relay developed in this research, is presented in order to provide an overall picture about the function of the developed system. This is followed by detailed explanations on the implementation of the line protection IED application.

The power system, on which the developed IED is tested and validated, is simulated in RTDS™. It is a real-time digital simulator based on electromagnetic transient (EMT) simulation (this simulator, from this point onwards, shall be referred to as the RTDS). It is also the primary SV source considered in this work. Depicted in Figure 12, is the schematic of the

experimental setup (related to the distance protection scheme) developed for this research. The dashed-box in Figure 12 represents the implemented IED that is existing outside the RTDS on a desktop computer. Real IEC 61850 communication is used for transferring information between the RTDS and the IED. All other components are modelled inside the RTDS simulation case, using its standard library modules. The power system section under consideration is an overhead transmission line connecting two AC networks.

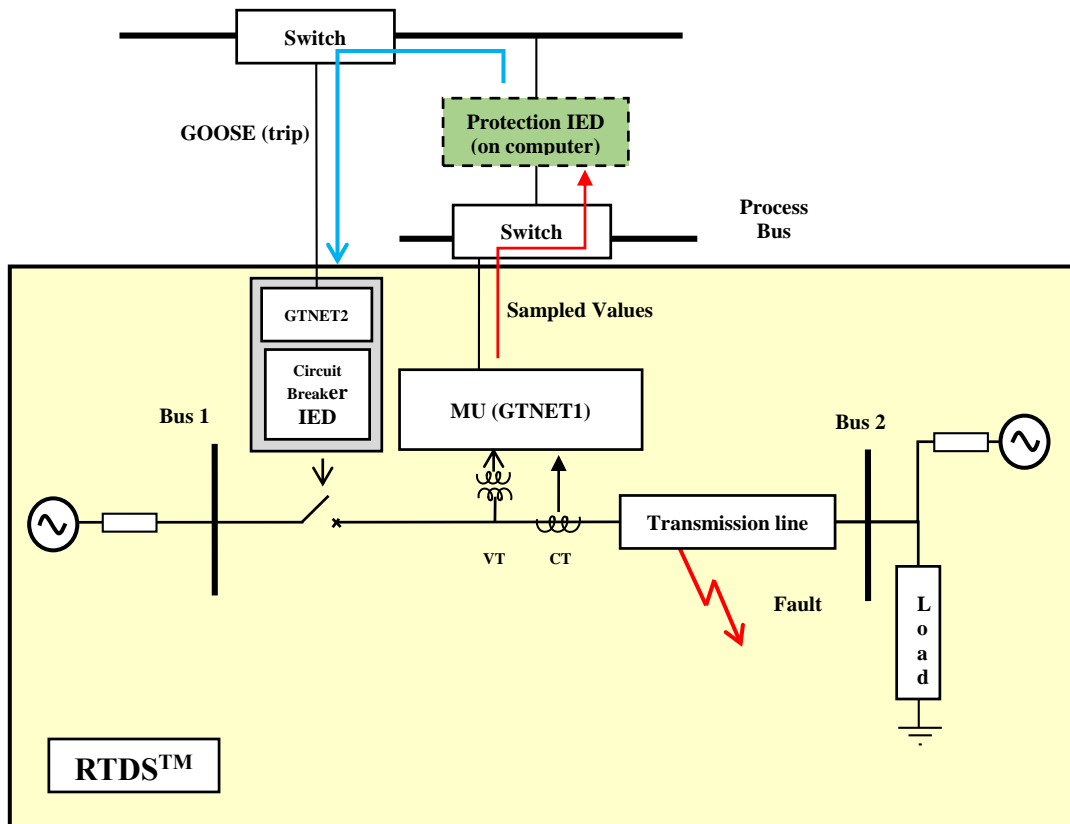


Figure 12: Schematic of the apparatus for the distance protection scheme

Implementation of the IEC 61850 substation architecture and communication system is also represented in Figure 12. The network interface

card of the RTDS, referred to as the GTNET card [28], supports the two protocols GOOSE and SV. For this work, two such GTNET cards are used, one for each protocol.

Sampled values (SV module) module in the RTDS is compliant with IEC 61850-9-2 LE, thus, publishes four currents and voltages each to form a virtual MU inside the RTDS. Detailed modelling of this MU will be explained later. This SV module is connected with GTNET1, which is dedicated for SV communication. In this study, the published SV streams are the instantaneous currents and voltages of the three phases and the neutral, measured at Bus 1, as shown in Figure 12.

The SV stream published by GTNET1 goes through a high speed (1 Gbps) Ethernet network (the process bus) into the line protection IED (implemented on the desktop computer), where it is subscribed and decoded to be used in protection algorithms. Once the relay detects a disturbance by internal processing of the received information, it issues a trip signal via a GOOSE message. This GOOSE message is routed through a separate 100 Mbps network and is subscribed by the second GTNET card (GTNET2) of the RTDS. The GOOSE module in RTDS simulation then decodes the information inside the message and acts accordingly by tripping the circuit breaker in the simulated network.

Moreover, from here onwards, the near end refers to Bus 1 and the far end refers to Bus 2 of the transmission line, as shown in Figure 12.

Furthermore, all distances (for instance, distance to the location of a fault) are measured from Bus 1.

## 3.2 Line Protection IED Application

The basic line protection relay (IED) application developed in “C” programming language runs on desktop computer with a Linux operating system. Basic implementation structure of the developed IED is illustrated in Figure 13 below. The IED application (the line protection relay), once configured and initiated, is looking for a source that is publishing SV (according to IEC 61850-9-2-LE). The process of matching IEC 61850 configurations of the source with those of the destination is called mapping, which will be discussed under a different topic later.

Once a connection is established with a SV source (in this scenario, with the RTDS), the application starts receiving SV. These SV packets are then stored in a circular data buffer. Concurrently, another tread of the application reads SV packets from the same buffer and then, decodes them to acquire the instantaneous currents and voltage values contained within. These values are then subjected to further processing as shown in Figure 13.

As the next step, any DC offsets contained within the currents and voltages are filtered-out using a digital mimic filter (a low pass filter). Afterwards, discrete Fourier transform is performed using this filtered data, in order to extract the current and voltage phasors. Impedance estimations are



carried out using the said phasors, which are then fed into the distance relay characteristics. If the estimated impedance is within a zone, a trip signal is issued via a GOOSE message. Important sections of the above implementations are explained in detail in the next sub-sections.

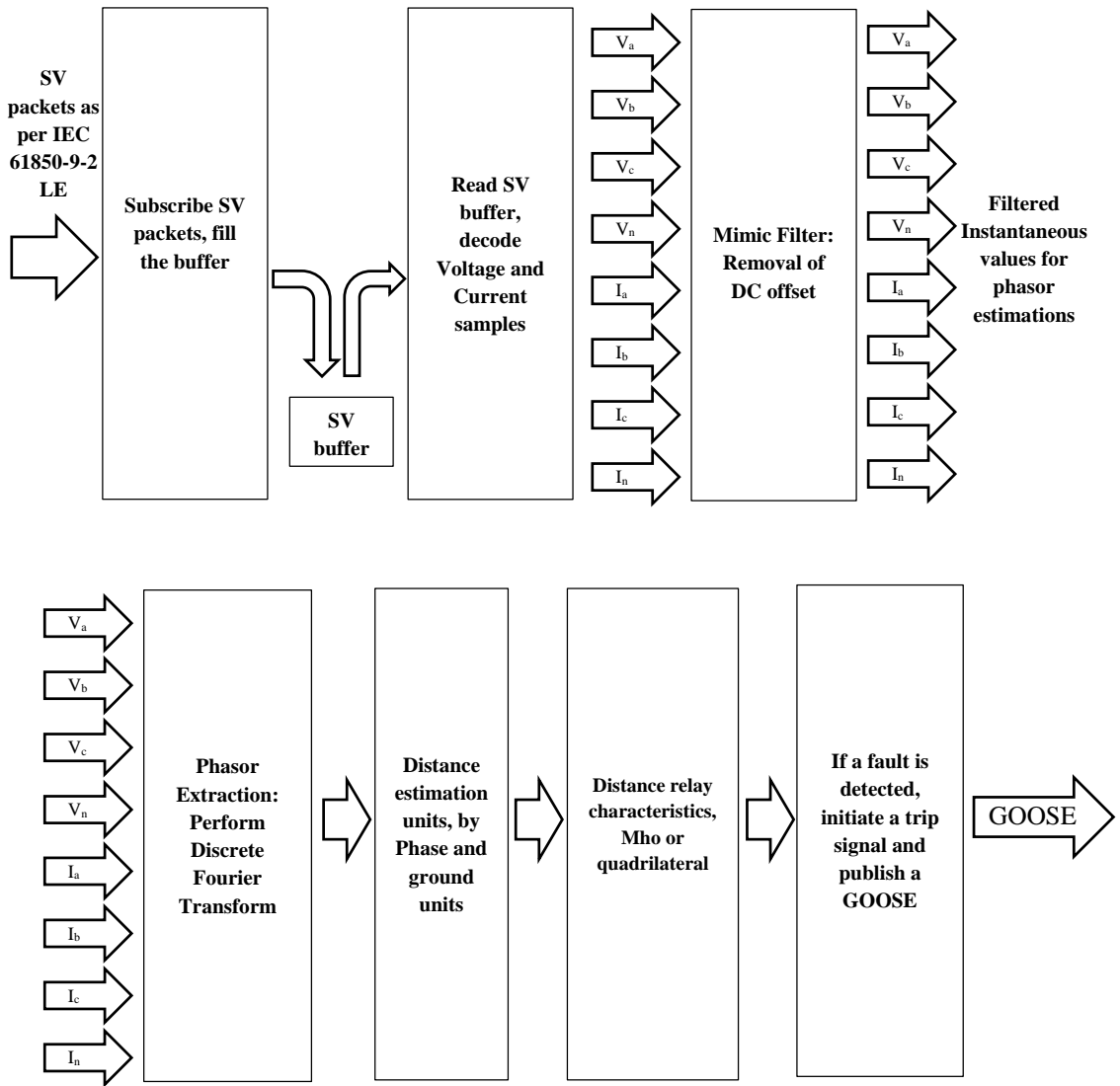


Figure 13: Implementation structure of the line protection IED; only the distance protection function is illustrated

### 3.2.1 Implementation of IEC 61850 Services

This application uses a set of software libraries developed by Kalkitech Pvt. Ltd, India, to accomplish the basic IEC 61850 services such as publishing, subscribing, storing and decoding of SV and GOOSE messages. The Kalkitech IEC 61850 library consists of six modules:

1. Initialization Module.
2. Server Module.
3. Goose Publisher Module.
4. Goose Subscriber Module.
5. Sampled value Subscriber Module.
6. Sampled value Publisher Module.

Each of these modules contains different sets of APIs (Application Programming Interface) for IEC 61850 services, which are listed in Appendix A-I. This high level API library is built on SISCO SCL MMS Ease Lite [29], which is a source code package for the Manufacturing Message Specification (MMS) protocols, IEC 61850 that has been optimized for use in IEDs such as RTUs, reclosers, PLCs, meters and other resource constrained embedded applications. However, several of the functions in Kalkitech IEC 61850 library needed to be modified to achieve the desired functionality in this IED application.

### 3.2.2 Digital Mimic Filter

Depending on factors such as fault inception angle and X/R ratio of the network, current and voltage waveforms following a fault may contain decaying DC offsets. These DC offsets cause the phasor estimations (obtained using DFT) to be erroneous by inducing small oscillations on them. To eradicate this problem, a high pass filter is often used in modern digital relays and it is referred to as the “mimic filter”.

It can be proven from basic circuit theory that if an AC signal with an exponentially decaying DC component is passing through a filter with the transfer function,

$$H(s) = K(1 + s\tau) \quad \text{-----}(3)$$

Where,  $\tau$  is equal to the time constant of the decaying DC component, the output waveform exhibits no DC component. The discrete version of the above transfer function can be written as [30],

$$H(z) = K(1 + \tau) - K\tau z^{-1} \quad \text{-----}(4)$$

Applying the mimic filter to a discrete sinusoidal signal  $x(k)$  given by,

$$x(k) = A_1 e^{-\frac{k\Delta t}{\tau}} + A_1 \sin \left[ \left( \frac{2\pi \cdot \Delta t \cdot k}{W} \right) + \phi \right] \quad \text{-----}(5)$$

Where,  $W$  is the number of samples per cycle and  $\Delta t$  is the sampling interval.

Applying the mimic filter to  $x(k)$  would yield,

$$y(k) = K[(1 + \tau_d) \cdot x(k) - \tau_d \cdot x(k - 1)] \quad \text{-----}(6)$$

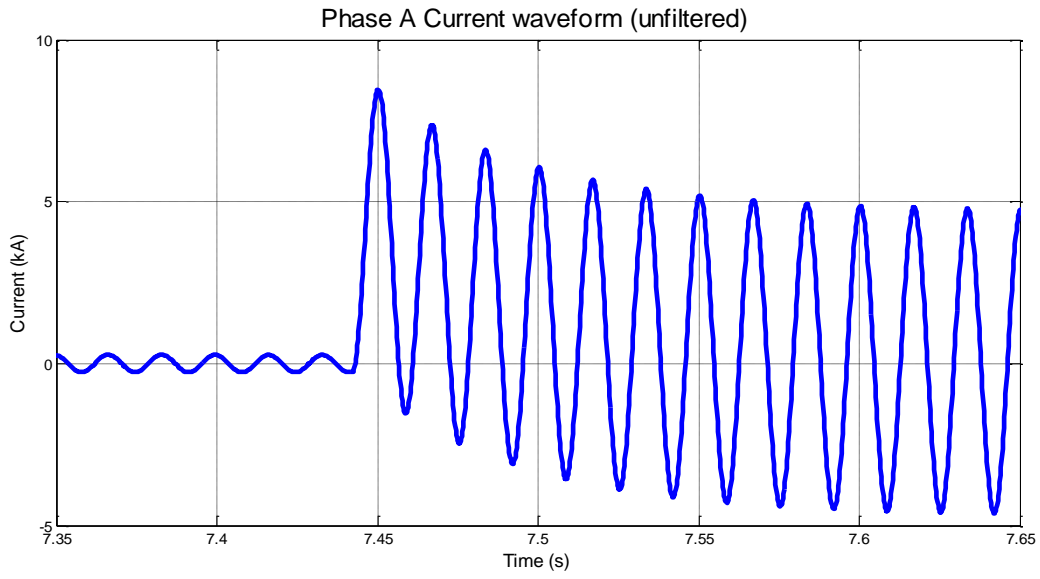
In (6),  $\tau$  is expressed as a number of samples ( $\tau_d$ ). It can be proven that for the fundamental component, the gain  $K$  is given by [30],

$$K = \frac{1}{\sqrt{\left( (1 + \tau_d) - \tau_d \cdot \cos\left(\frac{2\pi}{W}\right) \right)^2 + \left( \tau_d \cdot \cos\left(\frac{2\pi}{W}\right) \right)^2}} \quad \text{-----}(7)$$

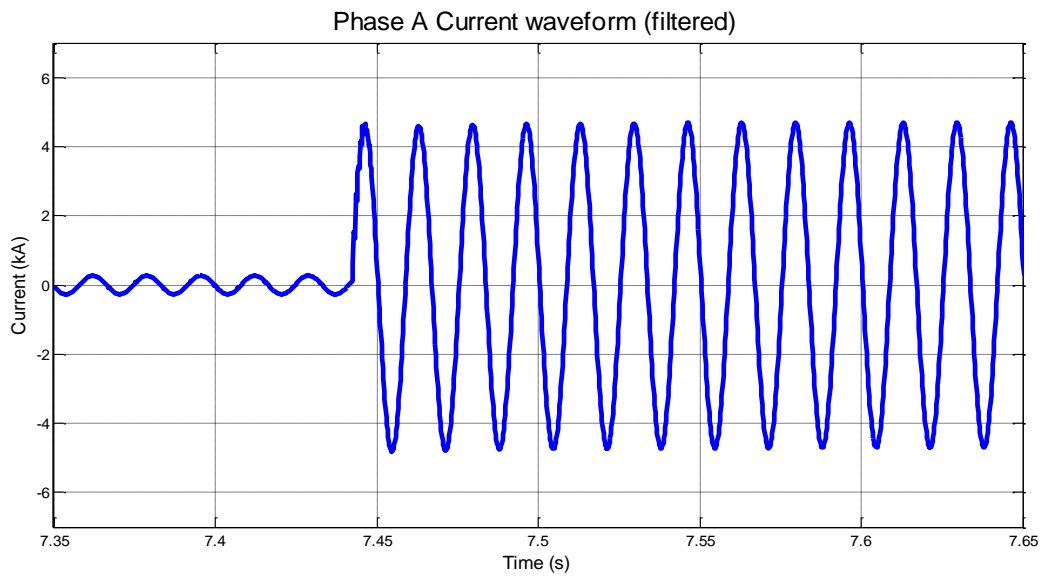
Further, this mimic filter introduces a phase shift to the AC signal which can be expressed as,

$$\psi = \tan^{-1} \left[ \frac{\tau_d \cdot \cos\left(\frac{2\pi}{W}\right)}{(1 + \tau_d) - \tau_d \cdot \cos\left(\frac{2\pi}{W}\right)} \right] \quad \text{-----}(8)$$

Implementation of the mimic filter for the IED is carried out using the above design. There, the number of samples per cycle,  $W$ , is 80 and  $\tau_d$  is a setting dependent on the power system X/R ratio. For this work, this user settable parameter is set at 640 samples (8 cycles). On the other hand, it is also important to know that this filter introduces a delay of 1 sample (equivalent to a time delay of 0.20833 ms at 80 samples per cycle) to the phasor estimation process. An example of a current waveform with a dc offset before and after the mimic filter is given in Figure 14. These sample results obtained with  $\tau_d = 640$  samples (8 cycles) shows the effectiveness of the mimic filter.



(a)



(b)

Figure 14: (a) Unfiltered current waveform, (b) Filtered current waveform

### 3.2.3 Phasor Extraction using Discrete Fourier Transform

A number of algorithms can be used for phasor estimation in power systems. Commonly used algorithm classes are Discrete Fourier Transform (DFT) based methods, optimization based methods such as Least Square Estimation, wavelet based methods and dynamic phasor based methods [31]. DFT based algorithms are simple and widely employed in modern digital relaying for phasor estimations, and hence, used in this work to extract the phasors from sampled data.

From the relationship between the Discrete Fourier Transform and the Fourier series, the fundamental frequency component extracted from N number of samples of the given waveform,  $x(t)$ , can be written as,

$$X_1 = \frac{\sqrt{2}}{N} \sum_{n=0}^{N-1} x(n, \Delta t) \cdot \cos\left(\frac{2\pi n}{N}\right) - j \cdot \frac{\sqrt{2}}{N} \sum_{n=0}^{N-1} x(n, \Delta t) \cdot \sin\left(\frac{2\pi n}{N}\right) \quad \text{-----}(9)$$

Where,  $\Delta t$  is the sampling interval. In power system protection, current and voltage waveforms having a nominal frequency of  $f_0$ , are assumed to have the general format,

$$x(t) = X_m \cos(2\pi f_0 t + \phi) \quad \text{-----}(10)$$

When the signal is sampled at W samples per cycle (a sampling frequency of  $W \cdot f_0$ ), and  $\phi$  is the phase angle between the first sampling point and the peak of the signal, it can be written as,

$$x(n) = X_m \cos(n\theta + \phi) \quad \text{-----}(11)$$

$$X_{1\text{Re}} = \frac{\sqrt{2}}{N} \sum_{n=0}^{N-1} x(n) \cdot \cos(n\theta) \quad \text{and} \quad X_{1\text{Im}} = \frac{\sqrt{2}}{N} \sum_{n=0}^{N-1} x(n) \cdot \sin(n\theta) \quad \text{-----}(12)$$

Where,  $\theta=2\pi/W$  is the phase angle corresponding to the sampling interval.

Then the fundamental phasor (denoted by subscript <sub>1</sub>) is given by,

$$X_1^{N-1} = X_{1\text{Re}} - j \cdot X_{1\text{Im}} \quad \text{-----}(13)$$

When using the recursive algorithm to extract the phasor, the general form of the real and imaginary parts of the fundamental phasor can written as, (where (N+r) is the last sample of the window)

$$X_{1\text{Re}}^{N+r} = X_{1\text{Re}}^{N+r-1} + \frac{\sqrt{2}}{N} (x_{N+r} - x_r) \cdot \cos(r\theta) \quad \text{-----}(14)$$

$$X_{1\text{Im}}^{N+r} = X_{1\text{Im}}^{N+r-1} + \frac{\sqrt{2}}{N} (x_{N+r} - x_r) \cdot \sin(r\theta) \quad \text{-----}(15)$$

This can be expressed in the following format as well.

$$X_{1\text{Re}}(K) = \frac{\sqrt{2}}{W} \sum_{n=K-W}^{K-1} x(n) \cdot \cos(n\theta) \quad \text{-----}(16)$$

$$X_{1\text{Im}}(K) = \frac{\sqrt{2}}{W} \sum_{n=K-W}^{K-1} x(n) \cdot \sin(n\theta) \quad \text{-----}(17)$$

$$X_1(K) = X_{1\text{Re}}(K) - j \cdot X_{1\text{Im}}(K) \quad \text{-----}(18)$$

Where, W is the sampling window size and (K-1) is the last sample of the sampling window (with the first and the last sample numbers being 0 and (N-1) for N samples). This means K increases, starting from the sampling window size up to the number of samples, N.

The relevant parameters for phasor extraction using the DFT in the IED are given below.

$$f_0 = 60 \text{ Hz}, \quad W = 80 \text{ samples/cycle}, \quad W \cdot f_0 = 4800 \text{ Hz} \quad \text{-----(19)}$$

$$\Delta t, \text{ sampling interval} = \frac{1}{4800} = 0.00020833 \text{ s} \quad \text{-----(20)}$$

Here, the DFT is performed using a sliding data window of 80 data points, which is implemented by a dynamic data structure called “linked list”. An example phasor estimation performed in the IED is given in Figure 15 below. Note that the algorithm takes one sample window, in this case 80 samples, to settle down at the new value after a change. Plotted in the top most graph is the instantaneous values of a current, obtained from the SVs received by the IED.



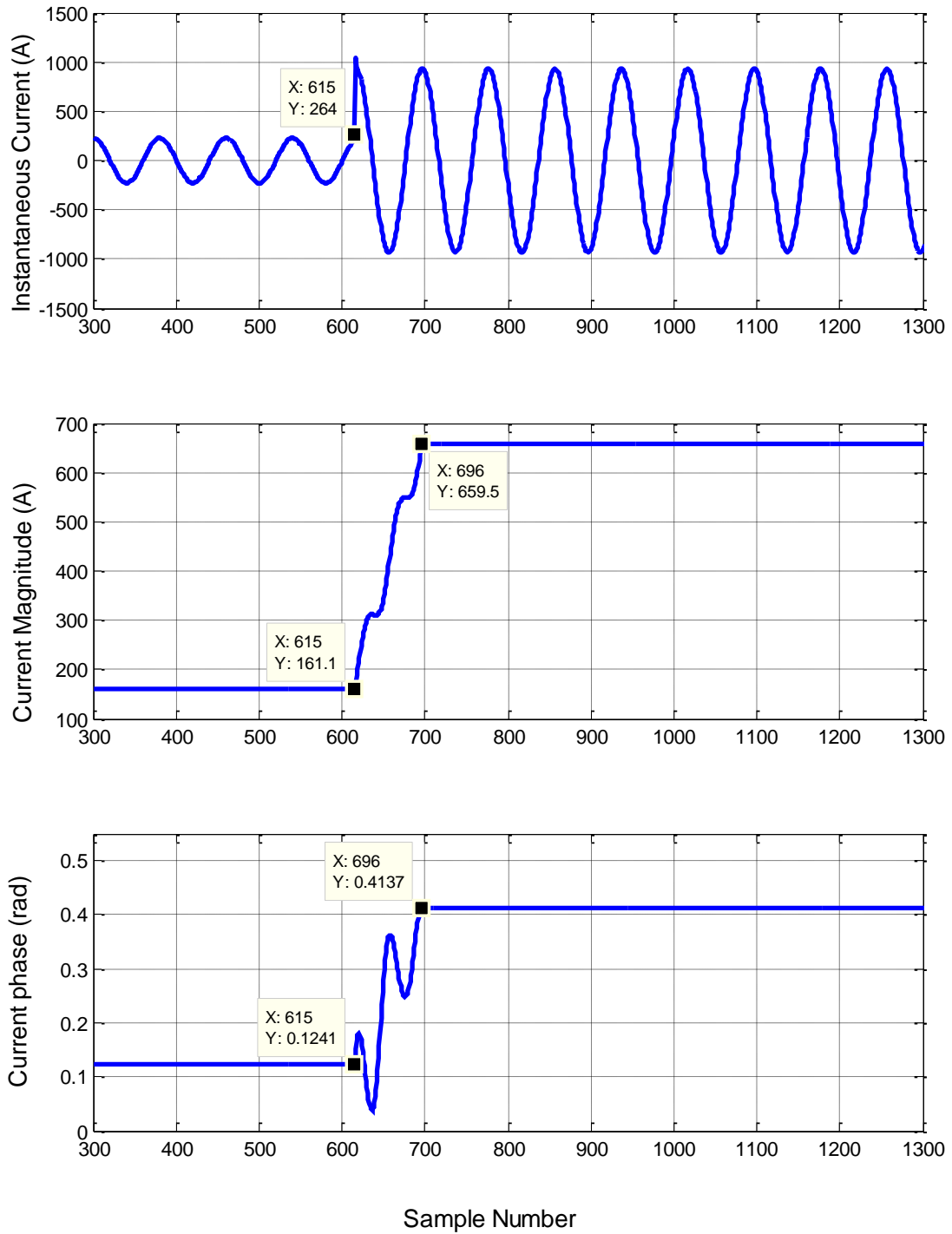


Figure 15: Magnitude and phase of the extracted current phasor plotted against the sample number

### 3.3 IEC 61850 Communication Configurations

Specific configurational procedures should be carried out before commencing communication according to IEC 61850 standard. A process called mapping is of particular importance, where entities such as published variables and data objects of the publisher are mapped to appropriate inputs of the subscriber. Moreover, network parameters such as MAC addresses and VLAN IDs should also be properly configured.

Since the communication in this work is bidirectional, data mapping should be carried out accordingly. That is, the data mapping should account for both the SV communication from the RTDS to the developed IED and the GOOSE communication from the developed IED to the RTDS. General procedures for publication and subscription of information in IEC 61850 are explained in the upcoming sub-sections in order to provide a comprehensive picture of the information exchange occurring in this work.

#### 3.3.1 Publication and Subscription of Information in IEC 61850

The publication and subscription of information in IEC 61850 are accomplished by following rigorous procedures. According to IEC 61850, all engineering design and data flow configuration in a project should be carried out in the system configuration tool, employing a unified approach [32]. However, the use of a system configuration tool for overall system

configurations is not well established in existing commercial IEC 61850 implementations. The prevailing norm is to use the proprietary (vendor-specific) IED configuration tools to setup the IEDs. Typically followed steps for setting up an IED for IEC 61850 based communication are explained below (which is also the method employed in this research as well).

### *3.3.1.1 Publication Procedure*

Firstly, the entities required to be published are put together into a group, which is called as a “dataset”. These entities are often Functionally Constrained Data Attributes (FCDA), although other entities in IEC 61850 product hierarchy such as logical nodes and data objects can also be published. Any number of datasets can be created as the requirements of the project demand. Then a control block is created including a particular dataset, and this control block contains additional information such as MAC address, application ID, VLAN (virtual local area network) ID and VLAN priority. A particular message published according to IEC 61850 is governed by its control block. This procedure of publication is common for both GOOSE and SV, even though their message initiation is different from each other. i.e., a new GOOSE message is initiated by a GOOSE control block once it detects a change in any of its dataset variables, whereas a SV control block publishes a new SV packet with all of its dataset variables, periodically.

Above mentioned configuration steps are carried out in the ICD file of the publisher's IED configuration tool. That file is then saved as a CID file and loaded to the respective publisher IED. This same file is also exported into the subscriber's IED tool for subscription configurations.

### *3.3.1.2 Subscription Procedure*

In contrast to the publication process, the method of subscription of messages in IEC 61850 is not entirely consistent. The method of subscription defined in IEC 61850 is using the Input/ExtRef element, which enables the binding of the external signals to an internal address of the IED. The nature of existing IEC 61850 implementations by almost all IED vendors is such that data mapping can only be performed with the subscriber's own IED configuration tool.

In the usual procedure, the CID files of all the publisher IEDs are imported into the subscriber's IED configuration tool, and required publisher variables are mapped into the internal variables of the subscriber IED. All these configuration information is contained in the subscriber's CID file, which is saved and, subsequently loaded into the corresponding IED. Moreover, the syntax for signal mapping in subscription is not defined in IEC 61850. As a result, syntaxes used vary from vendor to vendor and these are found enclosed inside private (<private>) sections in the subscriber's CID files.

### 3.3.2 Network Interface Card of the RTDS

Network Interface Card (NIC) of the RTDS, which is named “GTNET” card, supports five communication protocols in total, four of which can be kept installed through firmware. Moreover, only one chosen protocol of those four is functional at a given point of time. The functionality of the GTNET card has two aspects to it. Firstly, it can accept packets from a LAN, then, extract the information inside those packets and send it to the processor card (called PB5 card) of the RTDS to be used in the simulation. Secondly, it can get the values from the simulation, encode them into packets and send them out to be subscribed by other devices [28]. The list of supported protocols by the GTNET card are given below,

- GSE: IEC 61850 GOOSE/GSSE
- SV: IEC 61850-9-2 (Sampled Values)
- DNP3: Distributed Network Protocol
- PLAYBACK: Playback of large data sets
- PMU: IEEE C37.118 datastream output

The RTDS simulator used for this work has two GTNET cards, with GOOSE and SV as active protocols. A GTNET card has its own MAC address and IP address. In addition to the GTNET and the PB5 cards, few of the other card types in the simulator RTDS are also of significance to this study. One

such card is GTSYNC or synchronization card. Its purpose is to make sure that the RTDS simulation is in synchronism with an external, high precision time reference, which could be one of IEEE 1588 PTP (Precision Time Protocol), 1 PPS, or IRIG-B signals. For this research, the GTSYNC is provided with an IRIG-B signal, taken from a clock that is synchronized to a GPS signal. Clock used here is a SEL-2407, Satellite Synchronized Clock.

All Physical connections in the setup are shown in Figure 16. Connections among different cards inside the RTDS are shown in dashed lines.

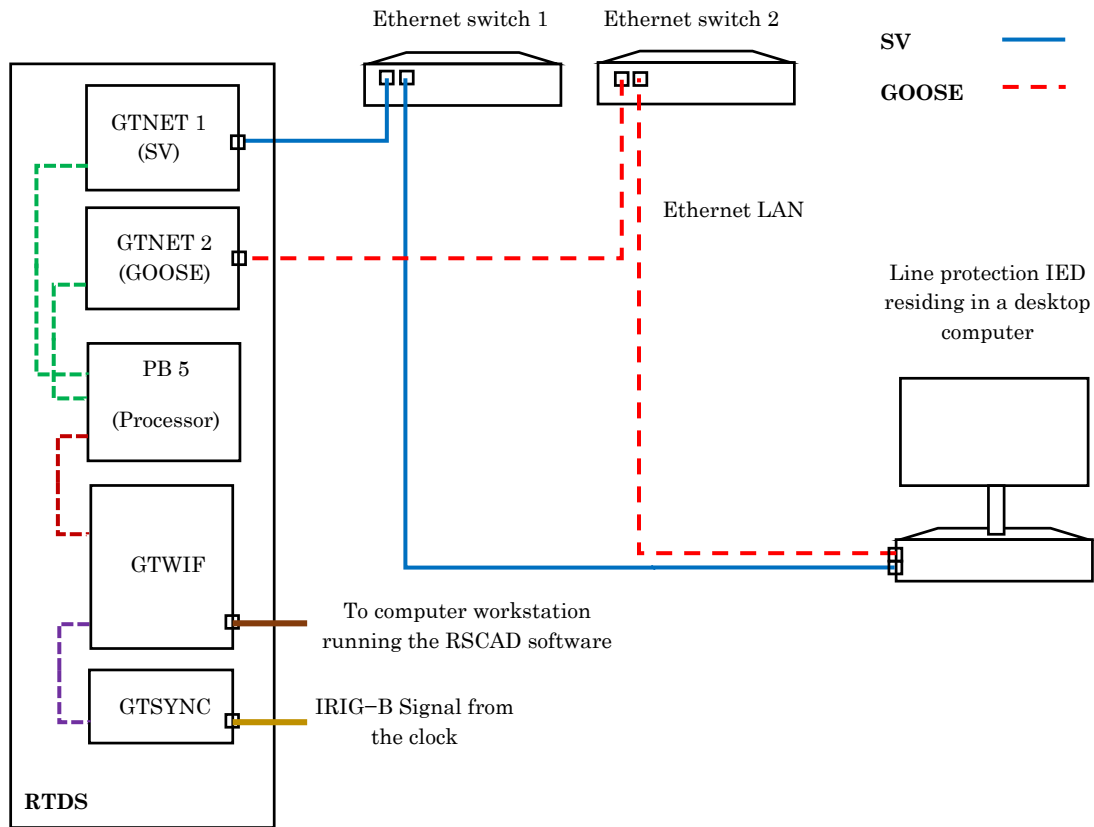


Figure 16: Physical connections in the LAN

GTWIF or the Workstation Interface Card of the RTDS manages all other cards in the simulator. It communicates with RSCAD, which is the software interface of the RTDS, in order to start/stop simulations and to exchange information regarding plotting, user initiated events etc. [28]. The connections of the Ethernet LAN, carrying GOOSE and SV between the RTDS and the developed line protection IED are also shown.

### 3.3.3 SV Publication from the RTDS

SVs in the RTDS are handled by the sampled value component in the RTDS simulation, as shown in Figure 17. It can be configured to either publish or receive SV and it supports both 9-2 LE and non-LE protocols. Here, non-LE refers to a protocol developed based on IEC 61869–9 and the Chinese national standard for SV merging units. In this work, the Sampled Value component is used only for SV publication, under 9-2 LE configuration, with a sampling rate of 80 samples per cycle (while 256 samples per cycle rate can also be used).

As depicted in Figure 17, the secondary three phase current and voltage signals of the two instrument transformers (IA, IB, IC and VA, VB, VC) are fed to a series of anti-aliasing low pass filters. A series of 6<sup>th</sup> order low-pass Butterworth filters is used for anti-aliasing. The cut-off frequency of these filters is set at 2.4 kHz, which is 50% of the sampling frequency of 9-2 LE (with the system frequency at 60 Hz, 80 samples per cycle is equivalent to 4.8 kHz). The filtered signals are then taken by the sampled value component to be

published as SVs through GTNET hardware. Furthermore, the combination of the anti-aliasing filters and the sampled values component can be considered as a virtual merging unit as per IEC 61850-9-2 LE. This margining unit is indicated in Figure 12 in above Section 3.1. Also notice that neutral current and voltage are calculated using the phase values.

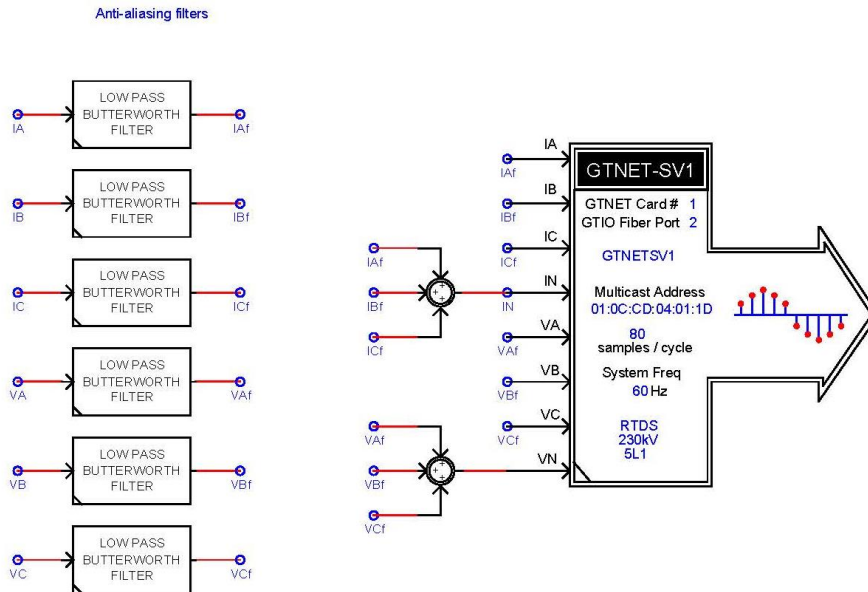


Figure 17: Anti-aliasing filters (left) and the sampled values component (right), residing in the RTDS simulation case

RTDS creates its own CID (the RTDS uses the extension .icd for CID file type as well, however to avoid confusion, it is referred to as the RTDS CID file) file for IEC 61850 communication configurations. This CID file contains a dataset, including eight FCDA. I.e. four FCDA from current transformer (CT) logical nodes (ex: TCTR1.MX.Amp.instMag.i) and four FCDA from voltage transformer (VT) logical nodes (ex: TVTR1.MX.Amp.instMag.i). As



explained in 3.3.1.1, this CID file has a SV control block to manage the publication of the said dataset. The CID file for SV publication of the RTDS is provided in Appendix A-II.

### 3.3.4 SV Subscription by the Line Protection IED

The ICD file for a given IED is provided by the manufacturer. For the line protection IED developed in this research, an ICD file is created manually, starting from scratch, using a commercial IEC 61850 SCL file editing software tool (Kalkitech™ SCLManager) with all the required logical node instances and data type definitions. Since there is no IED configuration tool for the laboratory developed IED, this ICD file is manually configured to create the CID file of the line protection IED. SV subscription in the IED is achieved by means of virtual current and voltage transformer LN instances. Here, the word “virtual” is used to describe the LN instances because they do not represent any physical (existing) elements in the substation (unlike the ones in the RTDS publisher CID file, which represent the actual current and voltage transformer of the substation). Notwithstanding, the advantage of this method is that subscription of SVs is only done at a single place of the IED and the local implementations of LN functions can access the subscribed data internally, without having to subscribe SVs individually to them. The current and the voltage transformer LN instances in the CID file of the IED are exact replicas

of their counterparts in RTDS CID file, thus, the signal mapping is one to one.

This is illustrated in Figure 18 below.

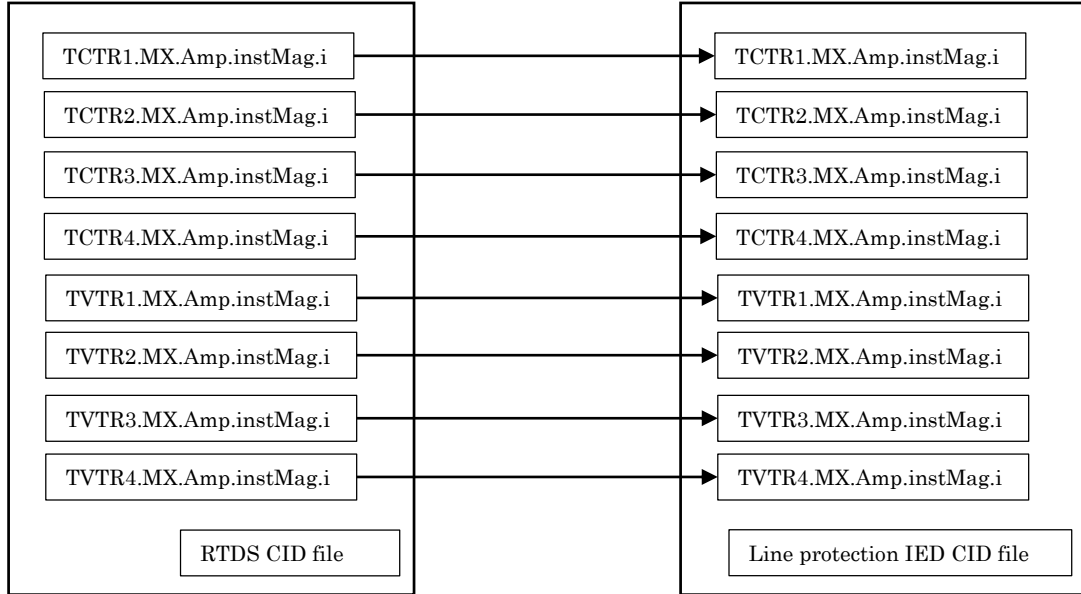


Figure 18: Signal mapping for SV subscription

### 3.3.5 GOOSE Publication from the Line Protection IED

Upon detection of a fault, the developed protection IED sends a GOOSE message to the circuit breaker simulated in the RTDS. For issuing of trip signals in the distance protection scheme, instances of the LN class “PDIS” (Distance Protection logical node) are used. However, there is no standard LN class available for transient based protection scheme, since it is a user defined, proprietary protection scheme. Therefore, instances of the LN class GGIO (Generic Process Input/Output) are used for this purpose.

### 3.3.6 GOOSE Subscription by the RTDS

In a RTDS simulation case, there can be many devices (circuit breaker controllers, protection relays, etc.) those use the information in GOOSE messages sent by external IEDs. However, since communication is handled by the GTNET cards, configuration of all IEC 61850 communication services is achieved through a common CID file that treats RTDS as a single IED. Information inside any GOOSE message received by a GTNET card is decoded by the relevant GTNET-GSE block in the RTDS simulation case and then assigned to an internal variable, as specified in the parameter section of the GTNET-GSE block. This internal variable usually is an input or an internal variable in a device simulated in RTDS. For GOOSE messaging, the RTDS only supports the LN class GGIO. One GTNET-GSE block in the RTDS can accommodate up to 64 GOOSE input/outputs, although the number of inputs

used here are 1 or 2, depending on the protection scheme in use. GOOSE messages published by the line protection IED are subscribed by the GTNET hardware of the RTDS as explained, and this is illustrated in Figure 19.

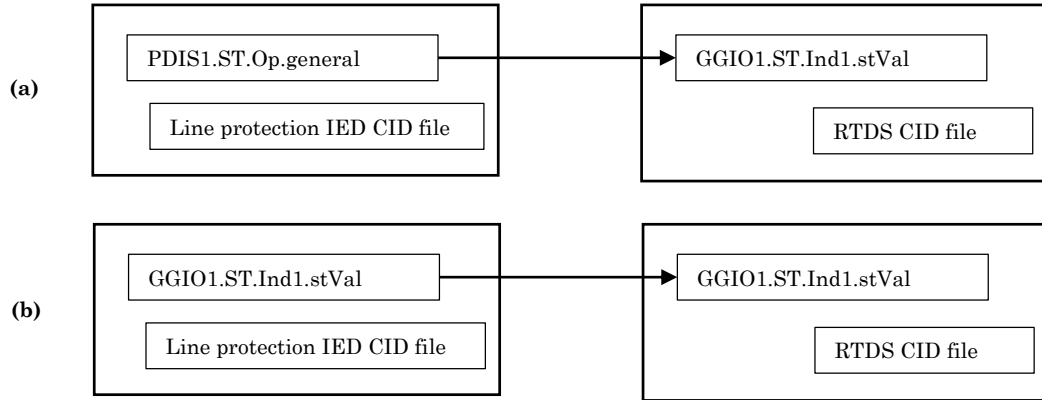


Figure 19: An example signal mappings for GOOSE subscription in; (a) Distance Protection scheme (b) Transients based protection scheme

Given in Figure 19 are two examples of signal mappings for GOOSE subscription for the two protection schemes. Note that the all published variables are binary values. Furthermore, for the distance protection scheme, the GTNET hardware and the GTNET-GSE component in the RTDS, forms what is referred to as a “breaker IED” (BIED) in the virtual environment of the simulation case. A BIED is the smart section of a circuit breaker (recognized as an IED in the perspective of IEC 61850) that controls its operation in a substation according to the control signals provided by the protection schemes or an operator. These devices reside in the process level and, are connected to the circuit breakers using hardwires internally.

Figure 20 illustrates the implementation of a breaker IED in the RTDS simulation. The decoded binary value of the subscribed GOOSE message (the trip signal) is assigned to the variable BRK, the value of which determines position of the circuit breaker (opened or closed).

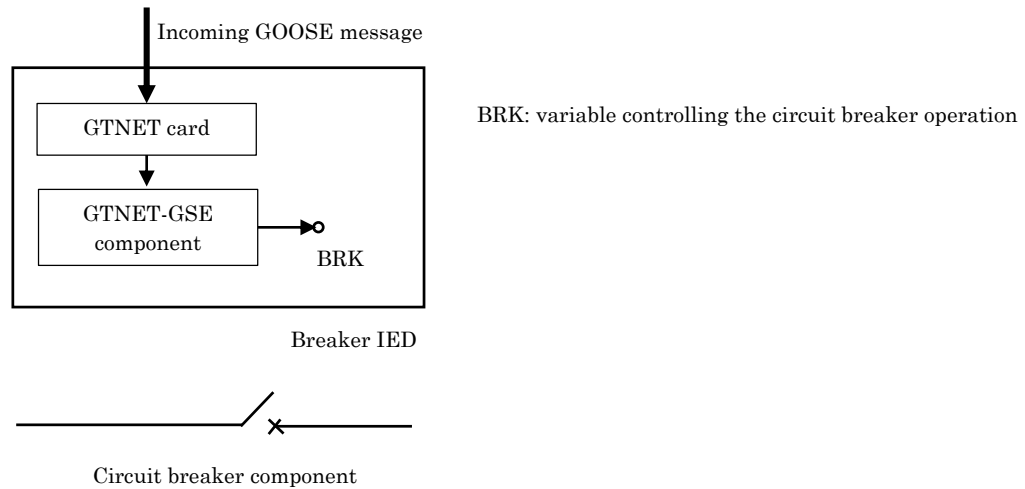


Figure 20: Illustration of the implementation of a breaker IED in the RTDS simulation

### 3.4 Time Delays in the Setup

The time taken from the implemented line protection IED to respond to a fault simulated in the RTDS is very large compared to the response time of actual relays. This time delay is measured as a round trip time (time take from the moment a fault is applied in the RTDS simulation to the arrival of the GOOSE trip from the relay), which is observed to be varying in rather a wide range from 10 ms to 2 s. This round trip time includes the processing times in the RTDS, communication network delays and the processing time in the implemented line protection IED.

It is found out that a major portion of this round trip time (approximately 95% of it) is caused between the arrival of SV packets at the IED (network card of the desktop computer) and passing of the decoded sampled values to signal processing modules. Closer examination showed that there is no SV packet loss, but just a random delay that is not accumulating. Although the exact reason behind this problem is not identified, it is assumed that the delays in the network interface card of the desktop computer and the non-real-time nature of its operating system are major contributing factors to the delays. However, irrespective of the delay, IED responds correctly to every fault. Due to this time delay, the time performance of the implemented line protection IED is not evaluated.

### 3.5 Chapter Summary

Chapter 3 rigorously explained the basic implementation of the line protection IED application. Its internal algorithms for filtering and phasor calculations were provided with necessary equations and algorithms. Some results were also provided for validation of the filtering and the phasor calculation. Moreover, all IEC 61850 communication related information, including publishing and subscribing procedures at both ends, were described in detail.

# Chapter 4

## Distance Protection Scheme

Distance protection scheme developed in the line protection IED has both Mho and quadrilateral characteristics at its disposal. The protection scheme is tested and verified on the power system simulated in the RTDS. Implementation details are described in the next few sections.

### 4.1 Distance Estimation Units

A distance protection relay has two types of distance estimation units; namely, phase units and ground units. Usually a distance protection scheme requires six units (three each from the two types), for it to identify all types of faults involving all three phases. The phase units identify three-phase (3- $\Phi$ ) faults and line to line (L-L) faults, whereas the ground units identify line to ground (L-G), line to line to ground (L-L-G) and three-phase to ground (3- $\Phi$ -G) faults. Moreover, independent voltage and current inputs are provided for each of these six units. Well-known equations for impedance estimations from

calculated voltage and current phasors, in a phase unit (AB) and a ground unit (AG) are given below.

$$Z_{AB} = \frac{V_{AB}}{I_A - I_B} = \frac{V_A - V_B}{I_A - I_B} \quad \text{-----(21)}$$

$$Z_{AG} = \frac{V_A}{I_A + 3K_0I_0} \quad ; \text{ where } K_0 = \frac{Z_0 - Z_1}{3Z_1} \quad \text{-----(22)}$$

Here,  $Z_{AB}$  and  $Z_A$  are impedances seen by the phase unit and the ground unit, respectively.  $V_{AB}$  is the line to line voltage between phases A and B, while  $V_A$  and  $V_B$  are corresponding line to neutral voltages. Similarly,  $I_A$  and  $I_B$  are line currents of the two phases, whereas  $I_0$  is the zero sequence current.  $Z_1$  and  $Z_0$  are, respectively, the positive and the zero sequence impedances of the protected line.  $K_0$  is referred to as the zero sequence compensation factor. This  $K_0$  is introduced in such a way that the impedances seen by the ground units also are the positive sequence impedance of the line (as is the case with the phase units).

In the implementation of the laboratory line protection IED (in computer application code), two functions are developed to calculate above phase unit and ground unit impedances, by taking the extracted phasors as arguments. For instance, calling of the phase unit function with arguments  $V_A$ ,  $V_B$ ,  $I_A$  and  $I_B$  would yield,  $Z_{AB}$ ; the impedance seen by the phase unit AB. Likewise, the two functions are called three times each, in order to determine all six impedance estimations. These impedance estimations are then passed as arguments to another function implementing the impedance characteristics.



## 4.2 Impedance Characteristics

### 4.2.1 Mho Characteristic

The impedance setting of the zone-1 shown in Figure 21 is at 80% of the positive sequence impedance of the protected transmission line, denoted as  $Z_1$  ( $Z_1 \angle \Phi$ ). The angle  $\Phi$  is the impedance angle of the line.

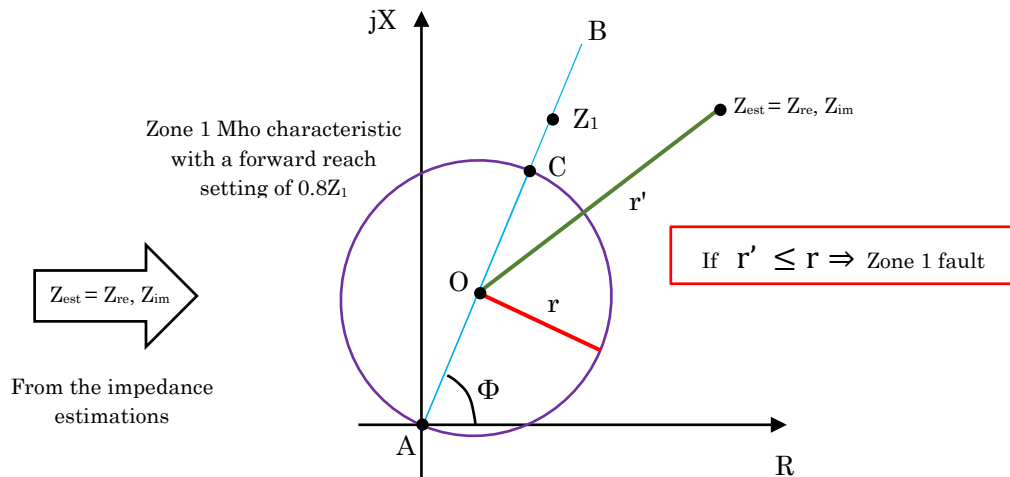


Figure 21: Implementation of zone 1 Mho characteristic

Notice that impedance line, AB, passes through the centre of the Mho circle on the R-X plane. Furthermore, the origin and the radius of the Mho circle are denoted as O and r, respectively. The x and y coordinates of the origin, O and the magnitude of the radius, r are expressed in terms of  $Z_1$  and  $\Phi$  as follows,

$$O = \left( x: \frac{0.8Z_1}{2} \cos(\Phi), y: \frac{0.8Z_1}{2} \sin(\Phi) \right) \quad \text{-----}(23)$$

$$r = \frac{0.8Z_1}{2} \quad \text{-----}(24)$$

The distance from O to the point representing the estimated impedance  $Z_{est}$  is given as  $r'$ , and it can be calculated in terms of  $x$ ,  $y$ ,  $Z_{re}$  and  $Z_{im}$  as,

$$r' = \sqrt{(x - Z_{re})^2 + (y - Z_{im})^2} \quad \text{-----}(25)$$

Where  $Z_{re}$  and  $Z_{im}$  are, respectively, the real and imaginary parts of the estimated impedance point,  $Z_{est}$ . It is clear that the estimated impedance point resides within the Mho characteristic circle, if (and only if) the radius of the circle is greater than the distance between its origin and the impedance point. The fulfilment of this condition, therefore, indicates that a zone 1 fault has been occurred. Required number of zones can be obtained by varying the radius of the Mho circle and extending a similar approach.

The forward reach (length AC in Figure 21) in secondary Ohms is the typical setting for zones 1 and 2 in a distance protection scheme using Mho characteristics. Zone 3 and beyond could incorporate a reverse reach as well. Further, the characteristic angle,  $\Phi$ , can also be a setting in some schemes.

### 4.2.2 Quadrilateral Characteristics

Zone 1 quadrilateral characteristic on R-X plane is depicted by the quadrilateral “abcd” in Figure 22.  $Z_{est}$ ,  $Z_1$  and  $\Phi$  have same meaning as in the previous sub-section.

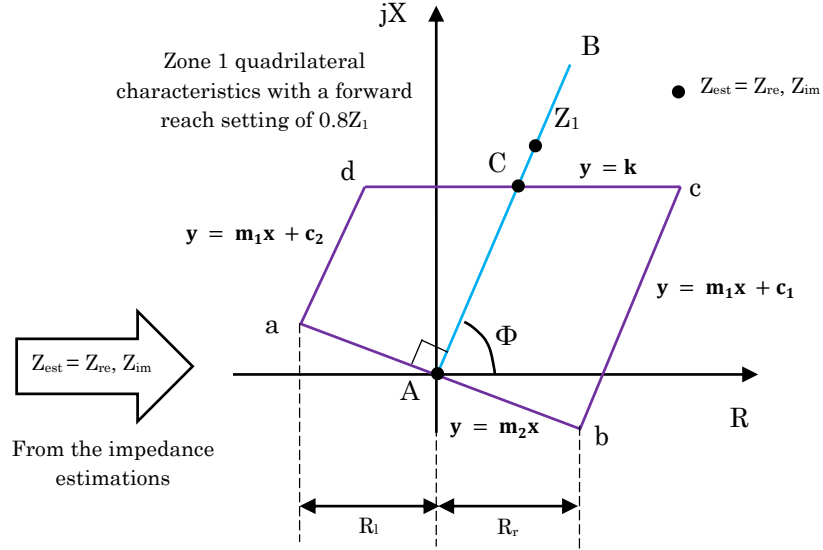


Figure 22: Implementation of zone 1 quadrilateral characteristic

Typically, a quadrilateral characteristic has three settings. They are forward reach (length AC), right reach ( $R_r$ ) and left reach ( $R_l$ ). Gradients and the intersections of the four straight lines that form the quadrilateral “abcd”, can be determined using the aforementioned setting as follows,

$$k = 0.8Z_1 \sin(\Phi)$$

$$m_1 = \tan(\Phi)$$

$$m_2 = \tan(\Phi + \pi/2) \quad \text{-----(26)}$$

$$c_1 = - \left[ R_r \tan(\Phi) + \frac{R_r}{\tan(\Phi)} \right]$$

$$c_2 = \left[ R_l \tan(\Phi) + \frac{R_l}{\tan(\Phi)} \right]$$

As before, the criterion for fault identification is to check whether the estimated impedance point lies inside the defined zone. This is occurring when the following four conditions are satisfied simultaneously.

$$Z_{im} > m_1 Z_{re} + C_1$$

$$Z_{im} < m_1 Z_{re} + C_2$$

$$Z_{im} < k$$

$$Z_{im} > m_2 Z_{re}$$

------(27)

And similar to Mho characteristics, the other zones can be implemented by simply increasing above mentioned the reach settings.

### 4.3 Fault Identification

Both types distance characteristics are implemented in a single function that takes estimated impedance as the input. Only one type of characteristic can be in use at a given time. This functions returns an indicator (with value 1) when it sees the estimated impedance point inside the predefined zone. Fault identification algorithm for the distance protection scheme is given in Figure 23.

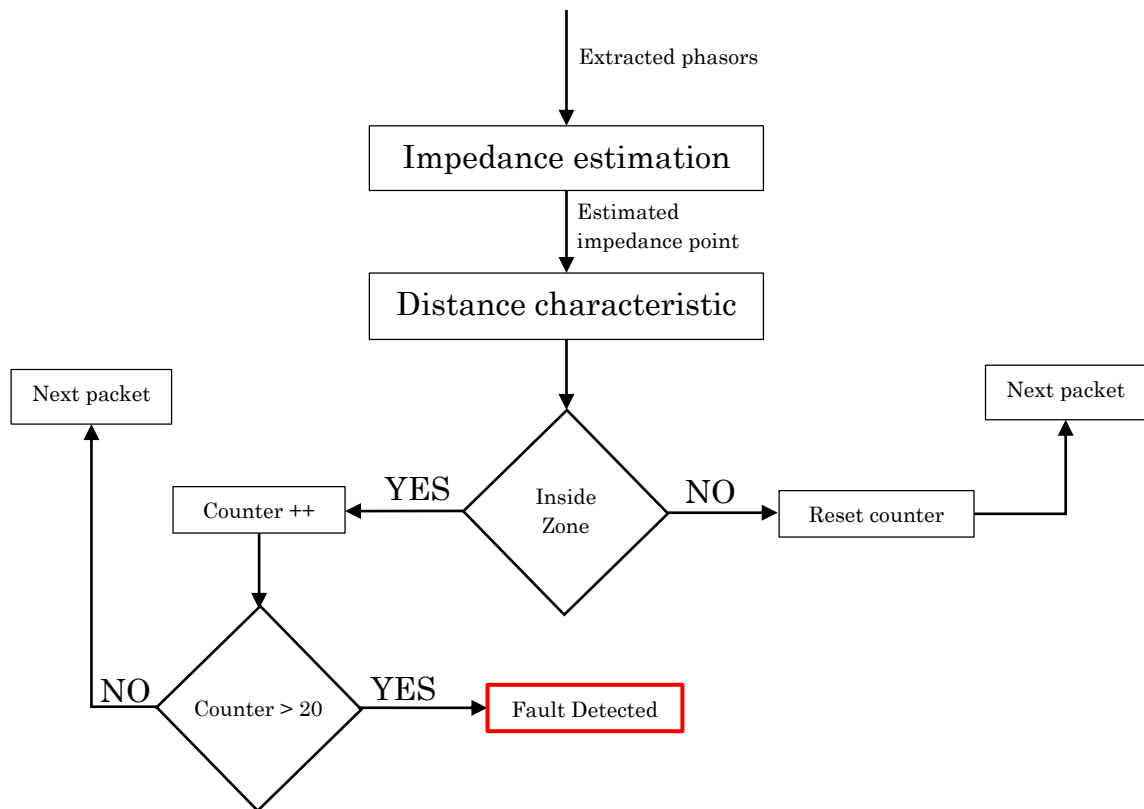


Figure 23: Fault Identification algorithm of the distance protection scheme

The IED is going through this process for each SV packet received. The algorithm demands that 20 consecutive impedance estimation points must be

within the zone for any disturbance to be identified as a fault. Here, 20 impedance estimation points corresponds to 20 samples, which is equivalent to a quarter of a cycle or 4.16 ms at 60 Hz. This is to ensure that the distance algorithm does not mal-operate for small disturbances in the system, thus providing robustness to the scheme. Further, this improves capability of the scheme to provide correct discrimination between zones for near-boundary faults as well (ex: 81% fault).

## 4.4 Validation of the Implemented Distance Protection Scheme

The single line diagram (SLD) of the simulated power system section, upon which the distance protection scheme is tested and validated is given below in Figure 24.

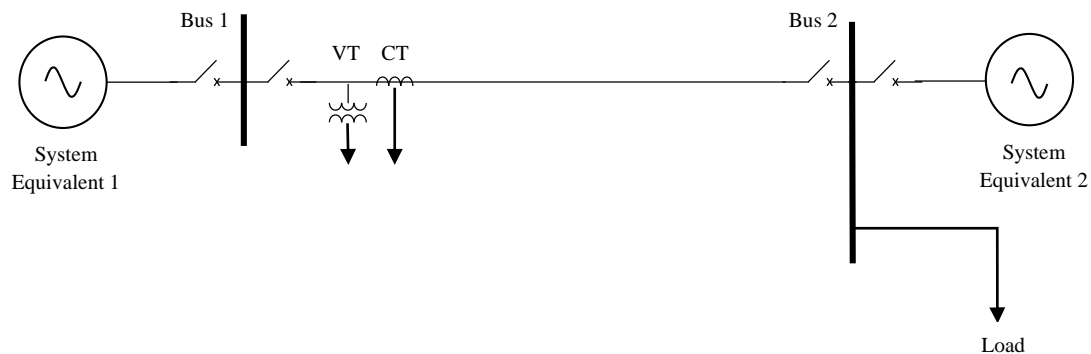


Figure 24: SLD of the simulated power system using which the implemented distance protection scheme is validated

The basic power system section simulated in RTDS is a 230 kV, 60 Hz, 200 km long overhead transmission line, connecting two AC networks. This system is used to test and validate the SV acquisition and basic calculations such as phasor extraction of the IED as well as the developed distance protection algorithm. Figure 12 in Section 3.1, which illustrates the apparatus used for testing the distance protection in detail, is repeated here in Figure 25 for the convenience of reference.

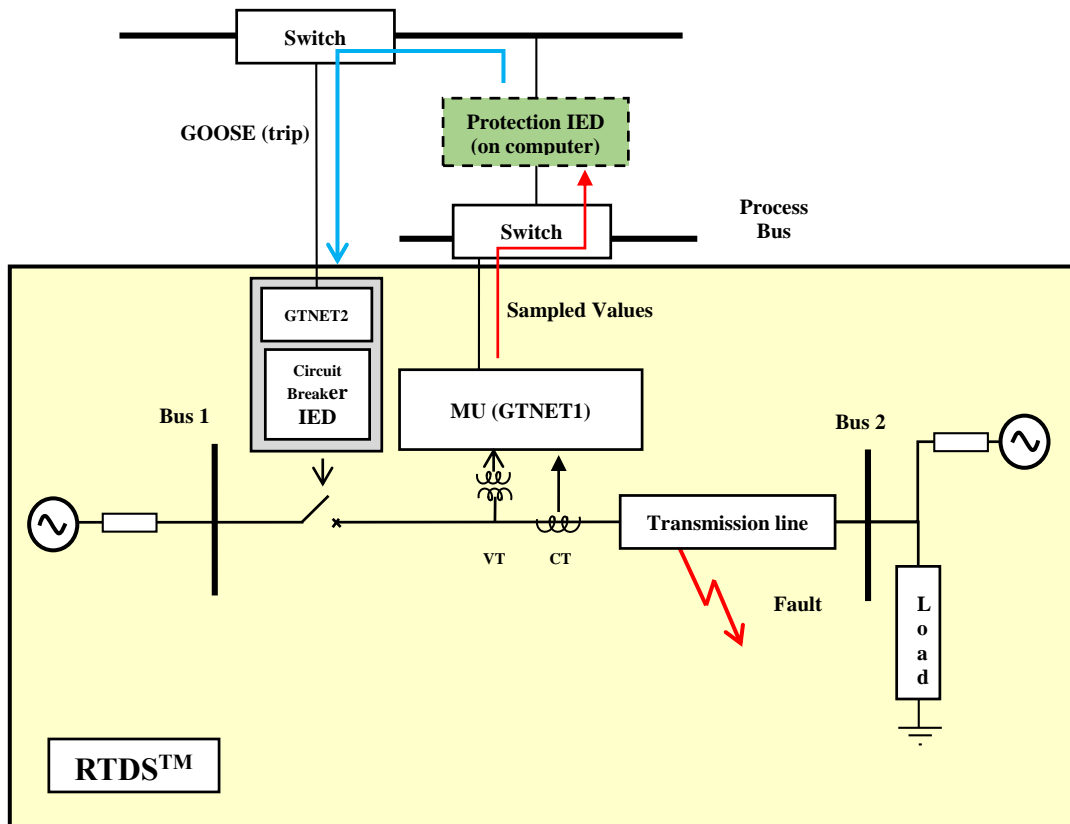


Figure 25: Schematic of the setup for testing the distance protection scheme

For this study, currents flowing out of the busbars are measured as positive and the simulation time-step used is 50  $\mu$ s. The transmission line is

modelled using a frequency dependent transmission line model (frequency dependent phase model) and the main parameters used are given in Appendix B. Current transformers (CT) and voltage transformers (VT) are modeled using standard library components in the RTDS. CT and VT ratios are 100 and 2000, respectively. A dynamic load is connected at bus 2 and its active and reactive power consumptions can be set as needed. The AC networks are modeled as Thevenin's equivalents with two 230 kV, 60 Hz sources. Impedances of the network equivalents 1 and 2 are  $176\angle 82^\circ \Omega$  and  $200\angle 82^\circ \Omega$ , respectively.

## 4.5 Results Comparison for Impedance Estimations

Table 1 presents impedance estimation results, comparing the impedance estimations taken from the IEC 61850 process bus compatible line protection IED developed in the laboratory with the values estimated by a commercial IED which takes current and voltage signals through the analog outputs of the RTDS. These are also compared with impedance calculations carried out in the RTDS, following similar steps as in the developed line protection IED. The commercial IED used here is a line protection relay; L-PRO 4000 manufactured by ERLphase Power Technologies Ltd. Moreover, the positive and zero sequence impedances of the protected transmission line are  $83.34\angle 86.43 \Omega$  and  $224.86\angle 72.30 \Omega$ , respectively.



Table 1: Comparison of phase unit impedance calculations

Applied Faults		Primary Impedance seen by the phase unit AB					
		Laboratory IED		L-PRO 4000		RTDS	
Fault type	Location	Magnitude ( $\Omega$ )	Angle ( $^{\circ}$ )	Magnitude ( $\Omega$ )	Angle ( $^{\circ}$ )	Magnitude ( $\Omega$ )	Angle ( $^{\circ}$ )
ABC	5%	4.67	79.57	4.60	88.00	4.74	80.86
	50%	42.46	84.16	42.30	86.00	42.55	85.75
	90%	77.36	85.06	76.40	86.00	77.44	86.28
AB	5%	4.75	79.91	4.50	84.00	4.70	80.82
	50%	42.63	84.75	41.50	86.00	42.75	85.91
	90%	77.20	85.59	76.30	86.00	77.65	86.27

The results presented in Table 1 and Table 2 show that the impedance estimations carried out in the laboratory developed IED matches with those taken from other sources to a large extent. Slight differences in the impedances estimated by the commercial relay may be due to the differences in the inputs: it takes voltages and currents through the analog outputs of RTDS simulator, where some small deviation could be introduced based on the scaling factors used in the digital to analog conversion block.

Table 2: Comparison of ground unit impedance calculations

Applied Faults		Primary Impedance seen by the ground unit AG					
		Laboratory IED		L-PRO 4000		RTDS	
Fault type	Location	Magnitude ( $\Omega$ )	Angle ( $^{\circ}$ )	Magnitude ( $\Omega$ )	Angle ( $^{\circ}$ )	Magnitude ( $\Omega$ )	Angle ( $^{\circ}$ )
A-G	5%	4.71	73.12	4.60	76.00	4.74	75.81
	50%	43.17	76.44	42.50	77.00	43.06	78.99
	90%	77.77	78.12	76.40	79.00	77.22	80.09
AB-G	5%	4.32	74.61	4.50	84.00	4.43	76.89
	50%	38.79	78.76	41.90	86.00	39.07	80.76
	90%	69.85	80.29	76.20	86.00	71.01	81.98
ABC-G	5%	4.69	80.57	4.60	88.00	4.75	81.29
	50%	42.16	85.81	41.60	87.00	42.78	86.20
	90%	77.99	85.00	76.80	86.00	77.52	86.31

## 4.6 Estimated Impedance Trajectories

Some details of the operation of the implemented distance scheme are examined to validate the correct operation. Figure 26 presents the convergence of estimated impedance into the Mho circle for a zone 1 fault. The estimated

impedance point travels from the pre-fault value into the zone and settles on the impedance line of the transmission line plotted in the R-X plane.

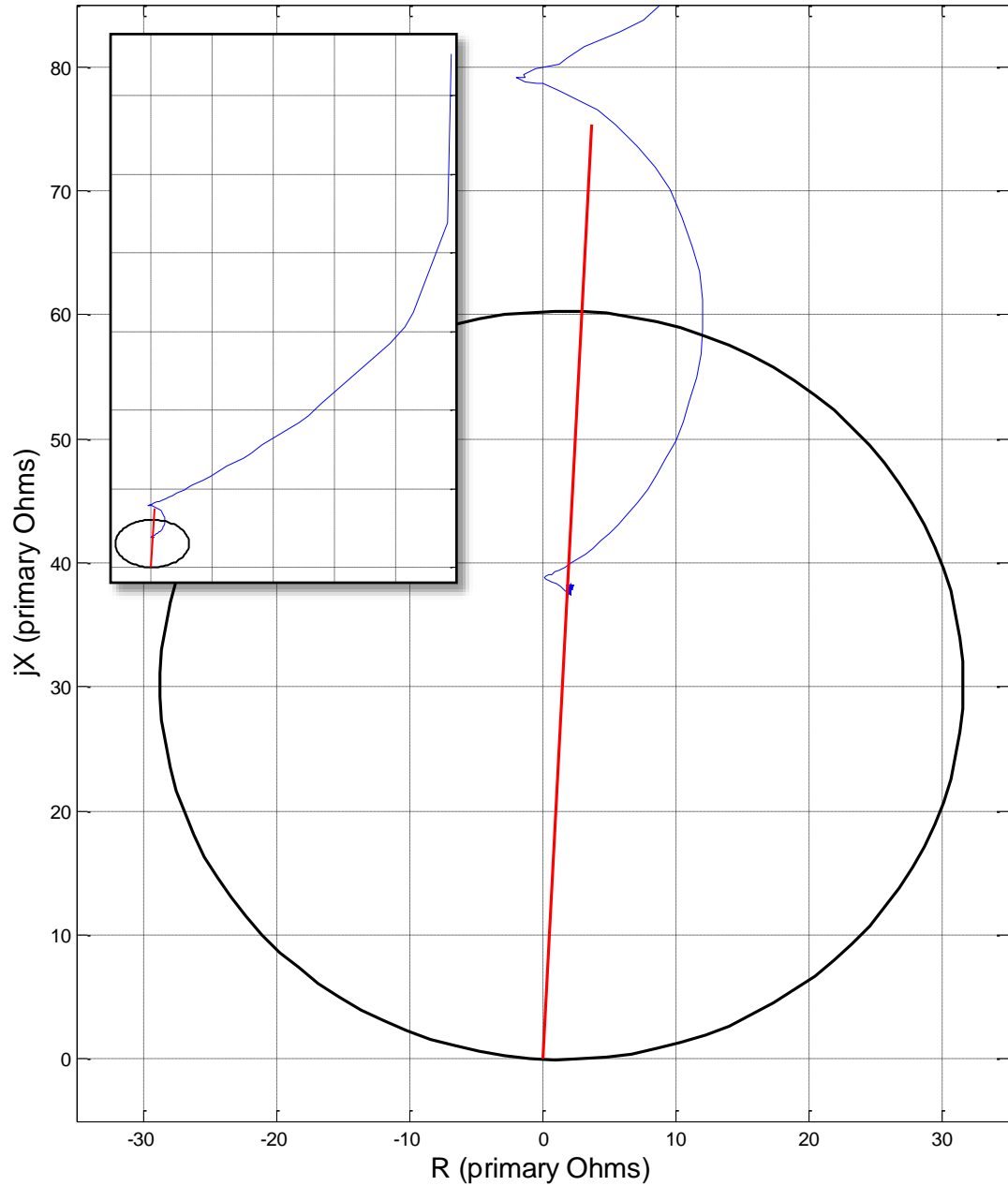


Figure 26: Trajectory of the estimated impedance of the line protection IED for a zone 1, AB fault, plotted on a R-X plane; Zone 1 Mho characteristics and impedance line are shown

## 4.7 Fault Detection Time

Time taken for the detection of a fault is illustrated in Figure 27. Here, Phase A current waveform, the estimated impedance scaled down by a factor of 10 and the initiation of the trip signal (indicated as a binary status value of the fault detection) is plotted.

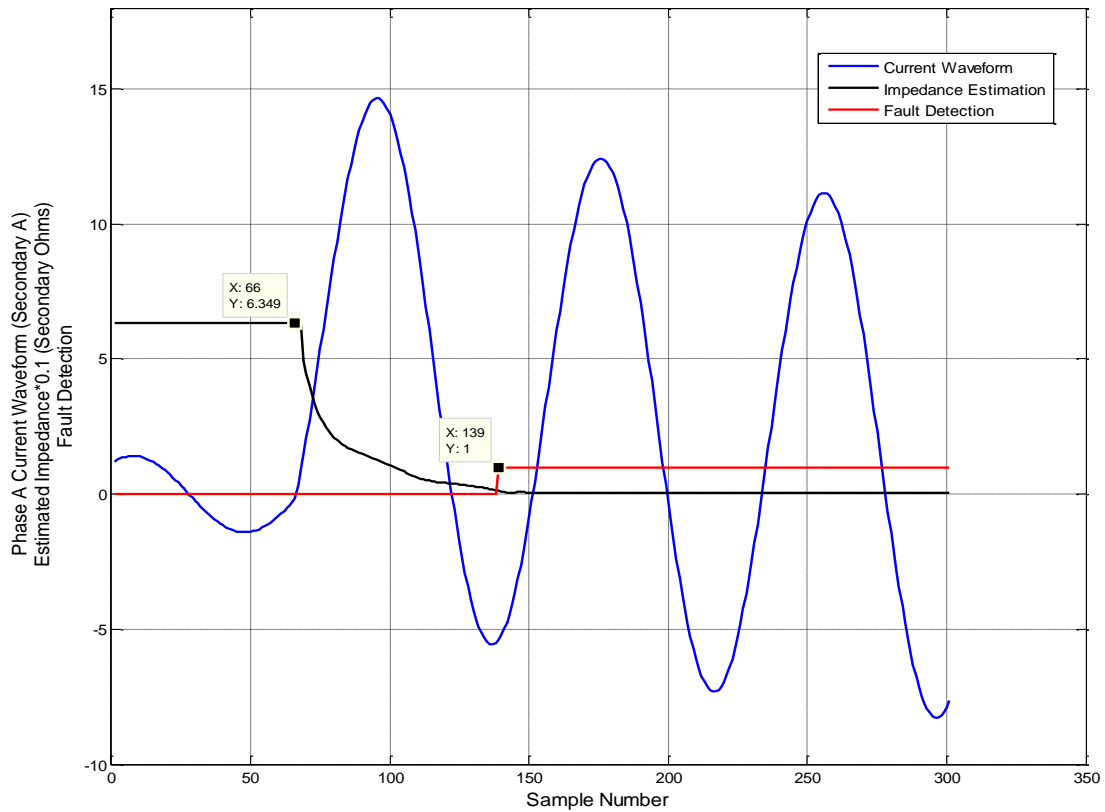


Figure 27: Fault detection in the distance protection scheme for a 10 % fault

Form Figure 27, it is observed that the time elapsed from the reception of the first SV packet after the fault to the fault detection is 73 samples, which is under one cycle. This is well within the typically acceptable tolerance for a distance protection algorithm. It is also observed that the time take by the

algorithm for fault detection is slightly increasing with the distance to the location of the fault. For a 90% fault, the number of samples taken by the algorithm for fault detection is 92 (as indicated in Figure 28), whereas that for a 10% fault is 73. This is a common characteristic of distance protection algorithms, a one even commercial distance relays exhibit.

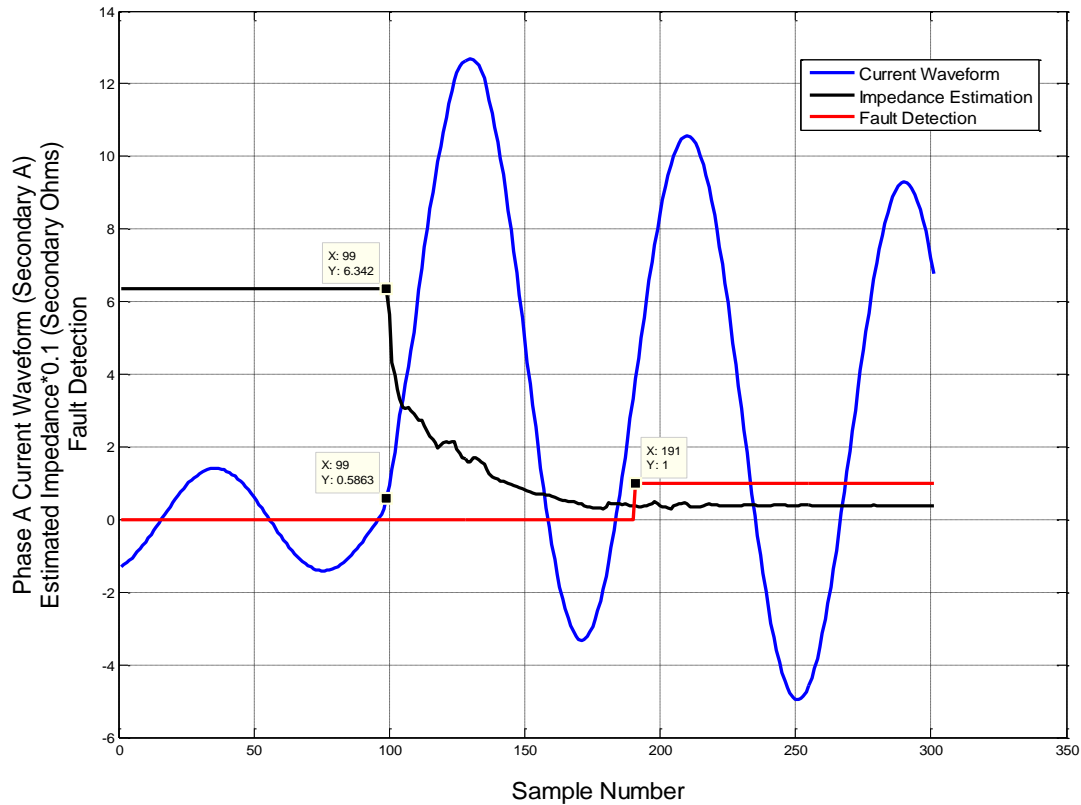


Figure 28: Fault detection in the distance protection scheme for a 90 % fault

Table 3 presents the time taken by the distance protection algorithm to detect various types of faults in terms of number of samples. The two instances that the algorithm fails to correctly identify the faults are high impedance faults, where the estimated fault impedances lie outside the protected zone settings of the relay.

Table 3: Fault detection time in terms of number of samples for distance protection algorithm

<b>Applied Faults</b>			<b>Time Taken</b> in number of samples (within brackets the number of power frequency cycles)
Fault type	Location	Fault Impedance ( $\Omega$ )	
<b>A-G</b>	5%	0	58 (0.725)
	50%	0	92 (1.15)
	90%	0	92 (1.15)
<b>A-G</b>	5%	50	Doesn't operate
	50%	30	89 (1.11)
	90%	30	Doesn't operate
<b>AB-G</b>	5%	0	59 (0.728)
	50%	0	82 (1.025)
	90%	0	89 (1.11)
<b>ABC-G</b>	5%	0	66 (0.728)
	50%	0	80 (1)
	90%	0	115 (1.4375)
<b>ABC</b>	5%	0	66 (0.728)
	50%	0	83 (1.0375)
	90%	0	116 (1.45)
<b>AB</b>	5%	0	70 (0.875)
	50%	0	86 (1.075)
	90%	0	129 (1.6125)

## 4.8 Results for Series Compensated Transmission Lines

Distance protection faces some challenges in protecting series compensated transmission lines. Due to voltage inversion, identification of faults happening at different parts of the transmission line can become difficult. The status of the bypass breaker, which may close during a fault, could complicate the fault discrimination, if not known.

Figure 29 presents a simple example where a conventional distance algorithm could malfunction due to the effect of the voltage inversion. It illustrates the estimated impedance trajectories for a bus 1 fault, with and without series compensation. Zone 1 Mho characteristic with a forward reach of 80% is also shown. These results are obtained when the relay is fed with the voltages measured on line side of the series capacitor.

It is obvious that with series compensation, the fault impedance is well-within zone 1, erroneously indicating a line fault. For distance relays fed with the line side voltage, certain reverse faults would appear as forward faults when the series capacitor is in service.

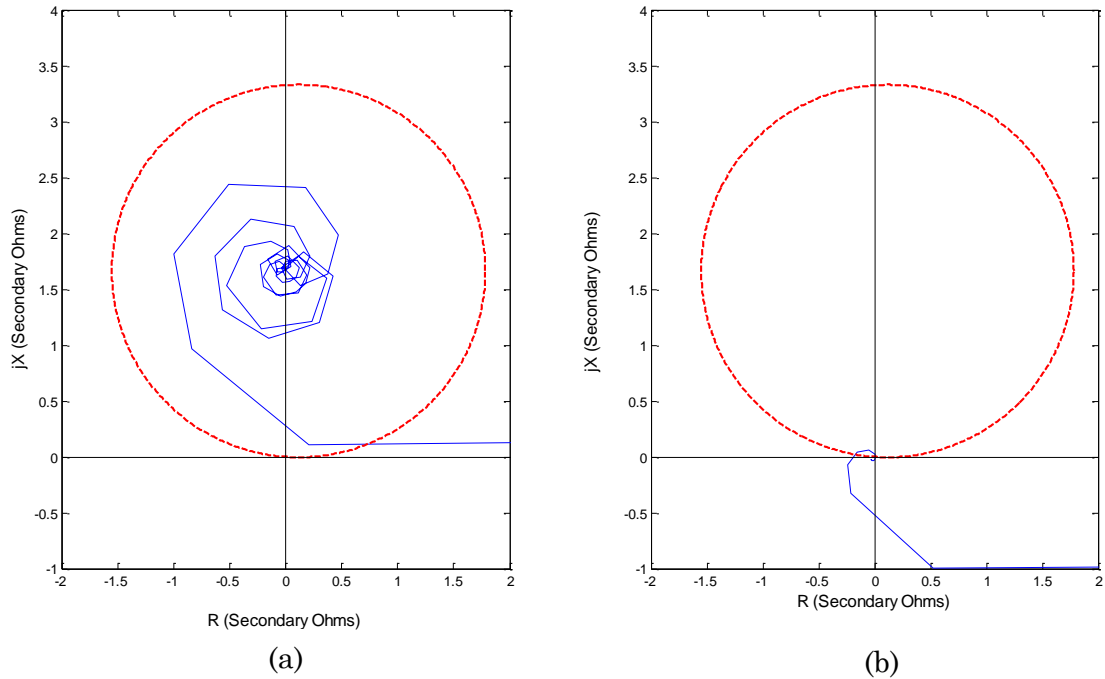


Figure 29: Estimated impedance trajectories for a bus 1 fault (a) with, and (b) without series compensation. Zone 1 Mho characteristic is also shown.

On the other hand, for relays fed with voltages measured on the bus side of the series capacitor, certain zone 2 faults would appear as zone 1 faults, causing the relay to overreach. This is shown in Figure 30 below. Zone 1 and zone 2 have forward reach settings of 80% and 120 % of the protected transmission line, respectively.

Due to these complications, it is advantageous to have more reliable means of protecting transmission lines with series compensation. Analysis of line current transients is one such method that has the potential to be successful in this regard.



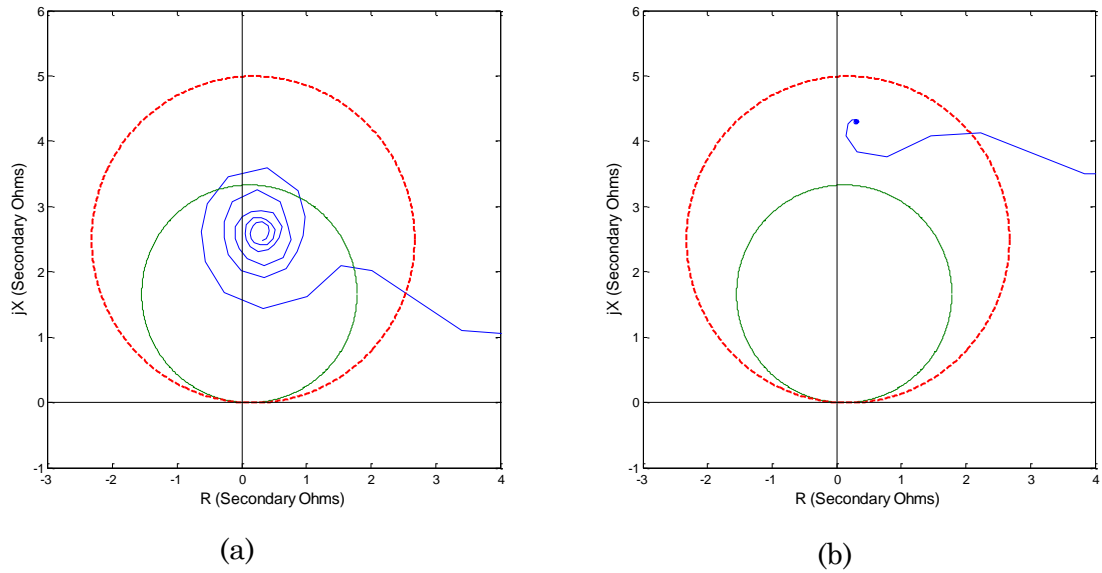


Figure 30: Estimated impedance trajectories for a bus 1 fault (a) with, and (b) without series compensation. Zones 1 and 2 Mho characteristic are also shown.

## 4.9 Chapter Summary

Chapter 4 presented the implementation details of the distance protection scheme in the line protection IED. Detailed descriptions about impedance estimation methods, development of impedance characteristics and fault identification algorithms were also provided. Steps of the validation process of the implemented scheme were then presented with a comparison of results with commercial IEDs. Finally, results for protection of series compensated lines were presented and associated protection challengers were highlighted.

## Chapter 5

# Transients Based Protection Scheme

Typical sampling rates modern digital relays operate, range from 20 to 32 samples per cycle [33]. In contrast, the SV protocol, when implemented according to IEC 61850-9-2 LE, has a significantly superior sampling rate and hence, can be used to implement non-conventional protection algorithms such as transients-based protection functions. It is observed that quite a number of recently the published research work on SV based process bus has focused on implementation and performance testing of protection algorithms [34], [35]. However, none of it seemed to have focused on transient protection, nor for that matter, has exploited the high sampling frequencies associated with 9-2 LE based SVs. This section proposes a method of implementing a transient based protection scheme that requires a high sampling rate as an application of SV protocol in accordance with IEC 61850-9-2 LE.

## 5.1 Concept of the Proposed Method of Line Protection

This work concentrates on a series compensated overhead transmission line, connecting two AC systems. At the terminating ends of the transmission line exist two line protection relays, which receive instantaneous values of local currents and voltages via Sampled Values (as per IEC 61850-9-2).

As explained earlier, occurrences such as faults, lightning strikes and switching operations in the power system generate high frequency current transients. Wave-front polarity of such a transient, observed at a particular point in the power system, depends on the location of that point with respect to the origin of the transient. The proposed method is based on the concept that the locality of a fault (internal or external) can be identified by comparing the polarities of the initial current transient seen at either end of the line [36]. The application of the concept to a single circuit, transmission line is depicted in Figure 31.

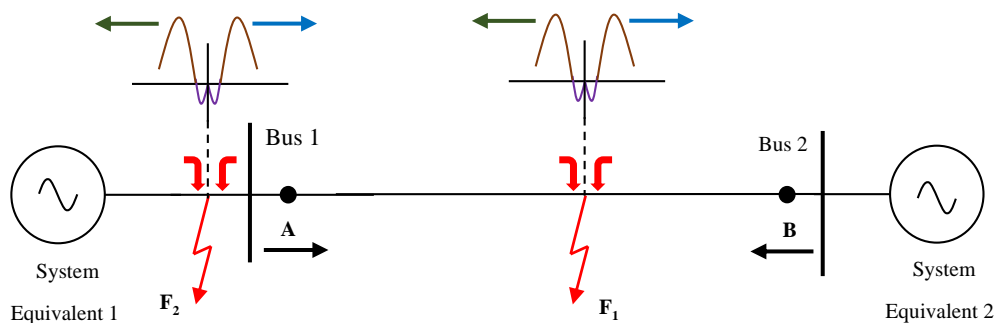


Figure 31: Origination of high frequency wave-fronts due to a fault

A fault in the system (such as  $F_1$  or  $F_2$ ) would generate current and voltage travelling waves with wave-fronts of the same polarity, traveling away from each other in opposite directions as shown. In the algorithm considered in this thesis, current transients are considered. Here, points A and B at the terminating ends of the line are considered as the two points of observation. The directions of current measurements are as indicated. When a fault occurs within the two points (i.e.: for an internal fault such as  $F_1$ ), it will be fed from both ends. This results in a sudden increase (or decrease, depending on the fault inception angle) in instantaneous current in the respective direction of measurement at both points of observation, A and B. Thus, the wave-fronts observed at either end are of the same polarity. In contrast, for an external fault such as  $F_2$  behind bus-1, both points experience only the fault current contribution coming from system 2, which is in the direction of observation at point B, and opposite to the direction of observation at point A. Hence, the observations at points A and B are of opposite polarities. This is true for any external fault. The similarity or difference in the observed wave front polarities at two line ends can, therefore, be utilized to distinguish between internal and external faults of a transmission line (a more rigorous explanation is given in Appendix D).

Nonetheless, it is important to understand that the polarity of the wave-front observed at a particular point depends on the inception angle of the fault as well. Moreover, several other factors including fault type, fault impedance,

line parameters as well as the sampling frequency and the signal processing technique used for filtering may have a bearing on the exact signature of such a high frequency transient.

As mentioned before, Wavelet Transform is a commonly used technique for analyzing fast aperiodic electromagnetic transients. In this study, Discrete Wavelet Transform (DWT) is used to decompose the observed currents into frequency bands and extract the high frequency transients superimposed on the power frequency currents. Instantaneous values of line currents are converted into modal components using constant Clarke transformation before extracting the high frequency transients from them. This transformation separates the ground mode component of the observed three phase currents that generally travels at a slower velocity, and allows accurate detecting and discriminating of faults of all different types by analyzing only the modal components.

## 5.2 Implementation of the Transient Protection Scheme

### 5.2.1 Clarke Transformation of the Line Currents

As the first step of implementation, the instantaneous values of three phase line currents subscribed by the relay as SVs are converted into modal components using the constant Clarke transformation matrix given in equation (28).

$$\begin{pmatrix} I_0 \\ I_\alpha \\ I_\beta \end{pmatrix} = \frac{1}{3} \begin{pmatrix} 1 & 1 & 1 \\ 2 & -1 & -1 \\ 0 & \sqrt{3} & -\sqrt{3} \end{pmatrix} \begin{pmatrix} I_a \\ I_b \\ I_c \end{pmatrix} \quad \text{-----(28)}$$

From the above transformation matrix, it is clear that all types of faults can be analysed by only using  $\alpha$  and  $\beta$  components (I.e.  $\alpha$  component contain transients for all types of fault expect those occurring between phases B and C. And  $\beta$  component reflects transients for all types of faults except an A-G fault).

### 5.2.2 Performing the Discrete Wavelet Transform

The discrete wavelet transform is performed using the multi-level filter bank implementation as explained in Section 0. However, only the level 1 detail coefficients are of interest for this work, for those yield the transient components in the highest available frequency band. Also due to limitation of computing resources, only  $I_\alpha$  is analysed in the implemented prototype relay. In an actual relay,  $I_\beta$  is also needed to be processed in a similar manner for it to enable detecting Phase-BC faults.

For the implementation of the DWT, “db4” (Daubechies 4) is chosen as the mother wavelet, after carrying out studies with several wavelet families on a trial and error basis (and also depending on the recommendations given in [19], [20]). Wavelet function of the db4 mother wavelet is given in Figure 10. The filter coefficients of the high pass filter,  $h[n]$ , are given in the Appendix C.

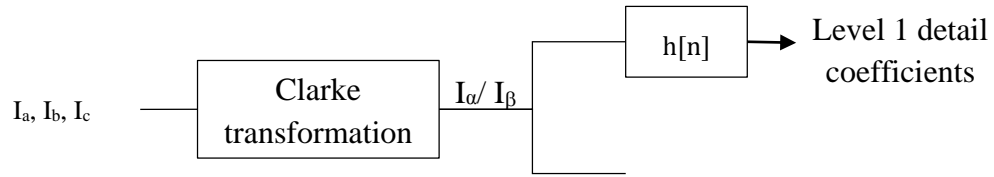


Figure 32: Implementation of the DWT

Figure 33 presents the high frequency transients extracted from  $I_\alpha$  using the DWT. It can be observed very clearly that the emergence of this transient coincides with the increase in the current due to the fault, hence the transient is understood to have been caused by the fault itself. Moreover, from the zoomed version of the transient, it can be seen that the wave-front polarity in this particular instance is negative.

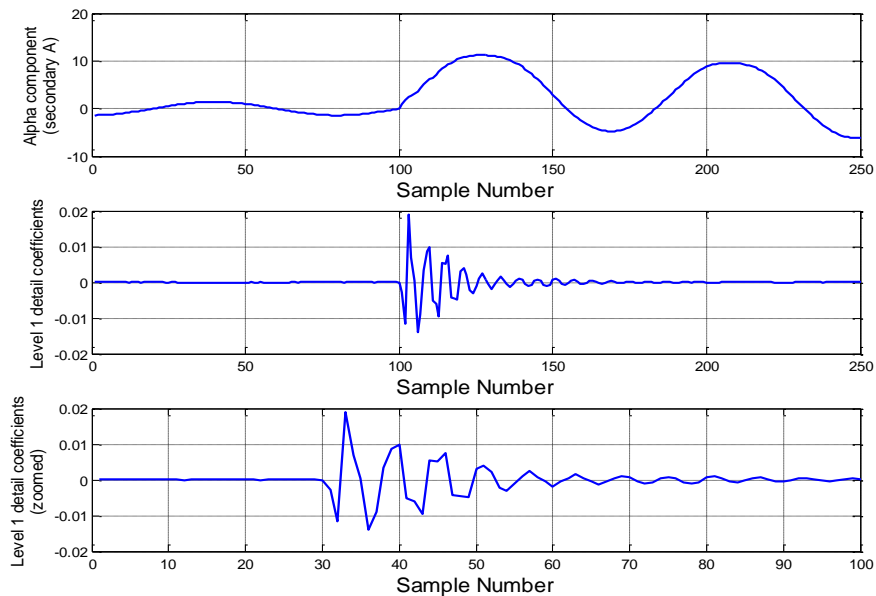


Figure 33: Extracted high frequency transient from  $I_\alpha$  (for a sampling frequency 80 samples per cycle)

Figure 34 shows the extracted high frequency transients from the same signal, when the sampling frequency of 256 samples per cycle (15.36 kHz).

These results obviously provide more information than those for 80 samples per cycle sampling frequency, nonetheless, do not make a qualitative difference to the proposed algorithm.

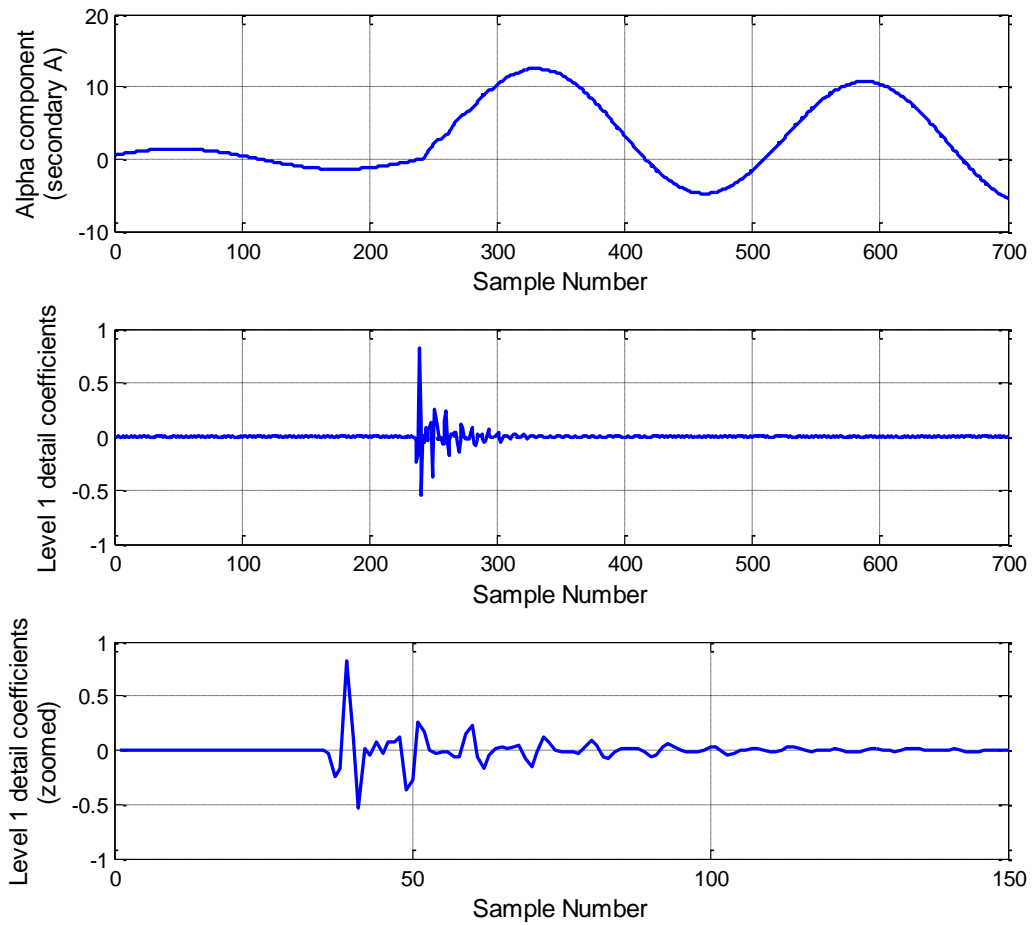


Figure 34: Extracted high frequency transient from  $I_a$  (for a sampling frequency 256 samples per cycle)



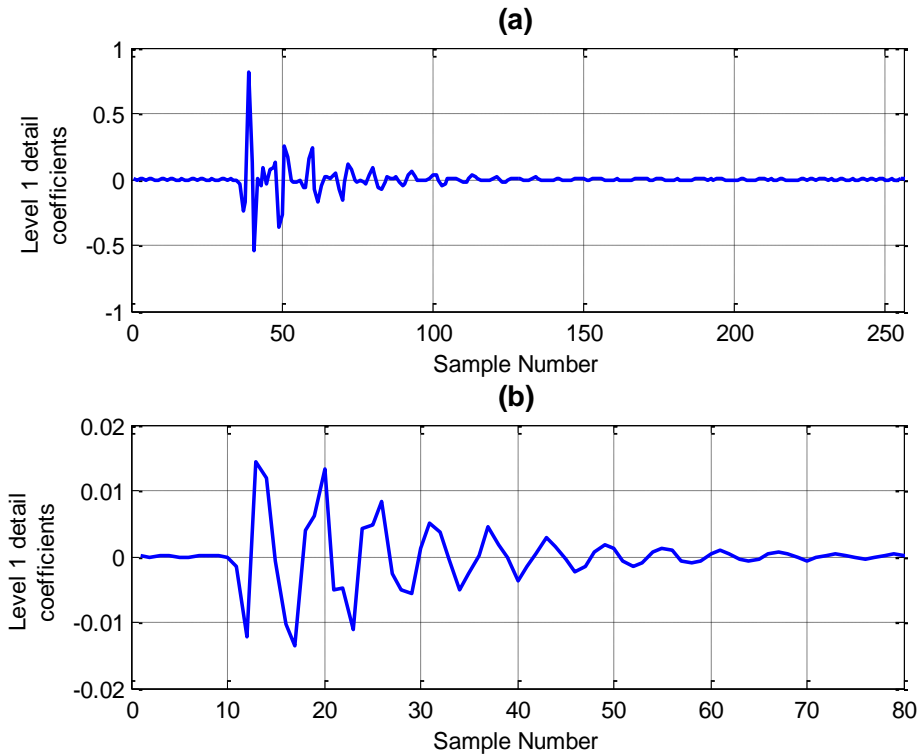


Figure 35: Detail wavelet coefficients at the near end for the same fault with a sampling rate of (a) 256 samples per cycle (b) 80 samples per cycle

Figure 35 presents a comparison of wavelet coefficients obtained at the near end for the same fault during a single cycle at 60 Hz. Results for both the sampling rates have the transient in them although their magnitudes and frequencies are different. Further, it is clear that both the sampling rates provide enough information (about the wave-front polarity) to be used in the proposed protection algorithm.

Notice that the near end refers to Bus 1 and the far end refers to Bus 2 of the transmission line, as shown in Figure 31. Furthermore, all distances (for instance, distance to the location of a fault) are measured from Bus 1.

Figure 36-(a) and (b) present the detail wavelet coefficients for the same fault with fault inception angles  $180^\circ$  apart. There, the reversal of the wave-front polarity is obvious. Further, (a), (c) and (d) of Figure 36 reveal the change of the signature of the transient with the location of the fault. It is evident that the observed transient is sustained for a longer period of time as the location of the fault moves away from the point of observation. The observed wave-front polarities, however, remain the same for faults at all three locations.

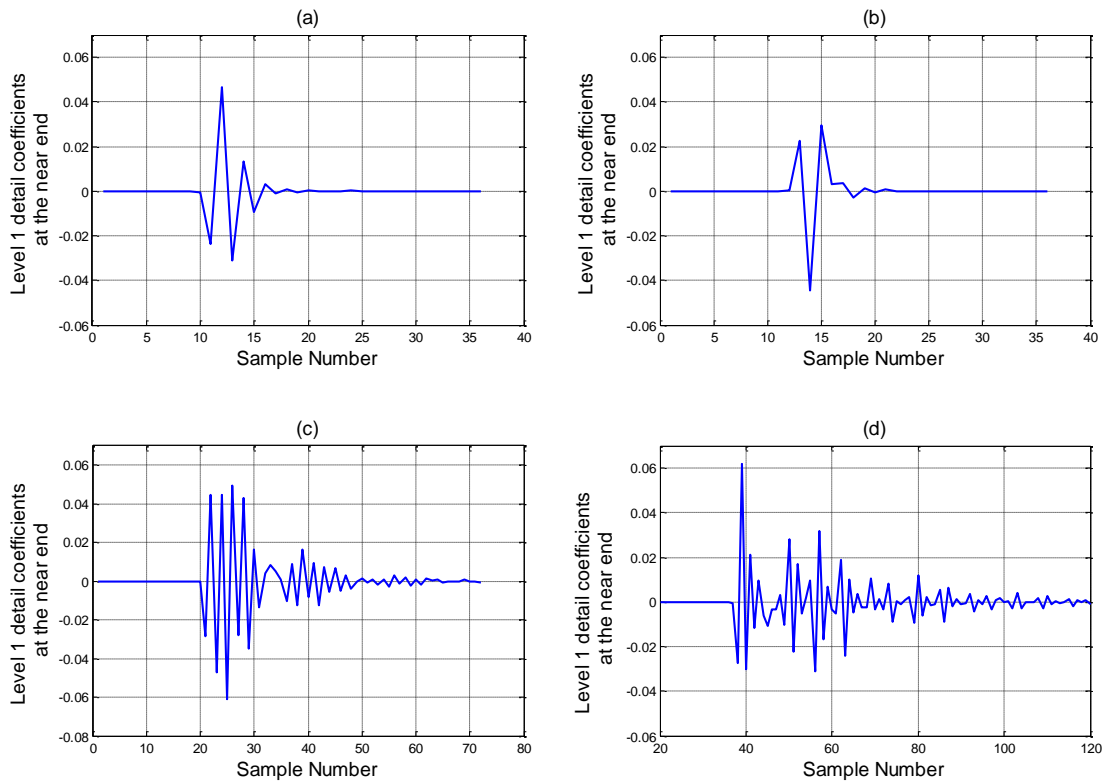


Figure 36: Detail wavelet coefficients at near end for (a) a 10% fault with fault inception angle at  $0^\circ$ , (b) a 10% fault with fault inception angle at  $180^\circ$ , (c) a 50% fault with fault inception angle at  $0^\circ$  and (d) a 90% fault with fault inception angle at  $0^\circ$ .

It is further observed from Figure 37 that the values of the detail wavelet coefficients following a fault are far greater than those appearing during the steady state. Therefore, a simple threshold can be used to identify the occurrence of a fault. In Figure 38, absolute values of the detail wavelet coefficients are shown with a pre-set threshold.

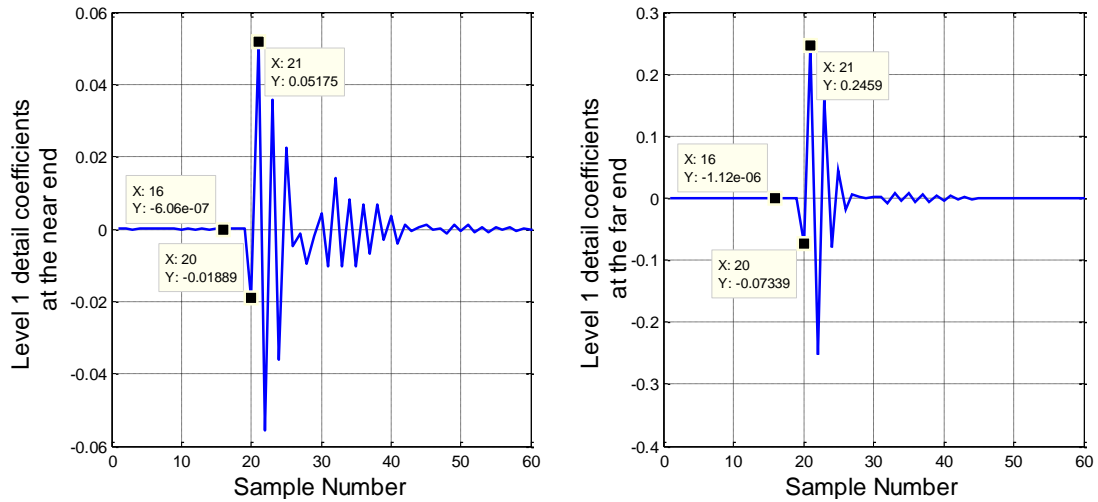


Figure 37: Detail wavelet coefficients at either end for a 50% fault

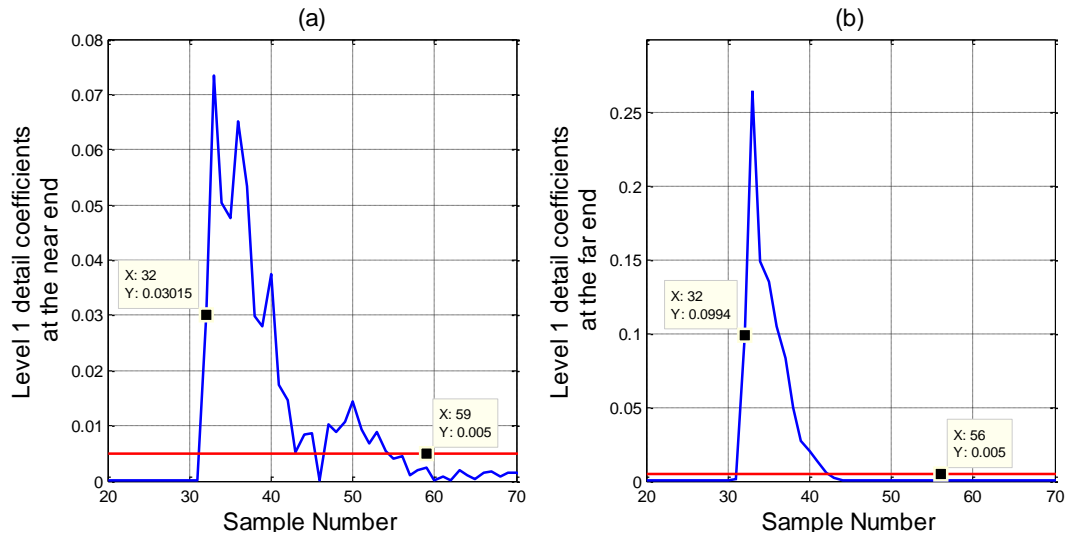


Figure 38: Absolute values of the detail wavelet coefficients at either end for a 50% fault

The value of the first point above the threshold is also indicated in Figure 38. The threshold is chosen empirically, based on the values observed for the detail wavelet coefficients for a larger number of faults and other disturbances. This is determined by adding some safety factor to the noise level observed during normal operation. It should also be checked against the ability of detecting high impedance faults (reasonably). There exists a compromise between the algorithm's capability to correctly identify the wave-front polarity, and its susceptibility to noise. In other words, if the threshold is set too high, the algorithm might miss the wave-front (especially, that of a high impedance fault), and intern, if it's too low, it can be triggered by noise.

### 5.2.3 Fault Identification

The fault identification method is as follows. The absolute value of the extracted high frequency transient (detailed coefficients of DWT) is computed and compared against a pre-set threshold value. When a coefficient value passes the threshold then, the original sign of that value is saved as the polarity of the wave-front. Once a fault is detected, a corresponding GOOSE message will be send, depending on the observed polarity. The reception of this GOOSE message would indicate the potential detection of a fault as well as the wave-front polarity of the fault generated current. The process of generating this GOOSE message is illustrated in Figure 39.

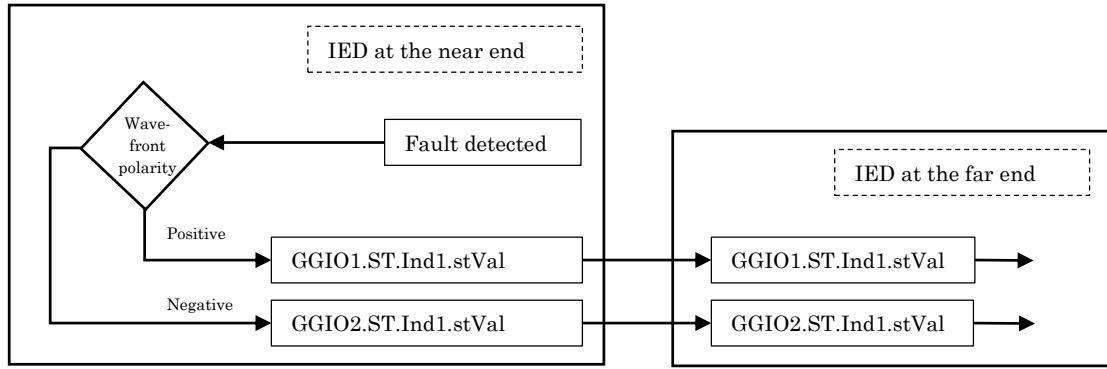


Figure 39: Sending of GOOSE messages corresponding to wave-front polarity

As shown in Figure 39, both positive and negative polarities have been assigned to a GOOSE output variable each, which initiates the corresponding GOOSE message once a fault detected. The line protection IED at the remotend subscribes the incoming message and compares the received wave-front polarity with its own. The IED at near end similarly subscribes the corresponding GOOSE messages sent from the remote end IED. The actions of the two IEDs are determined by the two wave-front polarities as described in Section 5.1.

### 5.3 Hybrid Protection Algorithm

From the earlier discussion on current transients in Section 5.1, it is clear that certain non-faulty conditions such as switching operations can also generate transients in line currents. This may cause a scheme that depends on wave-front polarities as the sole method of fault identification to mal-operate. In order to overcome this issue and also to increase the reliability and the

robustness of the scheme, a new hybrid protection algorithm is introduced by combining the transient based protection algorithm with distance protection. This combination enables the proposed method to effectively prevent non-faulty transient producing events from being identified as faults. The proposed hybrid line protection scheme is designed to operate similar to a transfer-trip scheme as shown in Figure 40.

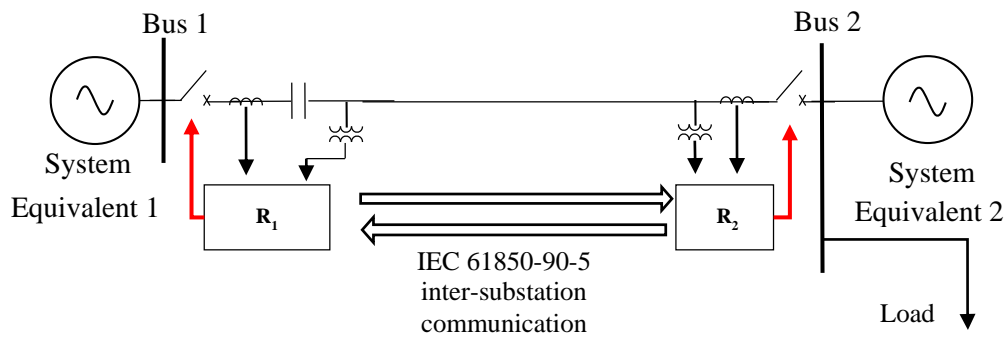


Figure 40: Illustration of the transfer-trip scheme

Upon detection of a disturbance, two protection IEDs (relays) R<sub>1</sub> and R<sub>2</sub> exchange the observed wave-front polarities with each other through GOOSE messages, as shown in Figure 40. Then at each IED, the locally observed wave-front polarity is compared with the remote end wave-front polarity received via GOOSE messages. If the two wave-fronts are of the same polarity, transient based line protection algorithm declares an internal fault. However, this transient based protection logic is supervised by a local measurement based distance element: a trip signal will be issued, only if the fault is confirmed by the supervising distance elements with modified characteristics.

A supervising distance element used in the hybrid algorithm is implemented with a zone having Mho characteristics, but with modified reach settings: a forward reach of 110% and a reverse reach of 10%, as shown in Figure 41. These reach values are selected to ensure that the estimated impedance would lie within the Mho circle for faults at all locations on the line, with the series capacitor in and out of service, assuming that voltage measurements are taken at line side of the series capacitor. The dashed line in Figure 41 is the transmission line impedance. The combined algorithm for fault detection is given below in Figure 42. According to the algorithm presented in Figure 42, the fault is detected and discriminated (whether it is inside the protected zone or not) by the transient based protection scheme, but trip signal is issued only if a line fault is confirmed by the distance protection.

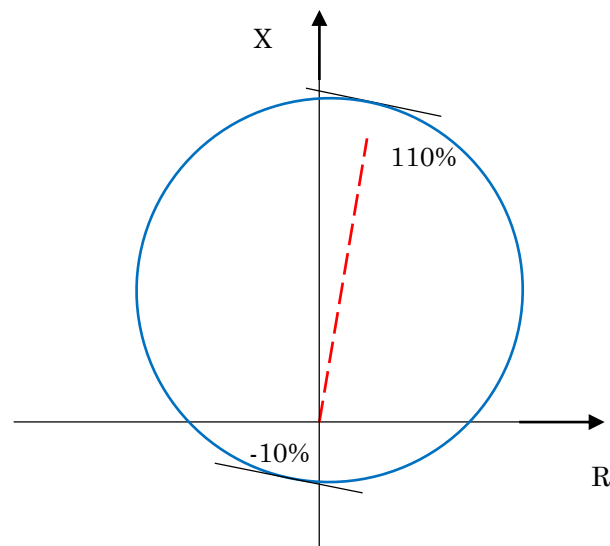


Figure 41: Modified Mho characteristics for the proposed protection method

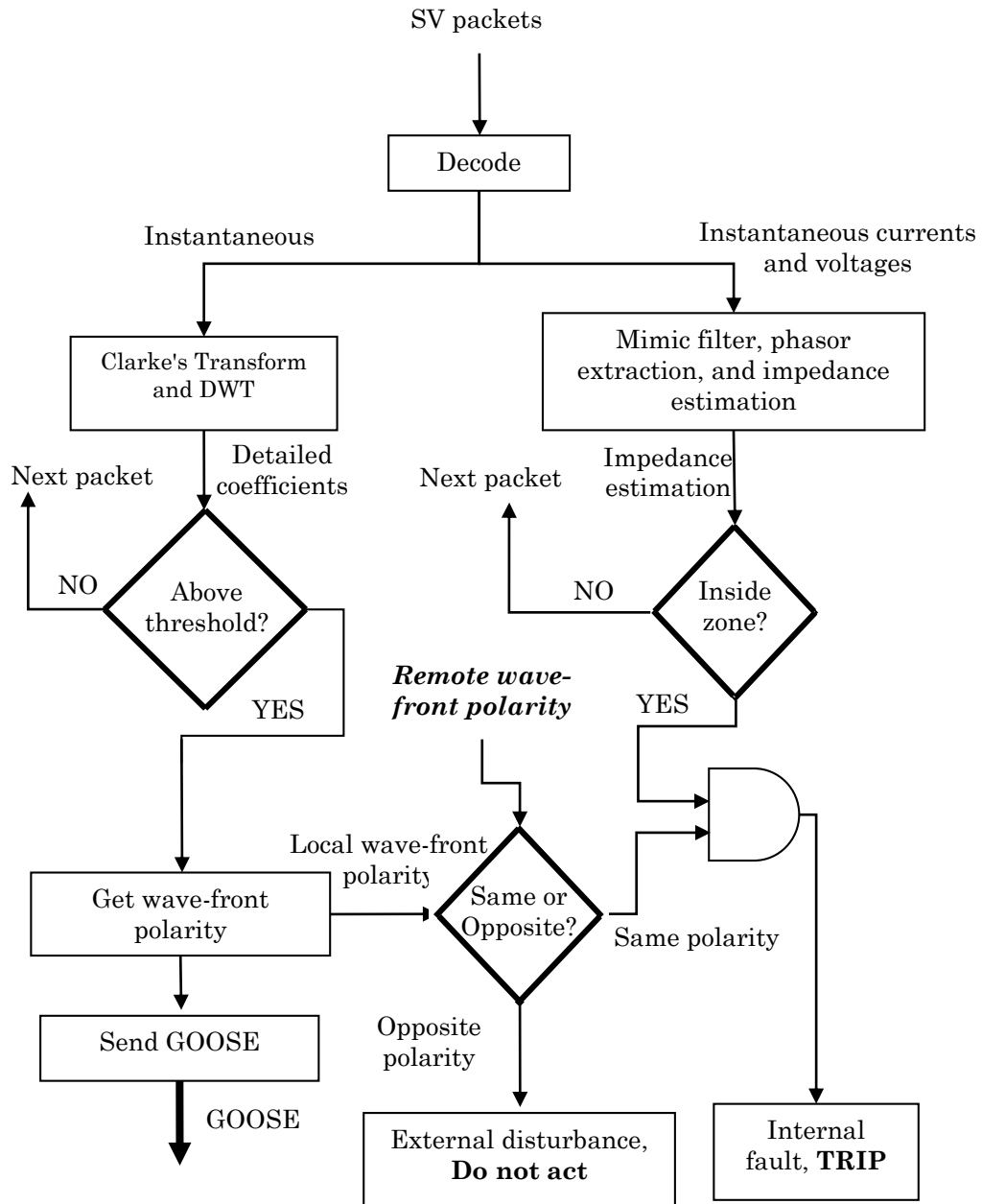


Figure 42: Combined algorithm of fault detection for the proposed hybrid protection scheme



## 5.4 Validation of the Hybrid Protection Scheme

The single line diagram (SLD) of the simulated power system section, upon which the transient protection scheme is tested and validated, is given below in Figure 43. The locations of the voltage and current measurements are also indicated.

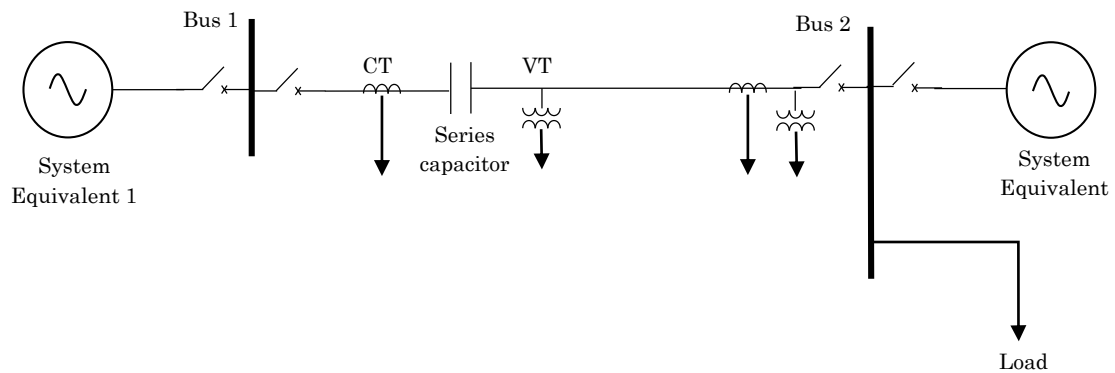


Figure 43: SLD of the simulated power system using which the implemented transient protection scheme is validated

To explore the full potential of the transients-based hybrid protection scheme, series compensation is introduced at the near end of the transmission line with a percentage compensation of 40 %. Furthermore, the series capacitors are modelled using the thyristor protected models with MOVs and bypass switches (important parameters are given in Appendix B). All other system parameters are similar to those used for the validation of the distance protection scheme.

The function of the relay at the far end of the line,  $R_2$ , is also implemented inside the RTDS simulation case. This is carried out employing

standard library components and using similar procedures and algorithms as in the relay prototype implemented on desktop computer. This too detects disturbances in the system and records the respective wave-front polarities as seen at its location. Therefore, the two relays considered for this scheme are the IED ( $R_1$  or  $IED_1$ ) and its virtual equivalent implemented in the RTDS case ( $R_2$  or  $IED_2$ ). Figure 44 below illustrates the corresponding schematic of the test apparatus.

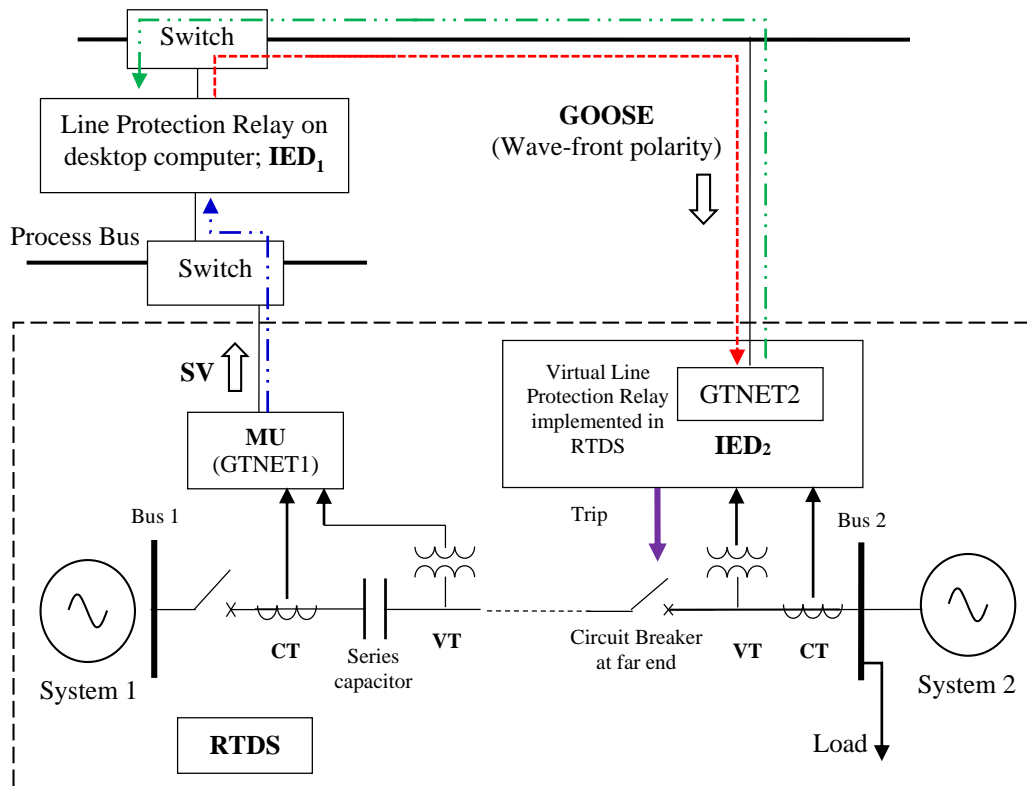


Figure 44: Schematic of the developed system for the hybrid protection scheme

Notice that, only one link of the transfer trip scheme (communication from  $IED_1$  to  $IED_2$ ) is implemented in the validation process. Since the operation of the protection system is not real-time (as explained in Section 3.4),

implementation of the other link does not yield a meaningful result. As shown in Figure 44, upon detection of a fault by the line protection IED ( $IED_1$ ), the wave-front polarity observed is sent via a GOOSE message (indicated in red) to  $IED_2$  at the far end of the line, which is implemented inside the RTDS. Then the  $IED_2$  compares it with the locally observed wave-front polarity and acts accordingly. In case of an internal fault, it would issue a trip signal to the circuit breaker at the far end to operate. Inter-substation communication between IEDs 1 and 2 are envisioned to be carried out using routable GOOSE messages as per IEC 61850-90-5. For this work, however, the said communication is accomplished by regular GOOSE messages, as both IEDs are located in the laboratory and connected to the same LAN. Although the second link is not implemented, the sending of the GOOSE message with the wave-front polarity observed by  $IED_2$  is indicated in the green line.

The graphs in Figure 45 present the three phase currents, voltages, model current component, detail WTCs (Wavelet Transform Coefficients), trajectories of the estimated impedance and the fault detection at either end during the fault. According to the WTCs computed at the two current measurement points, the fault is an internal fault. The estimated impedances at both ends converge and settle inside the special Mho zones defined for the respective relays, confirming the occurrence of a fault. The dotted blue lines the bottom most plots indicates the times when transient based algorithms detect the fault and initiate respective GOOSE messages with the polarity of

the wave front. The red solid lines show the times when the trip signals are initiated, after the confirmation by the impedance units.

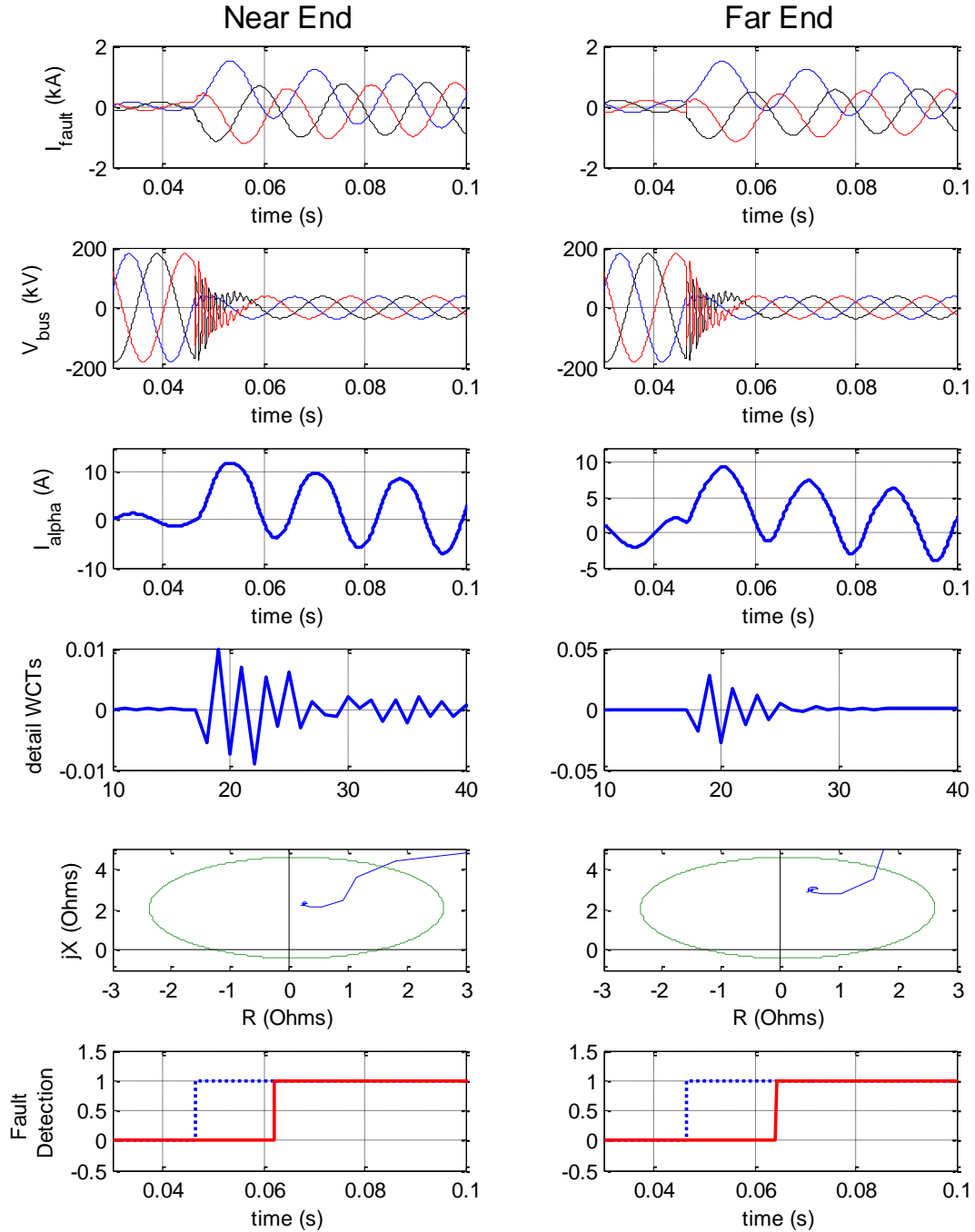


Figure 45: Three phase currents, voltages, model current component ( $I_{\alpha}$ ), detail WCTs, trajectories of the estimated impedance and the fault detection at either end for a 50%, ABC fault.

When the line is series compensated, there exist two options of voltage measurement at the near end (at bus 1) as mentioned in Section 2.2.2. They are the bus side voltage  $V_B$  and the line side voltage  $V_L$ , as given in Figure 46. Typically,  $V_L$  is used in series compensated line protection, therefore, all algorithms and settings in this application are devolved based on the assumption that the relay at the near end is fed with  $V_L$ .

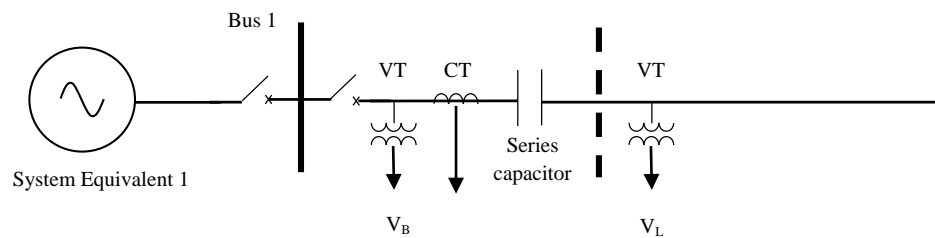


Figure 46: Voltage measurements at the bus side and the line side

Figure 47 presents the results for a bus 1 fault with a 40% of series compensation. A bus 1 fault is external to the two points of observation, therefore, the WTC are of opposite polarities. The algorithm corrected identifies this as an external fault although the estimated impedances are well within the zone.

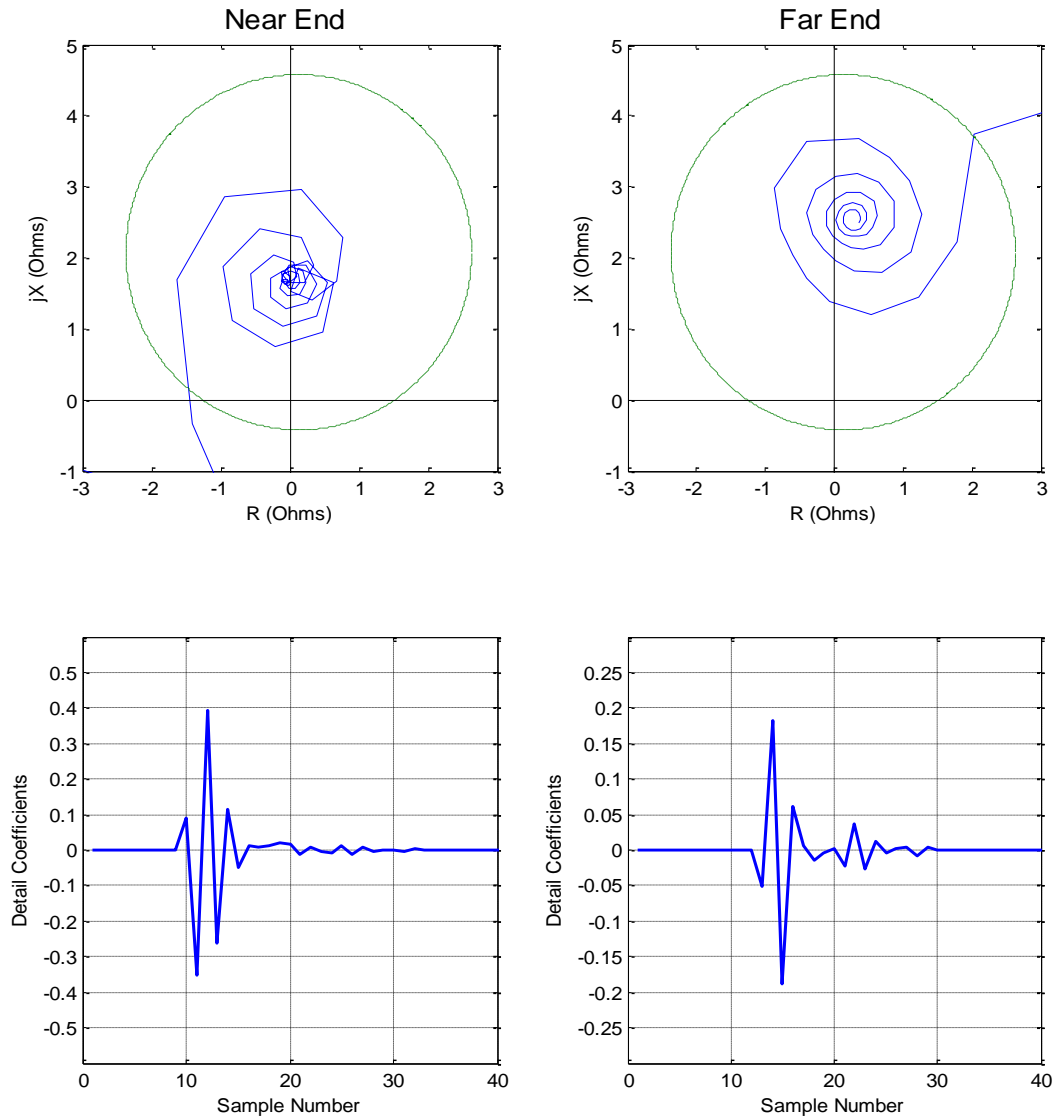


Figure 47: Trajectories of the estimated impedance and detail wavelet coefficients at either end for a bus 1, ABC fault, with the effect of voltage inversion

For certain reverse faults, the impedance seen by a distance relay at bus 1 would appear inside the forward protected zone. This is due to the effect of voltage inversion across the series capacitor. A conventional distance relay with a zone-1 forward reach characteristic of 80%, will misidentify such faults as internal faults, even though they are actually external faults.

Figure 48 and Figure 49 present similar results when the relay is fed with the bus side voltage,  $V_B$ , for a forward fault at 5% of the line.

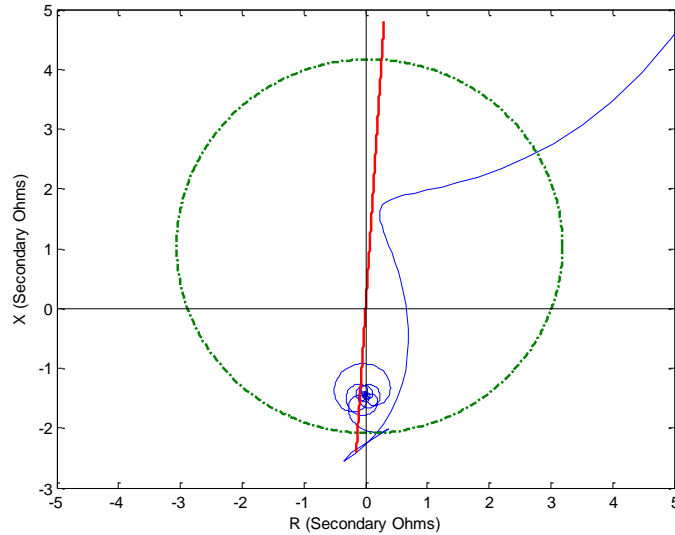


Figure 48: Trajectory of the estimated impedance for a 5% three phase fault with series capacitor in service, (with the effect of voltage inversion)

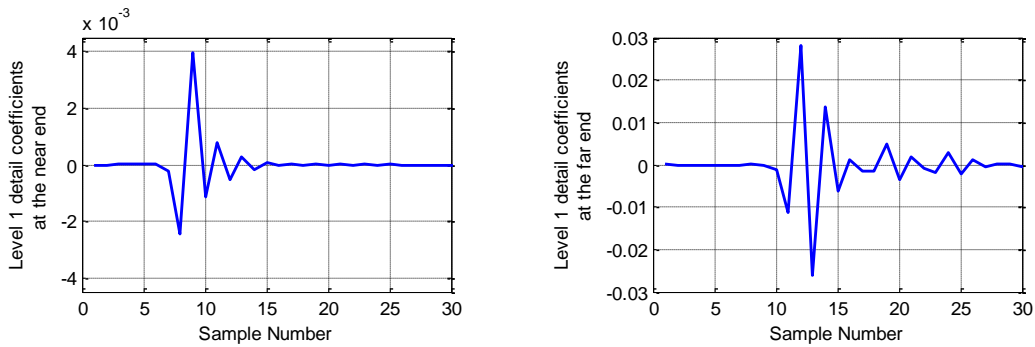


Figure 49: Detail wavelet coefficients at either end for a 5% three phase fault with series capacitor in service, (with the effect of voltage inversion)

When the voltage measurements are taken from the bus side of the capacitor, the reverse reach of the Mho circle must be increased as the impedance seen by the relay can now be negative. Here, a reverse reach of 50% is used. Now, for a bus 1 fault, although the estimated impedance lies within

the negative zone, the wave-front polarities are still of the same polarity. Hence, it is correctly identified as an internal fault.

The results presented above demonstrate the basic operation of the algorithm. That is, a fault is identified as internal only if the wave-front polarities are of the same polarity as well as the impedance seen is within the predefined zone.

The following (plotted in Figure 50, Figure 51, Figure 52 and Figure 53) are the wave-front polarities recorded at either end at several chosen locations of the transmission line for different scenarios.

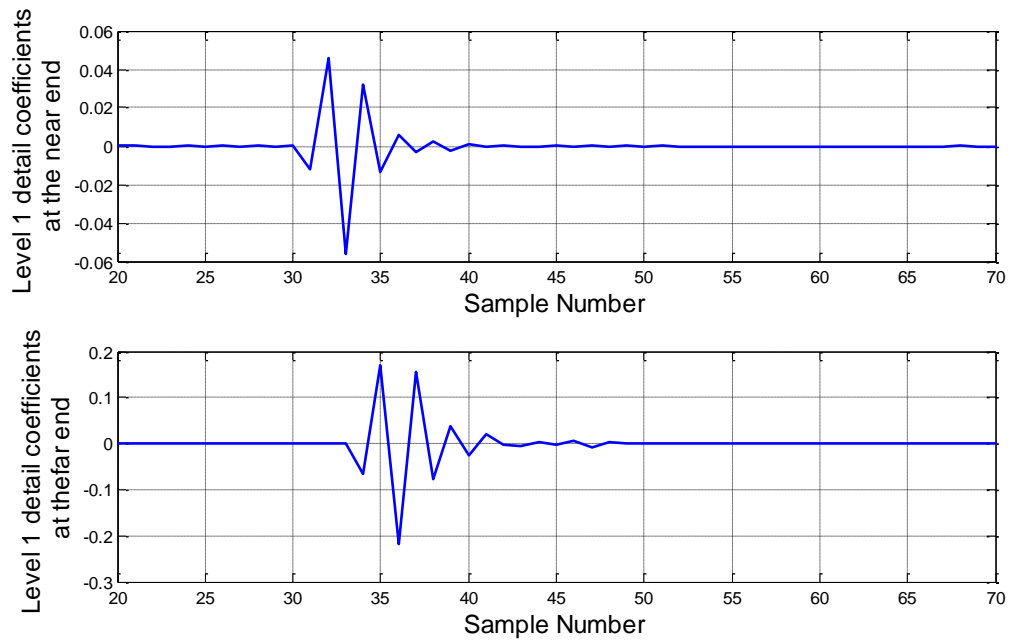


Figure 50: Detail wavelet coefficients at either end for a 10% AB fault



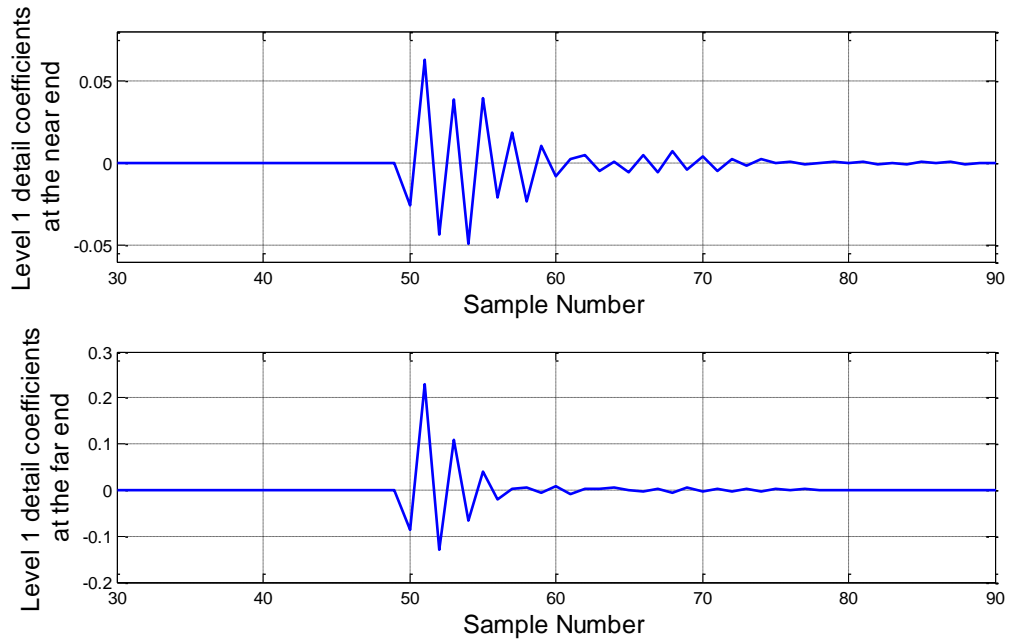


Figure 51: Detail wavelet coefficients at either end for a 50% AB fault

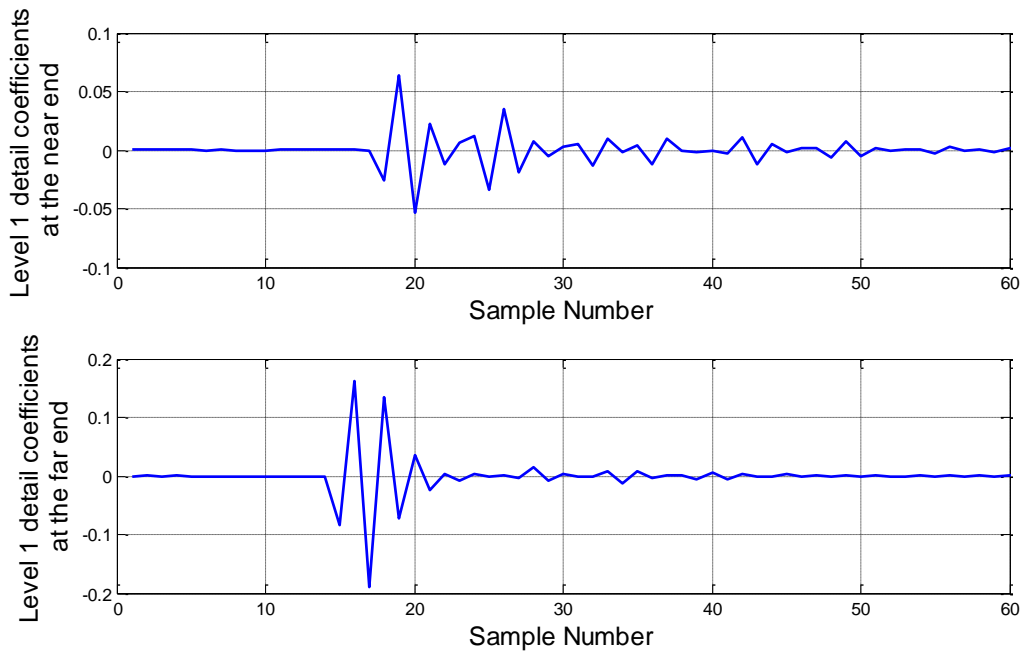


Figure 52: Detail wavelet coefficients at either end for a 90% AB fault

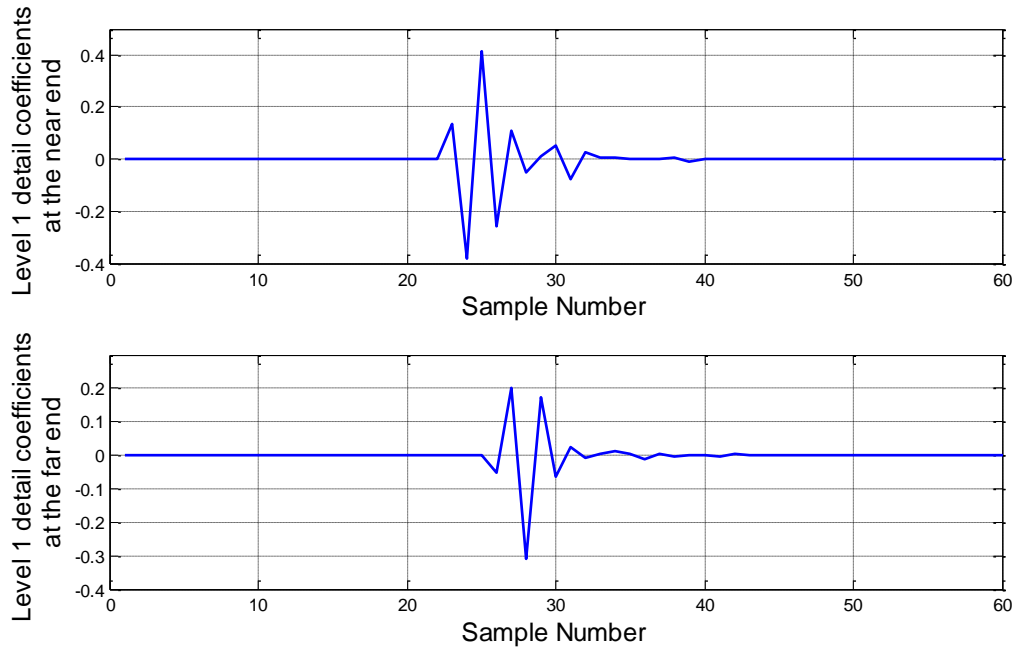


Figure 53: Detail wavelet coefficients at either end for an external fault (a bus 1 fault)

Above Figure 50, Figure 51 and Figure 52 show that the wave-front polarities observed at each end are of the same polarity for internal faults at different locations. On the other hand, for a bus 1 fault, which is external to the two points of observation, the observed wave-fronts are of opposite polarities as seen in Figure 53. These results, therefore, verify the theory formulated earlier regarding the fault identification using wave-front polarities. It is further noticed that the magnitude of the wavelet coefficients and the time of arrival of the wave-front understandably depend on location of the fault. For instance, for a 90% fault, the initial wave-front reaches the far end earlier than its counterpart reaches the near end, and the magnitude of the former is larger than that of the latter. These magnitudes, however, are also affected by other factors such as the type of the fault, pre-fault load current

magnitudes, source and fault impedances and also the inception angle. Although this is not detrimental to the function of the proposed hybrid algorithm, the threshold value against which the WTCs are compared to detect faults may need adjustments depending on the power system.

One of the most challenging tasks of transmission line protection is to effectively protect lines with series compensation. Traditional distance protection schemes tend to mal-function due to current or voltage reversals caused by the series capacitor. Another difficulty faced in distance protection is the detection of high impedance faults. Schemes with Mho characteristics, in particular, provide very little resistive coverage for downstream faults, while quadrilateral characteristics perform better in this regard. Also, for the faults located close to the far end (beyond 80%), the trip signal is delayed with traditional distance protection (without a transfer trip scheme) as they are detected in Zone 2.

The proposed method of line protection can be adopted to address both the issues mentioned above. While the proposed algorithm can effectively protect a series compensated line with existing settings, its protected zone (modified distance protection characteristic in Figure 41) is required to be redefined for it to cover high impedance faults as well. This is required in order to provide the necessary resistive coverage. In Figure 54, the detail wavelet coefficients at either end for a 5% fault with 40% series compensation are shown. And similarly in Figure 55, those for a 95% fault with a fault impedance

of  $50 \Omega$  (without series compensation) are shown. The wave-front polarities in both occasions correctly indicate an internal fault.

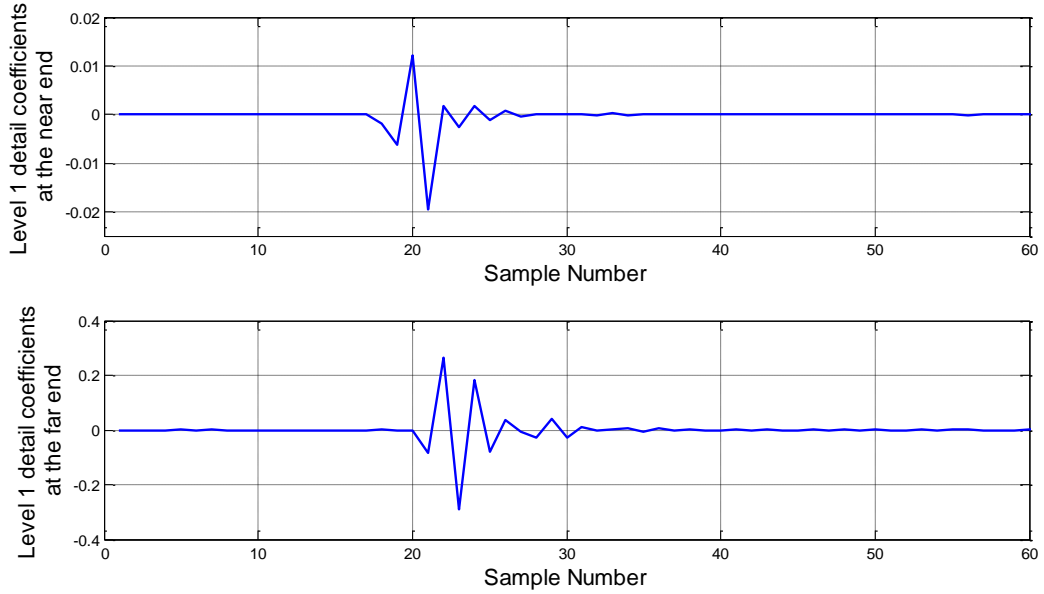


Figure 54: Detail wavelet coefficients at either end for a 5% AB fault with 40% series compensation

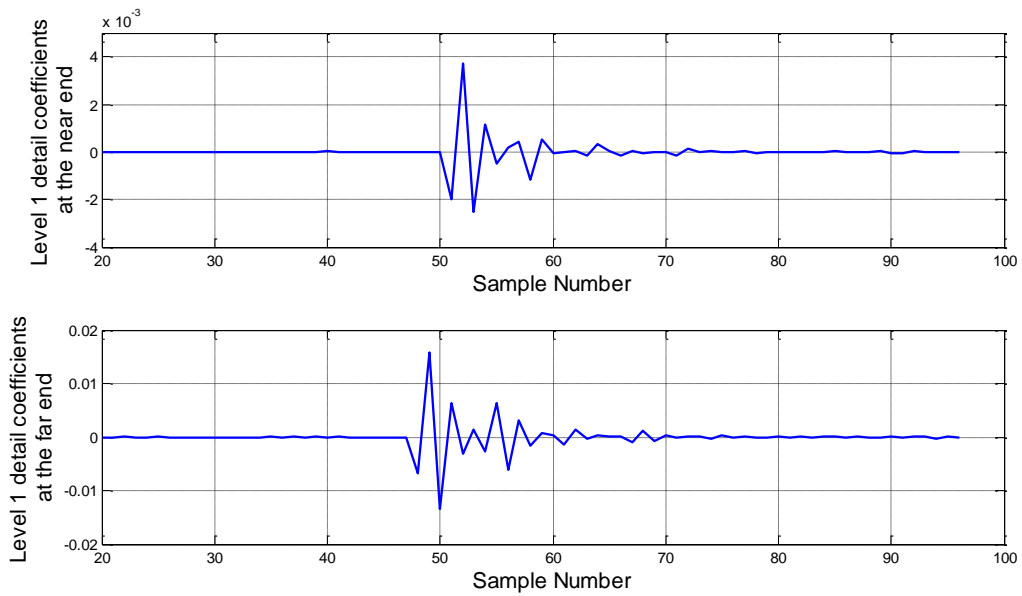


Figure 55: Detail wavelet coefficients at either end for a 95% AG fault with a  $50 \Omega$  fault impedance

Since the proposed hybrid protection scheme covers full length of the line, there is no intentional delay for any fault within the protected zone. However, the operation of transient based protection requires communication of wave-front polarities. However, this communication does not cause additional delay. Detection of fault and evaluation of wave-front polarities is very fast (less than 1 ms) and therefore, GOOSE messages from the respective remote ends can arrive at each IED well before the fault is confirmed by its distance element, which takes about one cycle (16.67 ms). This is clearly evident from Figure 56, which illustrates the time line of fault detection process. In this example, the time taken by the distance element is 86 samples, which is equivalent to 1.075 of a cycle at 60 Hz, while the detection by the transient based protection algorithm is almost immediate.

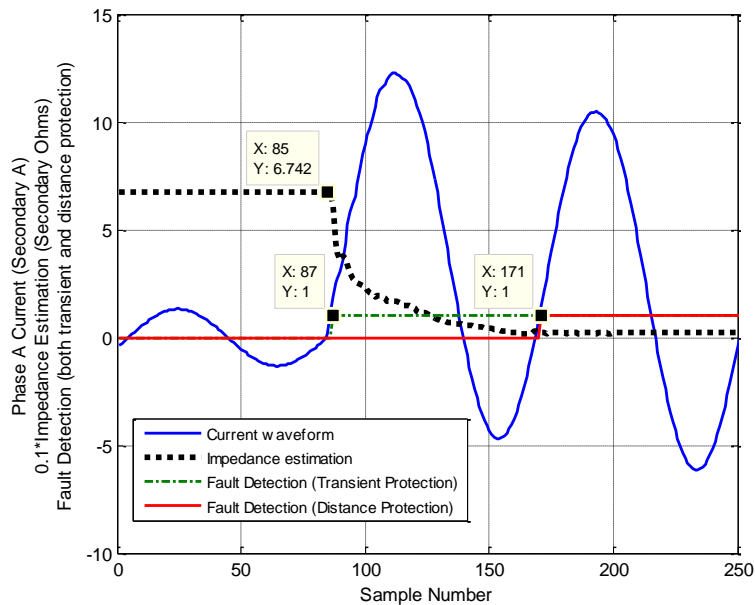


Figure 56: Fault detection in the proposed protection scheme for a solid AB fault, 5% away from bus-1.

## 5.5 Performance Evaluation of the Hybrid Protection Scheme

Performance of the proposed transient protection scheme is tested under a variety of faults and the results are tabulated below in Table 4.

Table 4: Performance of the proposed protection scheme under different fault conditions

<b>Applied Faults</b>				<b>Fault Detection</b>
<b>Fault type</b>	<b>Location</b>	<b>Fault Impedance (<math>\Omega</math>)</b>	<b>Series compensation</b>	
<b>AB</b>	5%	0	Yes	Yes
	50%	0	Yes	Yes
	95%	0	No	Yes
<b>ABC</b>	5%	0	Yes	Yes
	50%	0	No	Yes
	95%	0	No	Yes
<b>A-G</b>	5%	0	Yes	Yes
	50%	0	No	Yes
	95%	50	No	No
<b>AB-G</b>	5%	0	Yes	Yes
	50%	30	No	Yes
	95%	50	No	No
<b>ABC-G</b>	5%	0	Yes	Yes
	50%	0	Yes	Yes
	95%	0	Yes	Yes
<b>ABC</b>	Bus 1	0	No	No

With the current distance characteristic, the scheme doesn't work for high impedance faults occurring at far downstream locations, simply because the impedance point lies outside the protected zone. This hybrid protection scheme is also tested for a variety of percentage line compensations and for different source to impedance (SIR) ratios.

### 5.5.1 Behaviour for Non-faulty Conditions

The transients based protection scheme is also tested for some non-faulty conditions such as circuit breaker operations. Figure 57 shows the wave-front polarities observed for a closing operation of the circuit breaker at the near end.

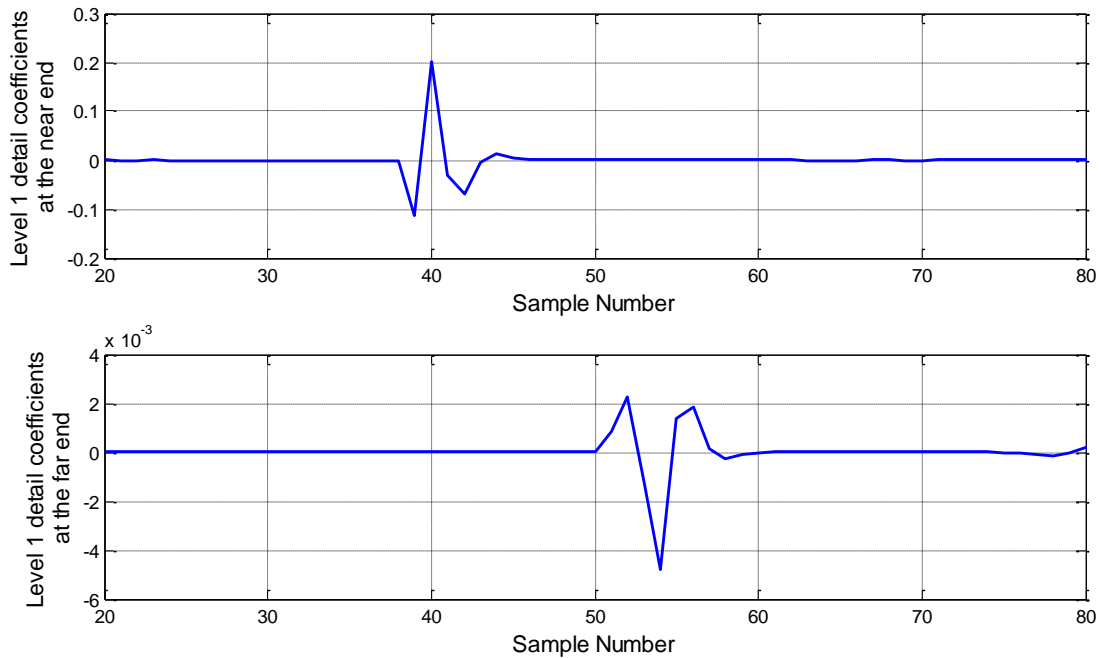


Figure 57: Detail wavelet coefficients at either end for a closing operation of the circuit breaker at the near end

Notice that the two wave-fronts are of opposite polarities similar to an external fault, despite the fact that it is an internal event (in this case). Therefore, this would not even trigger the transients-based section of the algorithm (impedance relay is obviously not triggered by this). Moreover, a similar behaviour is observed for the operation of the bypass switch of the series capacitor as shown in Figure 58.

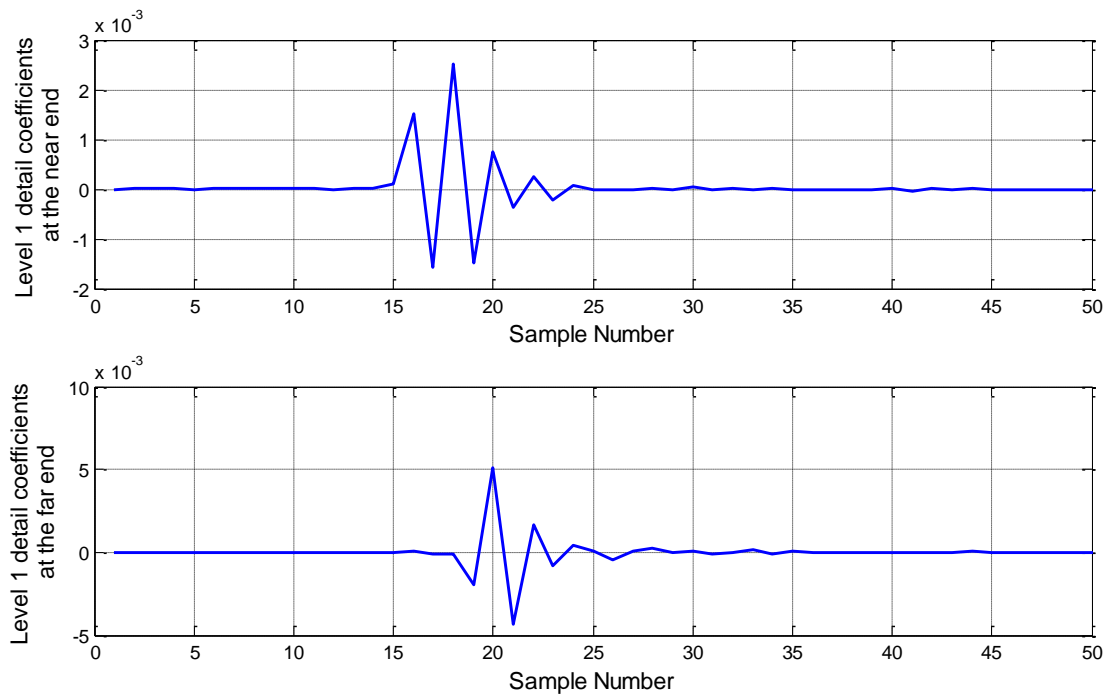


Figure 58: Detail wavelet coefficients at either end for a closing operation of the bypass switch of the series capacitor.



## 5.6 Effect of the Bit Resolution of the A/D Converter

The data types used in IEC 61850-9-2 LE for the representation instantaneous values of currents and voltages are “INT32” and “FLOAT32”. Both the data types are in 32 bit format. The RTDS has the capability to publish sampled valued with a resolution of 32 bits. However, the hardware analog to digital (A/D) converters in real merging units do not usually possess a 32 bit resolution. Typically, modern commercial merging units have a 16-20 bit resolution in their A/D converters [37], [38]. It is discovered that this bit resolution is of the utmost importance to the proposed transients based protection scheme. The analysis carried out regarding this showed that the high frequency transients become indistinguishable due to added noise, if the resolution of the currents measured are below a certain level. The following calculations are carried out assuming a bit resolution of 24.

Rated primary current of the CT = 100 A (rms). The CT ratio used is 100, therefore, the rated secondary current,  $I_{sec}$  is 1 A. Peak of the rated secondary current,  $I_{sec, pk}$  is  $1\sqrt{2}$  A = 1.41421 A. Assuming an accuracy limit of 20 for the CT, the maximum current that can be accurately measured by the CT is  $20 \cdot I_{sec, pk}$ .

$$20 = 2^{4.322} \rightarrow 5 \text{ bits} \quad \text{-----(29)}$$

Saving these 5 bits and 1 bit for the sign, would leave 18 bits to represent the regular secondary current. Therefore, the resolution of the secondary current provided by the MU is,

$$\frac{1.41421}{2^{18}} = 5.3948 \times 10^{-6} \text{A} = 5.3948 \mu\text{A} \quad \text{-----}(30)$$

Current resolutions calculated for 18 bit, 16 bit and 12 bit A/D converters, following the same procedure, are 0.3453 mA, 1.3811 mA and 22.097 mA, respectively. The wavelet coefficients observed after setting above current resolutions are given in Figure 59 below.

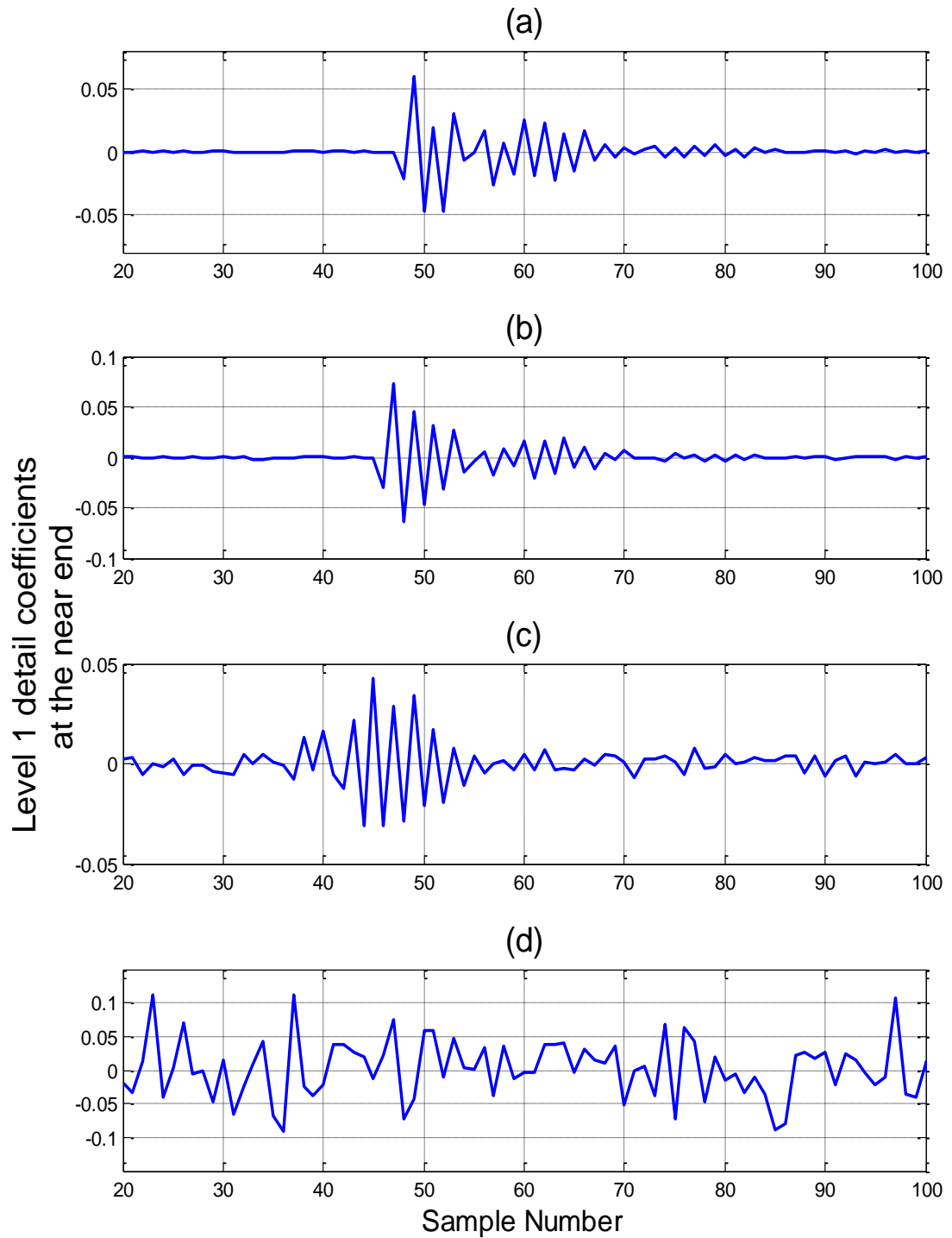


Figure 59: Detail wavelet coefficients at the near end for a 50% fault, with an assumed A/D converter bit resolution of (a) 24 bits, (b) 18 bits (c) 16 bits and (d) 12 bits

From the above results, it is clear that it is impossible to perform an analysis of transients of the type discussed in this thesis, with a bit resolution of 12. Results obtained for a bit resolution of 16 are also unworkable for identifying the wave-front polarity, although one can recognize the presence of the transient. Results for both bit resolutions 18 and 24 presents distinct transients and can be effectively used for the purpose of this study. It should be further noticed that the above calculations have not accounted for the noise generated by the electronic devices and other means. Generally, 2-3 bits are typically reserved as a safety margin for errors caused by the system noise. From the above discussion, it can be recommended that the A/D converter of the MU should have a bit resolution of 20 or above for SVs (published by that MU) to be used in a transient based protection scheme of this nature. (This requirement is predominantly regarding the current measurement).

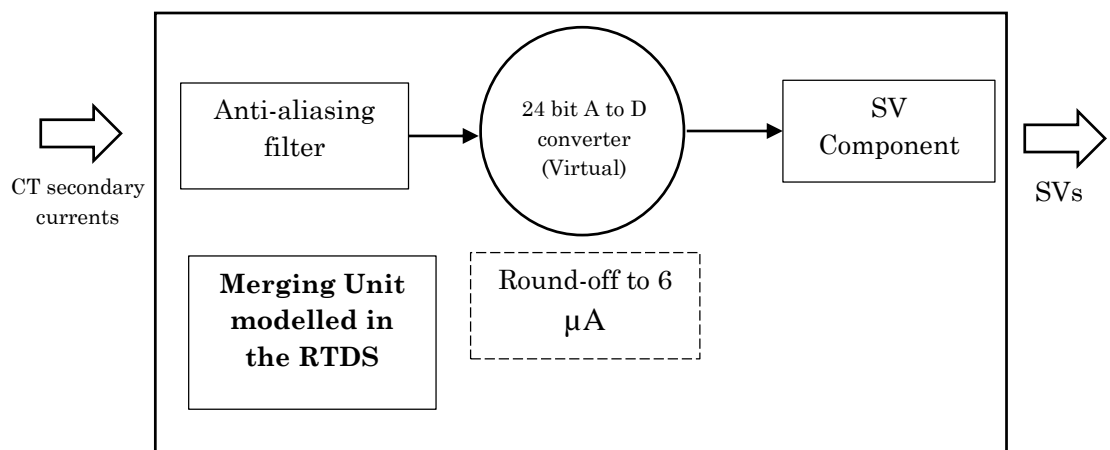


Figure 60: Modelling the effect of a 24 bit A to D converter

All the studies regarding the transient based scheme of this thesis are carried out assuming a bit resolution of 24. To model the effect of a 24 bit A/D converter, the output values of the anti-aliasing filters (as in Figure 17) are rounded off to the nearest 6  $\mu\text{A}$  (from 5.3948  $\mu\text{A}$ ).

With the modelling the effect of a 24 bit A/D converter, now the arrangement shown in Figure 60 implemented inside the RTDS, emulates the function of an actual merging unit with a substantial accuracy.

## 5.7 Chapter Summary

In Chapter 5, the steps followed in developing the transients based hybrid protection scheme were put forth. First the basic concept was described followed by the details explaining its implementation in an actual power system. This scheme too was validated using the RTDS and a number of results were presented in this chapter. Finally, modelling the effect of the bit resolution of an actual merging unit (MU) was analysed and important recommendations were provided.

# Chapter 6

## Conclusions

### 6.1 Contributions and Conclusions

In this thesis, implementation of an IEC 61850-9-2 LE, sampled values compatible line protection IED is presented. A distance protection algorithm and a transient based hybrid protection algorithm are successfully implemented on this IED, both of which are tested through hardware-in-the-loop simulations performed using a RTDS simulator. The main contributions made during the work done in completing this thesis and pertinent conclusions are listed below.

- An IEC 61850-9-2 LE sampled values compatible IED prototype was developed on a Linux based desktop computer. This prototype IED could successfully subscribe to sampled values published by a source with the correct configurations, decode the information, and pass the decoded sampled values to signal processing algorithms for further processing.

- An experimental setup was developed to test the process bus compatible IEDs by augmenting a test setup previously developed to test the station bus capability of IEC 61850 compatible IEDs. This development resulted in a fully IEC 61850 compliant laboratory setup.
- Two simultaneous signal processing algorithms, a Discrete Fourier Transform based phasor extraction algorithm and a Discrete Wavelet Transform based transient extraction algorithm, were successfully implemented on the prototype IED. Accuracy of signal processing was confirmed by extensive tests.
- A distance protection algorithm was implemented using the phasors extracted from IEC 61850-9-2 LE sampled values. Both Mho and quadrilateral characteristics were implemented. Operation of the distance protection was extensively tested and verified through hardware-in-the-loop simulations.
- A transient based protection algorithm was implemented on the prototype IED using IEC 61850-9-2 LE sampled values as inputs. The fault identification in this algorithm is based on the comparison of polarities of the fault generated travelling wave-fronts measured at two line ends. This algorithm was combined with distance protection to implement a reliable hybrid line protection scheme applicable for protection of series compensated transmission lines.

- This hybrid line protection scheme based on IEC 61850-9-2 LE sampled values was extensively tested and verified using the real-time digital simulator. The performance of the transient based algorithm and its sensitivity to various factors was investigated through experiments.
  
- ❖ Based on the studies conducted, it can be concluded that
  - When IEC 61850-9-2 sampled values are used as inputs, generic hardware such as the desktop PC used in this research can be used to implement process bus based IEDs. The prototype IED on desktop is a convenient platform for testing novel protection algorithms.
  - The hybrid protection scheme proposed in this research can effectively protect series compensated transmission lines from all types of faults without being affected by the voltage inversion due to series capacitor.
  - The sampled values as per IEC 61850-9-2 LE contain enough information for them to be used in the class of transient based protection algorithms implemented in this thesis.
  - When used for transient based protection algorithms, the analog to digital converter of the merging need to have a higher bit resolution. For the algorithm implemented in this research, the required minimum analog to digital conversion resolution was 20 bits.



- The fully IEC 61850 compliant laboratory setup developed for the purpose of this research can be used for further research on the IEC 61850 protection algorithms as well as for teaching purposes.

## 6.2 Future Work

The followings can be viewed as future extensions on the work presented in this thesis.

- Although the implemented prototype IED is adequate for verifying the protection algorithms, there was a time delay in acquisition of IEC 61850-90-2 sampled values (as explained in Section 3.4). The cause for this time delay could not be pinpointed, but it could be due to the network card used or due to the fact that the developed application is running on a regular operating system not optimized for real-time operation. Rectifying this problem is needed for achieving improved time performance and make the prototype more realistic.
- The protection of series compensated double circuit transmission lines is also an existing challenge in power system protection. The transient based protection algorithm can be further improved to accomplish this as well. One way of achieving this would be to incorporate a current comparison of the two circuits to the existing algorithm.
- Other protection schemes such as overcurrent protection can be added to the line protection IED. Furthermore, with some modifications to the existing libraries, a differential protection IED can also be implemented by subscribing two sampled values streams.

- Currents and voltages of the RTDS can be taken out as analog outputs, and then amplified and fed into the inputs of a real merging unit in the laboratory. This would provide the opportunity to use sampled values from an actual merging unit in the implemented IED and to investigate the issues accompanied with it, which might not be present in the sampled values published by the RTDS.

# References

- [1] ABB Review (Aug. 2010), Special Report IEC 61850, [Online] Available:  
[https://library.e.abb.com/public/a56430e1e7c06fdcf12577a00043ab8b/3BSE063756\\_en\\_ABB\\_Review\\_Special\\_Report\\_IEC\\_61850.pdf](https://library.e.abb.com/public/a56430e1e7c06fdcf12577a00043ab8b/3BSE063756_en_ABB_Review_Special_Report_IEC_61850.pdf).
- [2] K.P. Brand, C. Brunner and W. Wimmer, "Substation Automation Handbook" UAC 2003, ISBN 3-85759-951-5, 2003
- [3] E. Chikuni, "Power System and Substation Automation," Cape Peninsula University of Technology, South Africa, [Online] Available:  
[https://scadahacker.com/library/Documents/ICS\\_Basics/InTech%20-%20Power%20System%20and%20Substation%20Automation.pdf](https://scadahacker.com/library/Documents/ICS_Basics/InTech%20-%20Power%20System%20and%20Substation%20Automation.pdf)
- [4] R.E. Mackiewicz, "Overview of IEC 61850 and Benefits," in Power Systems Conference and Exposition, 2006. PSCE '06. 2006 IEEE PES, vol., no., pp.623,630.
- [5] IEC 61850. (2015, January 14). In Wikipedia, The Free Encyclopedia. Retrieved on February 25<sup>th</sup>, 2015, from [http://en.wikipedia.org/w/index.php?title=IEC\\_61850&oldid=642524536](http://en.wikipedia.org/w/index.php?title=IEC_61850&oldid=642524536).
- [6] IEC standard for Communication Networks and Systems in Substations, Part 5: Communication Requirements for Functions and Device Models, IEC 61850-5, First Edition, (Jul. 2003).

- [7] IEC standard for Communication networks and systems for power utility automation, Part 8-1: Specific communication service mapping (SCSM) – Mappings to MMS (ISO 9506-1 and ISO 9506-2) and to ISO/IEC 8802-3, IEC 61850-8-1, Second Edition, (Jun. 2011).
- [8] IEC standard for Communication networks and systems for power utility automation, Part 9-2: Specific communication service mapping (SCSM) – Sampled values over ISO/IEC 8802-3, IEC 61850-9-2, Second Edition, (Sep. 2011).
- [9] B.A.H. Wickremasuriya, K.K.M.S. Kariyawasam and A.D. Rajapakse “A Laboratory Setup for Teaching IEC 61850 based Substation Automation,” *2015 CIGRÉ Canada Conference*, in press.
- [10] D. McGinn, M. G. Adamiak, M. Goraj and J. Cardenas, "Reducing conventional copper signaling in high voltage substations with IEC 61850 process bus system," in *PowerTech, 2009 IEEE Bucharest*, vol., no., pp.1-8, June 28 2009-July 2 2009.
- [11] IEC standard for Communication Networks and Systems in Substations, Part 7-1: Basic communication structure for substation and feeder equipment - Principles and models, IEC 61850-7-1, First Edition, (Jul. 2003).
- [12] IEC standard for Communication networks and systems for power utility automation – Part 6: Configuration description language for

communication in electrical substations related to IEDs, IEC 61850-6, Second Edition, (Dec. 2009).

- [13] C. Fernandes, S. Borkar and J. Gohil, "Testing of Goose Protocol of IEC61850 Standard in Protection IED," International Journal of Computer Applications (0975 – 8887) Volume 93 – No 16, May 2014.
- [14] UCA International Users Group, "Implementation guideline for digital interface to instrument transformers using IEC 61850," R2-1, UCA Int. Users Group, Raleigh, NC, USA, 2004.
- [15] L. F. Santos, "Substation Automation Process Bus System design and experiences with IEC 61850-9-2 and NCITs", ABB Group, [Online]Available:[http://www02.abb.com/global/gad/gad02465.nsf/59bddcf5e4536d06c125778c0028fa3c/0bccb6b99be39eda83257a8b0056716c/\\$FILE/Process+Bus.pdf](http://www02.abb.com/global/gad/gad02465.nsf/59bddcf5e4536d06c125778c0028fa3c/0bccb6b99be39eda83257a8b0056716c/$FILE/Process+Bus.pdf).
- [16] IEC standard for Communication networks and systems for power utility automation - Part 90-5: Use of IEC 61850 to transmit synchrophasor information according to IEEE C37.118, First Edition (May 2012).
- [17] H. Falk, SISCO, USA, "IEC 61850-90-5 - an Overview", PAC World, December 2012 Issue, Retrieved on December 30<sup>th</sup>, 2015, from [https://www.pacw.org/issue/december\\_2012\\_issue/iec\\_61850905\\_an\\_overview/iec\\_61850905\\_an\\_overview/complete\\_article/1.html](https://www.pacw.org/issue/december_2012_issue/iec_61850905_an_overview/iec_61850905_an_overview/complete_article/1.html).

- [18] J. M. Gers and E. J. Holmes, "Protection of Electricity Distribution Networks" (2nd Edition), Institution of Engineering and Technology, 2004, ISBN: 978-0-86341-357-5.
- [19] E. Bakie, C. Westhoff, N. Fischer and J. Bell, "Voltage and Current Inversion Challenges When Protecting Series-Compensated Lines – A Case Study," in 42nd Annual Western Protective Relay Conference Spokane, Washington, October 20–22, 2015.
- [20] D.C. Robertson, O.I. Camps, J.S. Mayer and W. B. Gish, "Wavelets and electromagnetic power system transients," IEEE Transactions on Power Del., vol.11, no.2, pp.1050-1058, Apr 1996.
- [21] V. Giurgiutiu and L. Yu, "Comparison of Short-time Fourier Transform and Wavelet Transform of Transient and Tone Burst Wave Propagation Signals For Structural Health Monitoring," 4<sup>th</sup> International Workshop on Structural Health Monitoring, Stanford University, Stanford, CA, September, 2003.
- [22] N. Mehala and R. Dahiya, "A Comparative Study of FFT, STFT and Wavelet Techniques for Induction Machine Fault Diagnostic Analysis," 7th WSEAS int. conf. on computational intelligence, man-machine systems and cybernetics (CIMMACS '08)
- [23] N. Perera and A. D. Rajapakse, "Series-Compensated Double-Circuit Transmission Line Protection Using Directions of Current Transients",

- IEEE Transactions on Power Del., vol. 28, no. 3, pp.1566- 1575 , July 2013.
- [24] N. Perera, A. D. Rajapakse, and T. Buchholzer, “Isolation of faults in distribution networks with distributed generators,” IEEE Transactions on Power Del., vol. 23, no. 4, pp. 2347–2355, Oct. 2008.
- [25] N. Perera, A. D. Rajapakse, and D. Muthumuni, “Wavelet based transient directional method for busbar protection,” presented at the Int. Conf. Power Systems Transients (IPST), Delft, the Netherlands, Jun. 14–17, 2011.
- [26] M. Misiti and Y. Misiti, Georges Oppenheim and Jean-Michel Poggi, “Wavelet Toolbox User’s Guide for use with Matlab (Version 1)”, The MathWorks, Inc., March 1996.
- [27] Wavelet Properties Browser, In WAVELET BROWSER BY PYWAVELETS, Retrieved on December 30<sup>th</sup>, 2015, from <http://wavelets.pybytes.com/>.
- [28] RTDS Technologies Inc. “RTDS Hardware Manual - GTNET Network Interface Card,” January 2014 rev 03.
- [29] Systems Integration Specialists Company, Inc. (SISCO), “MMS Lite, IEC 61850 for Embedded Systems,” Retrieved on April 06<sup>th</sup>, 2016, from [http://www.sisconet.com/wp-content/uploads/2015/06/MktLit\\_MMS-Lite\\_062015.pdf](http://www.sisconet.com/wp-content/uploads/2015/06/MktLit_MMS-Lite_062015.pdf).



- [30] G. Benmouyal, "Removal of DC-offset in current waveforms using digital mimic filtering," *IEEE Transactions on Power Del.*, vol.10, no.2, pp.621-630, Apr 1995.
- [31] M. Paolone, *Synchrophasor fundamentals: from computation to implementation*, Tutorial, IEEE PES GM, Vancouver, July 21-25, 2013.
- [32] K.P. Brand, C. Brunner and W. Wimmer, "Design of IEC 61850 based Substation Automation Systems according to Customer Requirements," in *CIGRE Plenary Meeting*, Paris, 2004, Session of SC B5, Paper B5-103.
- [33] M. Kezunovic, J. Ren and S. Lotfifard, "Design, Modeling and Evaluation of Protective Relays for Power Systems" Edition 1, Springer International Publishing, 2016.
- [34] M.G. Kanabar, T.S. Sidhu and M.R.D. Zadeh, "Laboratory Investigation of IEC 61850-9-2-Based Busbar and Distance Relaying With Corrective Measure for Sampled Value Loss/Delay," *IEEE Transactions on Power Del.*, vol.26, no.4, pp.2587-2595, Oct. 2011.
- [35] D.M.E Ingram, P Schaub, R.R. Taylor and D.A. Campbell, "System-Level Tests of Transformer Differential Protection Using an IEC 61850 Process Bus," *IEEE Transactions on Power Del.*, vol.29, no.3, pp.1382-1389, June 2014.
- [36] N. Perera, K. Narendra and D. Fedirchuk, "Power system fault zone detection", U.S. Patent 20130015878 A1, Jan 17, 2013.

[37] PCS-221 Merging Unit, Datasheet, NR Electric Co., Ltd., Retrieved on December 30<sup>th</sup>, 2015, from <http://www.nrec.com/en/product/PCS-221.html>.

[38] Analog Merging Unit, Datasheet, VIZIMAX Inc., Retrieved on November 11<sup>th</sup>, 2015, from <http://www.vizimax.com/knowledge-center/85-english/mergingunit/266-datasheets>.

# Appendix A

## I. IEC 61850 Service Modules

In section I of Appendix A, some of the important information regarding the software libraries developed by Kalkitech Pvt. Ltd are provided. Information given below are taken from the user manual provided (University Of Manitoba, IEC61850 Library APIs. User Manual, V 0.4).

### **INITIALIZATION MODULE**

#### List of APIs

- Set\_Log\_Level
- Initialize\_61850\_Library
- Close\_61850\_Library

#### Configuration of Parameters

Definition of the structure

```
typedef struct {
    char startUp_File[K_STRING_SIZE];
    char scl_conf_file[K_STRING_SIZE];
    char ied_name[K_STRING_SIZE];
    char goose_network_ID[K_STRING_SIZE];
    char sv_network_ID[K_STRING_SIZE];
    char accPoint_name[K_STRING_SIZE];
}CONFIG;
```

With this structure, user can specify the configuration parameters.

- `startUp_File` - The startup file to be used by the IEC 61850 library.
- `scl_conf_file` - SCL Configuration file to be used by the IEC 61850 library.
- `ied_name` - IED name as in SCL the configuration file.
- `goose_network_ID` - Network card to be used by the Goose publisher/subscriber.
- `sv_network_ID` - Network card to be used by the SV publisher/subscriber.
- `accPoint_name` - Access point name as specified in SCL configuration file.

## **SERVER MODULE**

Server module handles all the IEC 61850 server functions. Before using any API's in this module, the IEC 61850 server must be initialized by the initialization module. Functions in this module include,

- Server.
- Report service.
- Read and write variable values.
- Register client writes by a user callback function.
- Read the events occurred

NOTE: It will not be allowed to read and write variable values and details if none of the functionality (goose publisher, goose subscriber, sampled value publisher, sampled value publisher or server) are running.

List of APIs

- Get\_Total\_Variable\_Count
- Get\_Variable\_Details
- Start\_Server
- Start\_Report\_Service
- Stop\_Server
- Stop\_Report\_Service
- Read\_Variable\_Value
- Write\_Variable\_Value
- Register\_Client\_Writes
- Get\_Event\_Count
- Get\_Event

## **GOOSE PUBLISHER MODULE**

This module is responsible for the GOOSE publisher function. This module publishes new GOOSE messages, when a dataset variable configured in any goose control block changes. And this also handles the retransmission of goose messages.

### List of APIs

- Start\_Goose\_Publisher
- Stop\_Goose\_Publisher
- Start\_Goose\_Retransmission
- Stop\_Goose\_Retransmission

## **GOOSE SUBSCRIBER MODULE**

### List of APIs

- Start\_Goose\_Subscriber
- Stop\_Goose\_Subscriber
- Register\_Goose\_Events

## **SAMPLED VALUE SUBSCRIBER MODULE**

This module handles all the sampled value subscription related activities. It discovers the configured sampled value streams from the network. User shall select the sampled value stream to subscribe from the network. Received sampled value packets will be stored, which allows user to analyze them.

### List of APIs

- Start\_SV\_Subscriber
- Stop\_SV\_Subscriber
- Discover\_SV\_Streams

- Register\_SV\_Stream
- Unregister\_SV\_Stream
- Get\_Subscribed\_SVPackets\_Count
- Get\_SV\_Packet

Definition of the Structure

```
typedef struct{
    short smp_count;
    short smp_rate;
    unsigned long seconds;
    unsigned long micro;
    unsigned long quality;
    int smp_data_len;
    char *smp_data;
}SV_DETAILS;
```

Structure is used to exchange sampled value information between user application and IEC 61850 library. IEC61850 library returns the subscribed SV packet details using this structure.

- smp\_count - sample count.
- smp\_rate - sample rate.
- Seconds - refresh time seconds.
- micro - refresh time micro seconds.
- quality - refresh time quality.
- smp\_data\_len - sample data length.
- smp\_data - Pointer to the sample data buffer.

# SAMPLED VALUE PUBLISHER MODULE

## List of APIs

- Start\_SV\_Publisher
- Stop\_SV\_Publisher
- Get\_SV\_Publisher\_Streams
- Fill\_SV\_Data

## II. CID file of the RTDS™ for SV publication

Given below is the CID file of the RTDS™ used for the publication of sampled values.

```
<?xml version="1.0" encoding="UTF-8"?>
<SCL xmlns="http://www.iec.ch/61850/2003/SCL" xmlns:xsi="http://www.w3.org/2001/XMLSchema-instance"
xsi:schemaLocation="http://www.iec.ch/61850/2003/SCL c:\SCL\SCL.xsd">
<Header id="9-2LE-Spec" nameStructure="IEDName" version="0.7" revision="1"/>
  <Substation name="RTDS">
    <VoltageLevel name="230kV">
      <Bay name="5L1">
        <ConductingEquipment name="Inn" type="CTR">
          <SubEquipment name="A" phase="A">
            <LNode iedName="GTNETSV1" IdInst="MU00" lnClass="TCCTR" lnInst="1"/>
          </SubEquipment>
          <SubEquipment name="B" phase="B">
            <LNode iedName="GTNETSV1" IdInst="MU00" lnClass="TCCTR" lnInst="2"/>
          </SubEquipment>
          <SubEquipment name="C" phase="C">
            <LNode iedName="GTNETSV1" IdInst="MU00" lnClass="TCCTR" lnInst="3"/>
          </SubEquipment>
          <SubEquipment name="N" phase="N">
            <LNode iedName="GTNETSV1" IdInst="MU00" lnClass="TCCTR" lnInst="4"/>
          </SubEquipment>
        </ConductingEquipment>
        <ConductingEquipment name="Unn" type="VTR">
          <SubEquipment name="A" phase="A">
            <LNode iedName="GTNETSV1" IdInst="MU00" lnClass="TVTR" lnInst="1"/>
          </SubEquipment>
          <SubEquipment name="B" phase="B">
            <LNode iedName="GTNETSV1" IdInst="MU00" lnClass="TVTR" lnInst="2"/>
          </SubEquipment>
          <SubEquipment name="C" phase="C">
            <LNode iedName="GTNETSV1" IdInst="MU00" lnClass="TVTR" lnInst="3"/>
          </SubEquipment>
          <SubEquipment name="N" phase="N">
            <LNode iedName="GTNETSV1" IdInst="MU00" lnClass="TVTR" lnInst="4"/>
          </SubEquipment>
        </ConductingEquipment>
      </Bay>
    </VoltageLevel>
  </Substation>
</SCL>
```



```

</Bay>
</VoltageLevel>
</Substation>
<Communication>
  <SubNetwork name="NONE" type="8-MMS">
    <ConnectedAP iedName="GTNETSV1" apName="P1">
      <SMV IdInst="MU00" cbName="MSVCB01">
        <Address>
          <P type="VLAN-ID">000</P>
          <P type="VLAN-PRIORITY">4</P>
          <P type="MAC-Address">01-0C-CD-04-01-1D</P>
          <P type="APPID">4000</P>
        </Address>
      </SMV>
    </ConnectedAP>
  </SubNetwork>
</Communication>
<IED name="GTNETSV1" manufacturer="RTDS Technologies Inc." >
  <Services>
    <ConfDataSet maxAttributes="100" max="2" modify="0"/>
    <ReadWrite/>
  </Services>
  <AccessPoint name="P1">
    <Server>
      <Authentication/>
      <LDevice inst="MU00">
        <LN0 InType="9-2LELLN0" InClass="LLN0" inst="">
          <DataSet name="PhsMeas1">
            <FCDA IdInst="MU00" InClass="TCTR" InInst="1" doName="Amp" daName="instMag.i" fc="MX"/>
            <FCDA IdInst="MU00" InClass="TCTR" InInst="1" doName="Amp" daName="q" fc="MX"/>
            <FCDA IdInst="MU00" InClass="TCTR" InInst="2" doName="Amp" daName="instMag.i" fc="MX"/>
            <FCDA IdInst="MU00" InClass="TCTR" InInst="2" doName="Amp" daName="q" fc="MX"/>
            <FCDA IdInst="MU00" InClass="TCTR" InInst="3" doName="Amp" daName="instMag.i" fc="MX"/>
            <FCDA IdInst="MU00" InClass="TCTR" InInst="3" doName="Amp" daName="q" fc="MX"/>
            <FCDA IdInst="MU00" InClass="TCTR" InInst="4" doName="Amp" daName="instMag.i" fc="MX"/>
            <FCDA IdInst="MU00" InClass="TCTR" InInst="4" doName="Amp" daName="q" fc="MX"/>
            <FCDA IdInst="MU00" InClass="TVTR" InInst="1" doName="Vol" daName="instMag.i" fc="MX"/>
            <FCDA IdInst="MU00" InClass="TVTR" InInst="1" doName="Vol" daName="q" fc="MX"/>
            <FCDA IdInst="MU00" InClass="TVTR" InInst="2" doName="Vol" daName="instMag.i" fc="MX"/>
            <FCDA IdInst="MU00" InClass="TVTR" InInst="2" doName="Vol" daName="q" fc="MX"/>
            <FCDA IdInst="MU00" InClass="TVTR" InInst="3" doName="Vol" daName="instMag.i" fc="MX"/>
            <FCDA IdInst="MU00" InClass="TVTR" InInst="3" doName="Vol" daName="q" fc="MX"/>
            <FCDA IdInst="MU00" InClass="TVTR" InInst="4" doName="Vol" daName="instMag.i" fc="MX"/>
            <FCDA IdInst="MU00" InClass="TVTR" InInst="4" doName="Vol" daName="q" fc="MX"/>
          </DataSet>
          <SampledValueControl name="MSVCB01" dataSet="PhsMeas1" smvID="EXER1MU0001" smpRate="80" nofASDU="1" confRev="0">
            <SmvOpts refreshTime="false" sampleSynchronized="true" sampleRate="false" security="false" dataRef="false"/>
          </SampledValueControl>
        </LN0>
        <LN desc="" InType="9-2LELPHD" InClass="LPHD" inst="1"/>
        <LN InType="9-2LETCTR" InClass="TCTR" inst="1"/>
        <LN InType="9-2LETCTR" InClass="TCTR" inst="2"/>
        <LN InType="9-2LETCTR" InClass="TCTR" inst="3"/>
        <LN InType="9-2LETCTR" InClass="TCTR" inst="4"/>
        <LN InType="9-2LETVTR" InClass="TVTR" inst="1"/>
        <LN InType="9-2LETVTR" InClass="TVTR" inst="2"/>
        <LN InType="9-2LETVTR" InClass="TVTR" inst="3"/>
        <LN InType="9-2LETVTR" InClass="TVTR" inst="4"/>
      </LDevice>
    </Server>
  </AccessPoint>
</IED>
<DataTypeTemplates>
  <LNodeType id="9-2LELPHD" InClass="LPHD">
    <DO name="PhyNam" type="9-2LEPHYNAM"/>
    <DO name="PhyHealth" type="9-2LEINS_HEALTH"/>
    <DO name="Proxy" type="9-2LEPROXY"/>
  </LNodeType>
  <LNodeType id="9-2LELLN0" InClass="LLN0">
    <DO name="Mod" type="9-2LEINC"/>
    <DO name="Beh" type="9-2LEINS_BEH"/>
    <DO name="Health" type="9-2LEINS_HEALTH"/>
    <DO name="NamPlt" type="9-2LELN0LPL"/>
  </LNodeType>
  <LNodeType id="9-2LETCTR" InClass="TCTR">
    <DO name="Mod" type="9-2LEINC"/>
    <DO name="Beh" type="9-2LEINS_BEH"/>
    <DO name="Health" type="9-2LEINS_HEALTH"/>
  </LNodeType>

```

```

        <DO name="NamPlt" type="9-2LELNLPL"/>
        <DO name="Amp" type="9-2LESVAmp"/>
    </LNodeType>
    <LNodeType id="9-2LETVTR" InClass="TVTR">
        <DO name="Mod" type="9-2LEINC"/>
        <DO name="Beh" type="9-2LEINS_BEH"/>
        <DO name="Health" type="9-2LEINS_HEALTH"/>
        <DO name="NamPlt" type="9-2LELNLPL"/>
        <DO name="Vol" type="9-2LESVVol"/>
    </LNodeType>
    <DOType id="9-2LEINS_BEH" cdc="INS">
        <DA name="stVal" bType="Enum" type="Beh" fc="ST" dchg="true">
            <Val>on</Val>
        </DA>
        <DA name="q" bType="Quality" fc="ST" valKind="RO" qchg="true"/>
        <DA name="t" bType="Timestamp" fc="ST" valKind="RO"/>
    </DOType>
    <DOType id="9-2LEINS_HEALTH" cdc="INS">
        <DA name="stVal" bType="Enum" type="HealthKind" fc="ST" dchg="true">
            <Val>Ok</Val>
        </DA>
        <DA name="q" bType="Quality" fc="ST" valKind="RO" qchg="true"/>
        <DA name="t" bType="Timestamp" fc="ST" valKind="RO"/>
    </DOType>
    <DOType id="9-2LESVAmp" cdc="SAV">
        <DA name="instMag" bType="Struct" type="9-2LEAV" fc="MX"/>
        <DA name="q" bType="Quality" fc="MX" valKind="RO" qchg="true"/>
        <DA name="sVC" bType="Struct" type="9-2LEsVCamp" fc="CF"/>
    </DOType>
    <DOType id="9-2LESVVol" cdc="SAV">
        <DA name="instMag" bType="Struct" type="9-2LEAV" fc="MX"/>
        <DA name="q" bType="Quality" fc="MX" valKind="RO" qchg="true"/>
        <DA name="sVC" bType="Struct" type="9-2LEsVCVol" fc="CF"/>
    </DOType>
    <DOType id="9-2LEINC" cdc="INC">
        <DA name="stVal" fc="ST" bType="Enum" type="Mod" dchg="true">
            <Val>on</Val>
        </DA>
        <DA name="q" bType="Quality" fc="ST" valKind="RO" qchg="true"/>
        <DA name="t" bType="Timestamp" fc="ST" valKind="RO"/>
        <DA name="ctlModel" fc="CF" bType="Enum" type="CtlModelKind">
            <Val>status-only</Val>
        </DA>
    </DOType>
    <DOType id="9-2LELN0LPL" cdc="LPL">
        <DA name="vendor" bType="VisString255" fc="DC"/>
        <DA name="swRev" bType="VisString255" fc="DC"/>
        <DA name="d" bType="VisString255" fc="DC"/>
        <DA name="configRev" bType="VisString255" fc="DC"/>
        <DA name="ldNs" bType="VisString255" fc="EX">
            <Val>IEC 61850-7-4:2003</Val>
        </DA>
    </DOType>
    <DOType id="9-2LELNLPL" cdc="LPL">
        <DA name="vendor" bType="VisString255" fc="DC"/>
        <DA name="swRev" bType="VisString255" fc="DC"/>
        <DA name="d" bType="VisString255" fc="DC"/>
    </DOType>
    <DOType id="9-2LEPROXY" cdc="SPS">
        <DA name="stVal" bType="BOOLEAN" dchg="true" fc="ST">
            <Val>>false</Val>
        </DA>
        <DA name="q" bType="Quality" fc="ST" valKind="RO" qchg="true"/>
        <DA name="t" bType="Timestamp" fc="ST" valKind="RO"/>
    </DOType>
    <DOType id="9-2LEPHYNAM" cdc="DPL">
        <DA name="vendor" bType="VisString255" fc="DC"/>
        <DA name="hwRev" bType="VisString255" fc="DC"/>
        <DA name="swRev" bType="VisString255" fc="DC"/>
        <DA name="serNum" bType="VisString255" fc="DC"/>
        <DA name="model" bType="VisString255" fc="DC"/>
        <DA name="location" bType="VisString255" fc="DC"/>
        <DA name="cdcNs" bType="VisString255" fc="EX"/>
    </DOType>
    <DAType id="9-2LEAV">
        <BDA name="i" bType="INT32"/>
    </DAType>
    <DAType id="9-2LEsVCamp">

```

```

        <BDA name="scaleFactor" bType="FLOAT32">
            <Val>0.001</Val>
        </BDA>
        <BDA name="offset" bType="FLOAT32">
            <Val>0</Val>
        </BDA>
    </DataType>
    <DataType id="9-2LEsVCVol">
        <BDA name="scaleFactor" bType="FLOAT32">
            <Val>0.01</Val>
        </BDA>
        <BDA name="offset" bType="FLOAT32">
            <Val>0</Val>
        </BDA>
    </DataType>
    <EnumType id="Beh">
        <EnumVal ord="1">on</EnumVal>
        <EnumVal ord="2">blocked</EnumVal>
        <EnumVal ord="3">test</EnumVal>
        <EnumVal ord="4">test/blocked</EnumVal>
        <EnumVal ord="5">off</EnumVal>
    </EnumType>
    <EnumType id="Mod">
        <EnumVal ord="1">on</EnumVal>
        <EnumVal ord="2">blocked</EnumVal>
        <EnumVal ord="3">test</EnumVal>
        <EnumVal ord="4">test/blocked</EnumVal>
        <EnumVal ord="5">off</EnumVal>
    </EnumType>
    <EnumType id="HealthKind">
        <EnumVal ord="1">Ok</EnumVal>
        <EnumVal ord="2">Warning</EnumVal>
        <EnumVal ord="3">Alarm</EnumVal>
    </EnumType>
    <EnumType id="CtlModelKind">
        <EnumVal ord="0">status-only</EnumVal>
        <EnumVal ord="1">direct-with-normal-security</EnumVal>
        <EnumVal ord="2">sbo-with-normal-security</EnumVal>
        <EnumVal ord="3">direct-with-enhanced-security</EnumVal>
        <EnumVal ord="4">sbo-with-enhanced-security</EnumVal>
    </EnumType>
</DataTypeTemplates>
</SCL>

```

### III. CID file of the Line Protection IED

```

<?xml version="1.0" encoding="UTF-8"?>
<!-- This file is generated using KALKI SCL Manager IEC61850 Configuration Tool (www.kalkitech.com)-->
<SCL xmlns="http://www.iec.ch/61850/2003/SCL" xmlns:xsd="http://www.w3.org/2001/XMLSchema">
  <Header id="" version="4.0.0 Beta" revision="" toolID="" nameStructure="IEDName" />
  <Communication>
    <SubNetwork name="subnetwork1" type="8-MMS">
      <Text>Station bus</Text>
      <BitRate unit="b/s">10</BitRate>
      <ConnectedAP iedName="smv" apName="accessPoint1">
        <Address>
          <P type="IP">192.168.100.81</P>
          <P type="IP-SUBNET">255.255.255.0</P>
          <P type="IP-GATEWAY">192.168.100.1</P>
          <P type="OSI-TSEL">0001</P>
          <P type="OSI-PSEL">00000001</P>
          <P type="OSI-SSEL">0001</P>
        </Address>
        <GSE IdInst="IDevice1" cbName="GoosePublisher">
          <Address>
            <P type="MAC-Address">01-0C-CD-01-01-CD</P>
            <P type="APPID">01</P>
            <P type="VLAN-ID">0</P>
            <P type="VLAN-PRIORITY">4</P>
          </Address>
        </GSE>
      </ConnectedAP>
    </SubNetwork>
  </Communication>

```

```

    </Address>
  </GSE>
</ConnectedAP>
</SubNetwork>
</Communication>
<IED name="smv">
  <Services>
    <DynAssociation />
    <GetDirectory />
    <GetDataObjectDefinition />
    <GetDataSetValue />
    <DataSetDirectory />
    <ReadWrite />
    <GetCBValues />
    <ConfLNs fixPrefix="true" fixLnInst="true" />
    <GOOSE max="5" />
    <GSSE max="5" />
    <FileHandling />
    <GSEDir />
    <TimerActivatedControl />
  </Services>
  <AccessPoint name="accessPoint1">
    <Server>
      <Authentication />
      <LDevice inst="IDevice1">
        <Private type="SMVMapping">GTNETSV1\MU02\LLN0$M$SMVCB01\PhsMeas1\EXER1MU0001\01-0C-CD-04-01-
1D|FF-FF-FF-FF-FF-FF|
          [NumDatasetVars|16|
            |Primitive|smv|Device1|TCTR1$MX$Amp$InstMag$|GTNETSV1\MU02.MSVCB01\SV_Publisher_Data\MU02\TCTR1$MX$Amp$InstMag$|
            |Primitive|smv|Device1|TCTR1$MX$Amp$|GTNETSV1\MU02.MSVCB01\SV_Publisher_Data\MU02\TCTR1$MX$Amp$|
            |Primitive|smv|Device1|TCTR2$MX$Amp$InstMag$|GTNETSV1\MU02.MSVCB01\SV_Publisher_Data\MU02\TCTR2$MX$Amp$InstMag$|
            |Primitive|smv|Device1|TCTR2$MX$Amp$|GTNETSV1\MU02.MSVCB01\SV_Publisher_Data\MU02\TCTR2$MX$Amp$|
            |Primitive|smv|Device1|TCTR3$MX$Amp$InstMag$|GTNETSV1\MU02.MSVCB01\SV_Publisher_Data\MU02\TCTR3$MX$Amp$InstMag$|
            |Primitive|smv|Device1|TCTR3$MX$Amp$|GTNETSV1\MU02.MSVCB01\SV_Publisher_Data\MU02\TCTR3$MX$Amp$|
            |Primitive|smv|Device1|TCTR4$MX$Amp$InstMag$|GTNETSV1\MU02.MSVCB01\SV_Publisher_Data\MU02\TCTR4$MX$Amp$InstMag$|
            |Primitive|smv|Device1|TCTR4$MX$Amp$|GTNETSV1\MU02.MSVCB01\SV_Publisher_Data\MU02\TCTR4$MX$Amp$|
            |Primitive|smv|Device1|TVTR1$MX$Vol$InstMag$|GTNETSV1\MU02.MSVCB01\SV_Publisher_Data\MU02\TCTR1$MX$Vol$InstMag$|
            |Primitive|smv|Device1|TVTR1$MX$Vol$|GTNETSV1\MU02.MSVCB01\SV_Publisher_Data\MU02\TCTR1$MX$Vol$|
            |Primitive|smv|Device1|TVTR2$MX$Vol$InstMag$|GTNETSV1\MU02.MSVCB01\SV_Publisher_Data\MU02\TCTR2$MX$Vol$InstMag$|
            |Primitive|smv|Device1|TVTR2$MX$Vol$|GTNETSV1\MU02.MSVCB01\SV_Publisher_Data\MU02\TCTR2$MX$Vol$|
            |Primitive|smv|Device1|TVTR3$MX$Vol$InstMag$|GTNETSV1\MU02.MSVCB01\SV_Publisher_Data\MU02\TCTR3$MX$Vol$InstMag$|
            |Primitive|smv|Device1|TVTR3$MX$Vol$|GTNETSV1\MU02.MSVCB01\SV_Publisher_Data\MU02\TCTR3$MX$Vol$|
            |Primitive|smv|Device1|TVTR4$MX$Vol$InstMag$|GTNETSV1\MU02.MSVCB01\SV_Publisher_Data\MU02\TCTR4$MX$Vol$InstMag$|
            |Primitive|smv|Device1|TVTR4$MX$Vol$|GTNETSV1\MU02.MSVCB01\SV_Publisher_Data\MU02\TCTR4$MX$Vol$|
          </Private>
          <LN0 InClass="LLN0" InType="LLN04" inst="">
            <DataSet name="Dataset1" desc="Goose publisher dataset">
              <FCDA IdInst="IDevice1" InClass="GGIO" fc="ST" InInst="1" prefix="GSPUB_" doName="Ind1" daName="stVal" />
              <FCDA IdInst="IDevice1" InClass="GGIO" fc="ST" InInst="1" prefix="GSPUB_" doName="Ind2" daName="stVal" />
              <FCDA IdInst="IDevice1" InClass="GGIO" fc="ST" InInst="1" prefix="GSPUB_" doName="Ind3" daName="stVal" />
              <FCDA IdInst="IDevice1" InClass="GGIO" fc="ST" InInst="1" prefix="GSPUB_" doName="Ind4" daName="stVal" />
              <FCDA IdInst="IDevice1" InClass="GGIO" fc="ST" InInst="1" prefix="GSPUB_" doName="Ind5" daName="stVal" />
            </DataSet>
            <DOI name="Mod">
              <DAI name="stVal">
                <Val>on</Val>
              </DAI>
            </DOI>
            <DOI name="Beh">
              <DAI name="stVal">
                <Val>on</Val>
              </DAI>
            </DOI>
            <DOI name="Health">
              <DAI name="stVal">
                <Val>Ok</Val>
              </DAI>
            </DOI>
          </LN0>
        </LDevice>
      </Server>
    </AccessPoint>
  </IED>

```

```

</DAI>
</DOI>
<GSEControl name="GoosePublisher" appID="UoMg1" type="GOOSE" dataSet="Dataset1" confRev="1" />
</LN0>
<LN InClass="LPHD" InType="LPHD4" inst="1" prefix="">
<DOI name="PhyHealth">
<DAI name="stVal">
<Val>Ok</Val>
</DAI>
</DOI>
</LN>
<LN InClass="GGIO" InType="GGIO1" inst="1" prefix="GSPUB_">
<DOI name="Mod">
<DAI name="stVal">
<Val>on</Val>
</DAI>
</DOI>
<DOI name="Beh">
<DAI name="stVal">
<Val>on</Val>
</DAI>
</DOI>
<DOI name="Health">
<DAI name="stVal">
<Val>Ok</Val>
</DAI>
</DOI>
</LN>
<LN InClass="TCTR" InType="TCTR1" inst="1" prefix="">
<DOI name="Mod">
<DAI name="stVal">
<Val>on</Val>
</DAI>
</DOI>
<DOI name="Beh">
<DAI name="stVal">
<Val>on</Val>
</DAI>
</DOI>
<DOI name="Health">
<DAI name="stVal">
<Val>Ok</Val>
</DAI>
</DOI>
</LN>
<LN InClass="TVTR" InType="TVTR1" inst="1" prefix="">
<DOI name="Mod">
<DAI name="stVal">
<Val>on</Val>
</DAI>
</DOI>
<DOI name="Beh">
<DAI name="stVal">
<Val>on</Val>
</DAI>
</DOI>
<DOI name="Health">
<DAI name="stVal">
<Val>Ok</Val>
</DAI>
</DOI>
</LN>
<LN InClass="TCTR" InType="TCTR2" inst="2" prefix="">
<DOI name="Mod">
<DAI name="stVal">
<Val>on</Val>
</DAI>
</DOI>
<DOI name="Beh">
<DAI name="stVal">
<Val>on</Val>
</DAI>
</DOI>
<DOI name="Health">
<DAI name="stVal">
<Val>Ok</Val>
</DAI>
</DOI>

```

```

</LN>
<LN lnClass="TCTR" lnType="TCTR3" inst="3" prefix="">
  <DOI name="Mod">
    <DAI name="stVal">
      <Val>on</Val>
    </DAI>
  </DOI>
  <DOI name="Beh">
    <DAI name="stVal">
      <Val>on</Val>
    </DAI>
  </DOI>
  <DOI name="Health">
    <DAI name="stVal">
      <Val>Ok</Val>
    </DAI>
  </DOI>
</LN>
<LN lnClass="TCTR" lnType="TCTR3" inst="4" prefix="">
  <DOI name="Mod">
    <DAI name="stVal">
      <Val>on</Val>
    </DAI>
  </DOI>
  <DOI name="Beh">
    <DAI name="stVal">
      <Val>on</Val>
    </DAI>
  </DOI>
  <DOI name="Health">
    <DAI name="stVal">
      <Val>Ok</Val>
    </DAI>
  </DOI>
</LN>
<LN lnClass="TCTR" lnType="TCTR3" inst="5" prefix="">
  <DOI name="Mod">
    <DAI name="stVal">
      <Val>on</Val>
    </DAI>
  </DOI>
  <DOI name="Beh">
    <DAI name="stVal">
      <Val>on</Val>
    </DAI>
  </DOI>
  <DOI name="Health">
    <DAI name="stVal">
      <Val>Ok</Val>
    </DAI>
  </DOI>
</LN>
<LN lnClass="TCTR" lnType="TCTR3" inst="6" prefix="">
  <DOI name="Mod">
    <DAI name="stVal">
      <Val>on</Val>
    </DAI>
  </DOI>
  <DOI name="Beh">
    <DAI name="stVal">
      <Val>on</Val>
    </DAI>
  </DOI>
  <DOI name="Health">
    <DAI name="stVal">
      <Val>Ok</Val>
    </DAI>
  </DOI>
</LN>
<LN lnClass="TCTR" lnType="TCTR3" inst="7" prefix="">
  <DOI name="Mod">
    <DAI name="stVal">
      <Val>on</Val>
    </DAI>
  </DOI>
  <DOI name="Beh">
    <DAI name="stVal">
      <Val>on</Val>
    </DAI>
  </DOI>

```

```

</DAI>
</DOI>
<DOI name="Health">
  <DAI name="stVal">
    <Val>Ok</Val>
  </DAI>
</DOI>
</LN>
<LN InClass="TCTR" InType="TCTR3" inst="8" prefix="">
  <DOI name="Mod">
    <DAI name="stVal">
      <Val>on</Val>
    </DAI>
  </DOI>
  <DOI name="Beh">
    <DAI name="stVal">
      <Val>on</Val>
    </DAI>
  </DOI>
  <DOI name="Health">
    <DAI name="stVal">
      <Val>Ok</Val>
    </DAI>
  </DOI>
</LN>
<LN InClass="TVTR" InType="TVTR2" inst="2" prefix="">
  <DOI name="Mod">
    <DAI name="stVal">
      <Val>on</Val>
    </DAI>
  </DOI>
  <DOI name="Beh">
    <DAI name="stVal">
      <Val>on</Val>
    </DAI>
  </DOI>
  <DOI name="Health">
    <DAI name="stVal">
      <Val>Ok</Val>
    </DAI>
  </DOI>
</LN>
<LN InClass="TVTR" InType="TVTR2" inst="3" prefix="">
  <DOI name="Mod">
    <DAI name="stVal">
      <Val>on</Val>
    </DAI>
  </DOI>
  <DOI name="Beh">
    <DAI name="stVal">
      <Val>on</Val>
    </DAI>
  </DOI>
  <DOI name="Health">
    <DAI name="stVal">
      <Val>Ok</Val>
    </DAI>
  </DOI>
</LN>
<LN InClass="TVTR" InType="TVTR2" inst="4" prefix="">
  <DOI name="Mod">
    <DAI name="stVal">
      <Val>on</Val>
    </DAI>
  </DOI>
  <DOI name="Beh">
    <DAI name="stVal">
      <Val>on</Val>
    </DAI>
  </DOI>
  <DOI name="Health">
    <DAI name="stVal">
      <Val>Ok</Val>
    </DAI>
  </DOI>
</LN>
<LN InClass="TVTR" InType="TVTR2" inst="5" prefix="">
  <DOI name="Mod">

```

```

    <DAI name="stVal">
      <Val>on</Val>
    </DAI>
  </DOI>
</DOI>
<DOI name="Beh">
  <DAI name="stVal">
    <Val>on</Val>
  </DAI>
</DOI>
<DOI name="Health">
  <DAI name="stVal">
    <Val>Ok</Val>
  </DAI>
</DOI>
</LN>
<LN InClass="TVTR" InType="TVTR2" inst="6" prefix="">
  <DOI name="Mod">
    <DAI name="stVal">
      <Val>on</Val>
    </DAI>
  </DOI>
  <DOI name="Beh">
    <DAI name="stVal">
      <Val>on</Val>
    </DAI>
  </DOI>
  <DOI name="Health">
    <DAI name="stVal">
      <Val>Ok</Val>
    </DAI>
  </DOI>
</LN>
<LN InClass="TVTR" InType="TVTR2" inst="7" prefix="">
  <DOI name="Mod">
    <DAI name="stVal">
      <Val>on</Val>
    </DAI>
  </DOI>
  <DOI name="Beh">
    <DAI name="stVal">
      <Val>on</Val>
    </DAI>
  </DOI>
  <DOI name="Health">
    <DAI name="stVal">
      <Val>Ok</Val>
    </DAI>
  </DOI>
</LN>
<LN InClass="TVTR" InType="TVTR2" inst="8" prefix="">
  <DOI name="Mod">
    <DAI name="stVal">
      <Val>on</Val>
    </DAI>
  </DOI>
  <DOI name="Beh">
    <DAI name="stVal">
      <Val>on</Val>
    </DAI>
  </DOI>
  <DOI name="Health">
    <DAI name="stVal">
      <Val>Ok</Val>
    </DAI>
  </DOI>
</LN>
</LDevice>
</Server>
</AccessPoint>
</IED>
<DataTypeTemplates>
<LNNodeType id="LLN04" InClass="LLN0">
  <DO name="Mod" type="INC_0" />
  <DO name="Beh" type="INS_0" />
  <DO name="Health" type="INS_1" />
  <DO name="NamPlt" type="LPL_2_NamPlt" />
</LNNodeType>
<LNNodeType id="LPHD4" InClass="LPHD">

```



```

<DO name="PhyNam" type="DPL_1_PhyNam" />
<DO name="PhyHealth" type="INS_2_PhyHealth" />
<DO name="Proxy" type="SPS_1" />
</NodeType>
<NodeType id="GGIO1" InClass="GGIO">
  <DO name="Mod" type="INC_0" />
  <DO name="Beh" type="INS_0" />
  <DO name="Health" type="INS_1" />
  <DO name="Ind1" type="SPS_1" />
  <DO name="Ind2" type="SPS_1" />
  <DO name="Ind3" type="SPS_1" />
  <DO name="Ind4" type="SPS_1" />
  <DO name="Ind5" type="SPS_1" />
</NodeType>
<NodeType id="TCTR1" InClass="TCTR">
  <DO name="Mod" type="INC_0" />
  <DO name="Beh" type="INS_0" />
  <DO name="Health" type="INS_1" />
  <DO name="NamPlt" type="LPL_1" />
  <DO name="Amp" type="SAV_1_Amp" />
</NodeType>
<NodeType id="TVTR1" InClass="TVTR">
  <DO name="Mod" type="INC_0" />
  <DO name="Beh" type="INS_0" />
  <DO name="Health" type="INS_1" />
  <DO name="NamPlt" type="LPL_1" />
  <DO name="Vol" type="SAV_1_Amp" />
</NodeType>
<NodeType id="TCTR2" InClass="TCTR">
  <DO name="Mod" type="INC_0" />
  <DO name="Beh" type="INS_0" />
  <DO name="Health" type="INS_1" />
  <DO name="NamPlt" type="LPL_1" />
  <DO name="Amp" type="SAV_1_Amp" />
</NodeType>
<NodeType id="TCTR3" InClass="TCTR">
  <DO name="Mod" type="INC_0" />
  <DO name="Beh" type="INS_0" />
  <DO name="Health" type="INS_1" />
  <DO name="NamPlt" type="LPL_1" />
  <DO name="Amp" type="SAV_1_Amp" />
</NodeType>
<NodeType id="TVTR2" InClass="TVTR">
  <DO name="Mod" type="INC_0" />
  <DO name="Beh" type="INS_0" />
  <DO name="Health" type="INS_1" />
  <DO name="NamPlt" type="LPL_1" />
  <DO name="Vol" type="SAV_1_Amp" />
</NodeType>
<DOType id="INC_0" cdc="INC">
  <DA name="stVal" type="Mod" bType="Enum" fc="ST" dchg="true" />
  <DA name="q" bType="Quality" fc="ST" qchg="true" />
  <DA name="t" bType="Timestamp" fc="ST" />
  <DA name="ctlModel" type="ctlModel" bType="Enum" fc="CF" />
</DOType>
<DOType id="INS_0" cdc="INS">
  <DA name="stVal" type="Beh" bType="Enum" fc="ST" />
  <DA name="q" bType="Quality" fc="ST" />
  <DA name="t" bType="Timestamp" fc="ST" />
</DOType>
<DOType id="INS_1" cdc="INS">
  <DA name="stVal" type="Health" bType="Enum" fc="ST" />
  <DA name="q" bType="Quality" fc="ST" />
  <DA name="t" bType="Timestamp" fc="ST" />
</DOType>
<DOType id="LPL_2_NamPlt" cdc="LPL">
  <DA name="vendor" bType="VisString255" fc="DC" />
  <DA name="swRev" bType="VisString255" fc="DC" />
  <DA name="d" bType="VisString255" fc="DC" />
  <DA name="configRev" bType="VisString255" fc="DC" />
  <DA name="IdNs" bType="VisString255" fc="EX" />
</DOType>
<DOType id="DPL_1_PhyNam" cdc="DPL">
  <DA name="vendor" bType="VisString255" fc="DC" />
</DOType>
<DOType id="INS_2_PhyHealth" cdc="INS">
  <DA name="stVal" type="PhyHealth" bType="Enum" fc="ST" dchg="true" />
  <DA name="q" bType="Quality" fc="ST" qchg="true" />

```

```

<DA name="t" bType="Timestamp" fc="ST" />
</DOType>
<DOType id="SPS_1" cdc="SPS">
<DA name="stVal" bType="BOOLEAN" fc="ST" dchg="true" />
<DA name="q" bType="Quality" fc="ST" qchg="true" />
<DA name="t" bType="Timestamp" fc="ST" />
</DOType>
<DOType id="LPL_1" cdc="LPL">
<DA name="vendor" bType="VisString255" fc="DC" />
<DA name="swRev" bType="VisString255" fc="DC" />
<DA name="d" bType="VisString255" fc="DC" />
</DOType>
<DOType id="SAV_1_Amp" cdc="SAV">
<DA name="instMag" type="AnalogueValue_1" bType="Struct" fc="MX" />
<DA name="q" bType="Quality" fc="MX" qchg="true" />
</DOType>
<DAType id="AnalogueValue_1">
<BDA name="i" bType="INT32" />
</DAType>
<EnumType id="Mod">
<EnumVal ord="1">on</EnumVal>
<EnumVal ord="2">blocked</EnumVal>
<EnumVal ord="3">test</EnumVal>
<EnumVal ord="4">test/blocked</EnumVal>
<EnumVal ord="5">off</EnumVal>
</EnumType>
<EnumType id="ctlModel">
<EnumVal ord="0">status-only</EnumVal>
<EnumVal ord="1">direct-with-normal-security</EnumVal>
<EnumVal ord="2">sbo-with-normal-security</EnumVal>
<EnumVal ord="3">direct-with-enhanced-security</EnumVal>
<EnumVal ord="4">sbo-with-enhanced-security</EnumVal>
</EnumType>
<EnumType id="Beh">
<EnumVal ord="1">on</EnumVal>
<EnumVal ord="2">blocked</EnumVal>
<EnumVal ord="3">test</EnumVal>
<EnumVal ord="4">test-blocked</EnumVal>
<EnumVal ord="5">off</EnumVal>
</EnumType>
<EnumType id="Health">
<EnumVal ord="1">Ok</EnumVal>
<EnumVal ord="2">Warning</EnumVal>
<EnumVal ord="3">Alarm</EnumVal>
</EnumType>
<EnumType id="PhyHealth">
<EnumVal ord="1">Ok</EnumVal>
<EnumVal ord="2">Warning</EnumVal>
<EnumVal ord="3">Alarm</EnumVal>
</EnumType>
</DataTypeTemplates>
</SCL>

```

# Appendix B

## I. Transmission Line Parameters

Following are the main parameters used in the transmission line model

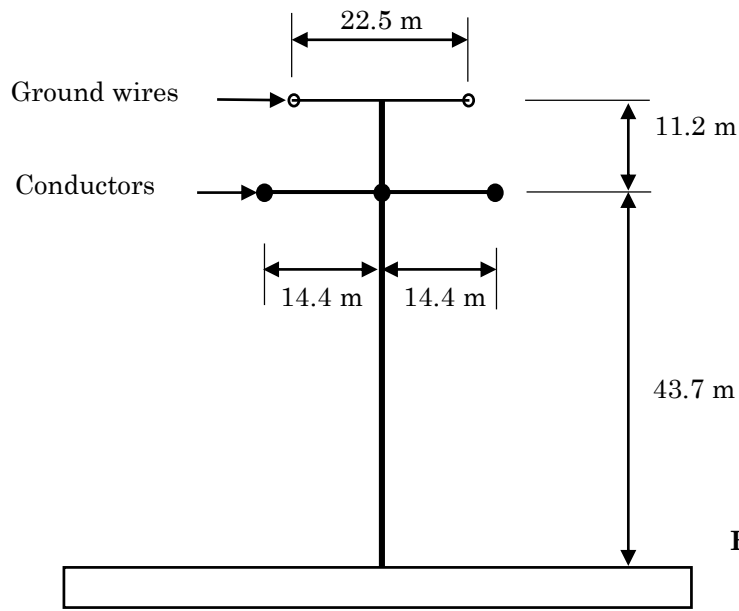


**Figure (a): Tower configuration**

- Model: Frequency Dependent phase model
- Line length: 200 km
- Ground Resistivity: 100  $\Omega\text{m}$
- Low frequency: 0.1 Hz
- High frequency: 1 MHz
- Steady state frequency: 60 Hz
- Number of conductors on tower: 3
- Number of ground wires on tower: 2

- Sub-conductor radius: 1.666 cm
- DC resistance per sub-conductor: 0.0472  $\Omega$ /km
- Shunt conductance:  $1 \times 10^{-11}$  mho/m (S/m)
- Sub-conductors per bundle: 2
- Sub-conductor spacing: 40 cm
- Ground wire radius: 0.489 cm
- DC resistance per wire: 1.463  $\Omega$ /km
- Sag at mid-span: 15 m (for both conductor and ground wire)

## II. Series Capacitor Parameters

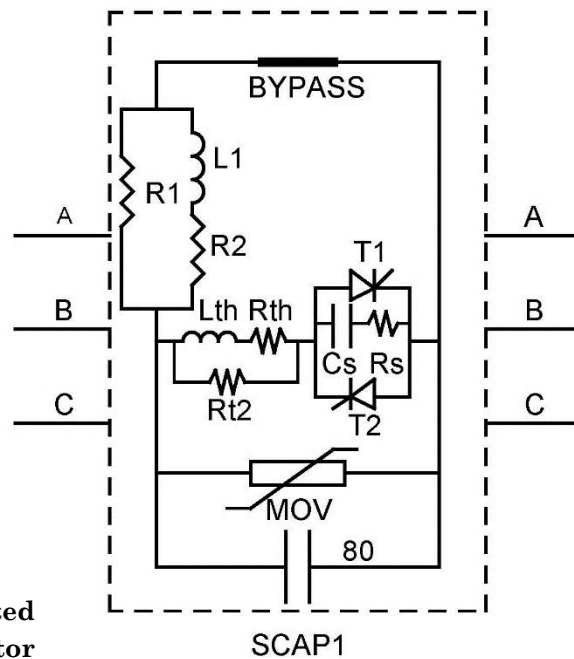


**Figure (b): Thyristor protected series capacitor**

- Series Capacitance: 80  $\mu\text{F}$

#### Arrestor parameters

- Discharge current: 10 kA
- Discharge voltage: 338 kV
- Energy decay time constant: 0.5 s

#### Parameters of the parallel thyristor branch

- $R_{\text{th}}$ : 1000  $\text{M}\Omega$
- $L_{\text{th}}$ : 1000 MH
- $R_{\text{t2}}$ : 1  $\Omega$
- $R_{\text{s}}$ : 1000  $\text{M}\Omega$
- $C_{\text{s}}$ : 1 pF
- Value on resistance: 10  $\mu\Omega$
- Value off resistance: 1  $\text{M}\Omega$

#### Parameters of the parallel thyristor branch

- $R_1$ : 1  $\Omega$
- $R_2$ : 0.01  $\Omega$
- $L_1$ : 2 mH

These are default values from the RTDS library component.

# Appendix C

Filter coefficients for the mother wavelet “Daubechies 4 (db4)”.

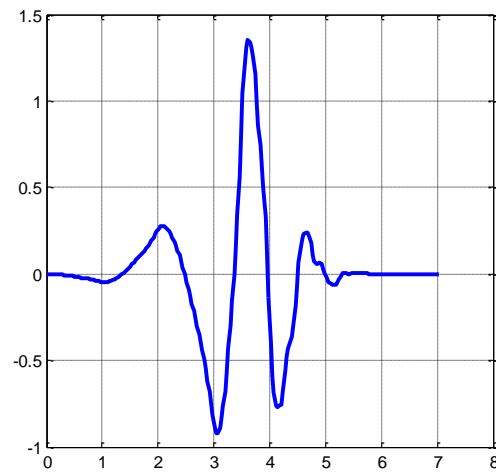


**Figure (c): “db4” mother wavelet function**

Coefficients for the decomposition high-pass filter  $h[n]$ .

$$h[0] = -0.23037781330885523$$

$$h[1] = 0.7148465705525415$$

$$h[2] = -0.6308807679295904$$

$$h[3] = -0.02798376941698385$$

$$h[4] = 0.18703481171888114$$

$$h[5] = 0.030841381835986965$$

$$h[6] = -0.032883011666982945$$

$$h[7] = -0.010597401784997278$$

# Appendix D

## I. Behaviour of traveling waves at a junction on a transmission line

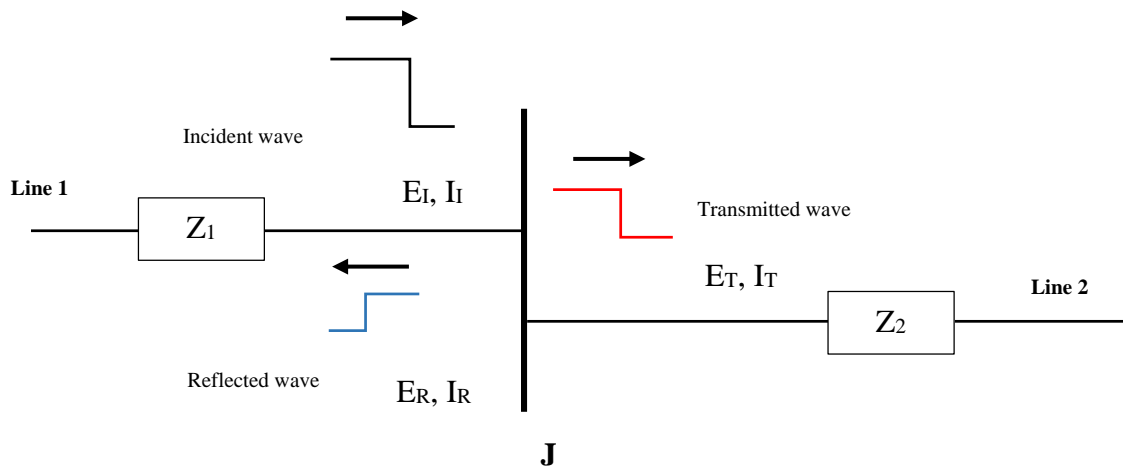


**Figure (d): Travelling wave at a junction**

Above Figure (d) illustrates the behaviour of a travelling wave at a junction formed by the connection of two transmission lines. The original wave, propagating through transmission line 1 towards the junction  $J$ , is called the incident wave. A portion of this wave is reflected back at the junction (the reflected wave) and the rest of it is transmitted into the second transmission line (the transmitted wave). Voltage and current magnitudes of the incident, the reflected and the transmitted waves are denoted by subscripts  $I$ ,  $R$  and  $T$ , respectively. These waves comply with the differential equation of the line as well as Kirchhoff's current and voltage laws.

Moreover, the surge impedances of the two transmission lines,  $Z_1$  and  $Z_2$ , relates the voltages of the lines to the respective currents. With this comprehension, following equations can be written,

$$E_I + E_R = E_T \quad \text{and} \quad I_I + I_R = I_T$$

$$E_I = Z_1 I_I, \quad E_T = Z_2 I_T \quad \text{and} \quad E_R = -Z_1 I_R$$

The transmitted and reflected voltages can be obtained by rearranging the above equations as follows:

$$E_T = \frac{2Z_2}{Z_1 + Z_2} \cdot E_I \quad \text{and} \quad E_R = \frac{Z_2 - Z_1}{Z_1 + Z_2} \cdot E_I$$

Similarly, transmitted and reflected currents are given by:

$$I_T = \frac{2Z_1}{Z_1 + Z_2} \cdot I_I \quad \text{and} \quad I_R = \frac{Z_1 - Z_2}{Z_1 + Z_2} \cdot I_I$$

Hence, the transmission and reflection coefficients,  $\alpha$  and  $\beta$ , respectively, for voltages and currents can be expressed as,

$$\alpha_E = \frac{2Z_2}{Z_1 + Z_2} \quad \text{and} \quad \beta_E = \frac{Z_2 - Z_1}{Z_1 + Z_2}$$

$$\alpha_I = \frac{2Z_1}{Z_1 + Z_2} \quad \text{and} \quad \beta_I = \frac{Z_1 - Z_2}{Z_1 + Z_2}$$



## Case I

Following Figure (e) depicts a transmission line linking two AC networks; a system similar to the one used for the transient protection scheme of this work. Now let's consider the behaviour of a current surge from system 1, at junction 1 (bus 1), occurring due to a solid fault in the transmission line. A fault occurring in the transmission line would effectively divide the line into two sections with respective surge impedances  $Z_2$  and  $Z_3$  as shown in the figure below. The equivalent surge impedance of system 1 is  $Z_1$ , whereas that of the line section from bus 1 to the location of the fault is  $Z_2$ . The first transient observed by the CT at point A due to this fault would be the transmitted current wave at junction 1.

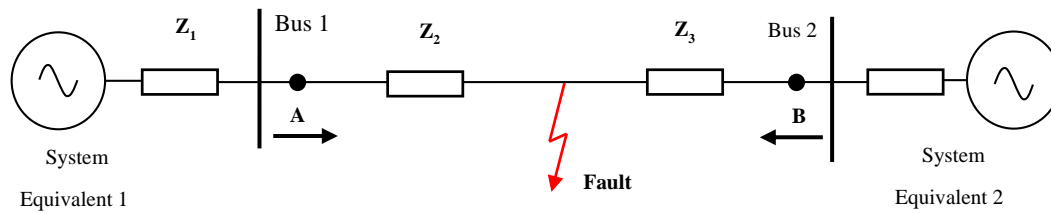


**Figure (e): Fault on the line; an internal fault**

The transmitted wave in terms of the incident wave is,

$$I_T = \frac{2Z_1}{Z_1 + Z_2} \cdot I_I = \frac{2(Z_1/Z_2)}{(Z_1/Z_2) + 1} \cdot I_I$$

From this it can be said that for all combinations of  $Z_1$  and  $Z_2$ , point A shall observe a fraction of the incident current wave, with its polarity unchanged (phase angles of  $Z_1$  and  $Z_2$  are typically quite close to each other, therefore, it is highly

unlikely that  $\frac{2Z_1}{Z_1+Z_2}$  would enforce a phase angle shift on  $I_1$  to reverse its polarity).

However, the magnitude of the transmitted wave depends upon the ratio  $Z_1/Z_2$ . The same argument can be extended to the behaviour of the current waves at junction 2 (bus 2) as well. Therefore, in theory, the two current measurement points shall observe initial transients of the same polarity for faults occurring on the line for all systems. The exact polarity depends on direction of change of the initial fault current, with respect to the pre-fault steady state current, which is determined by the fault inception angle.

## Case II

Now let's consider the behaviour of a travelling wave (current) for a solid fault at Bus 1. Now, the equivalent surge impedance of systems 1 and 2 are  $Z_1$  and  $Z_3$ , respectively, and that of the transmission line is  $Z_2$ .

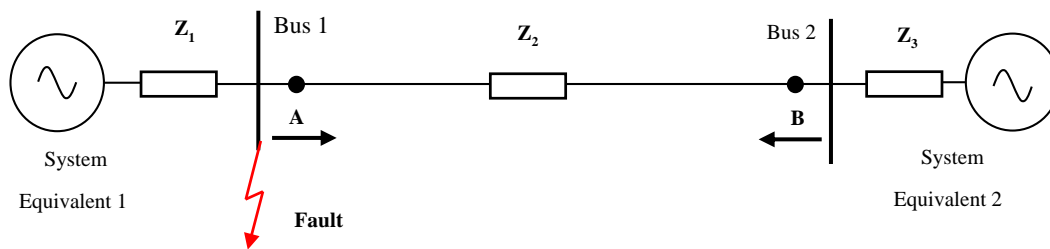


**Figure (f): Fault on the bus; an external fault**

Now the junction at bus 1 is on a short-circuit (therefore, the transmission and reflection coefficients are 2 and 1, respectively). However, since the line is short-circuited at bus 1, the current surge coming from system 1 will not go beyond bus 1 and hence, the current measurement at point A will not observe it.

On the other hand, current surge coming from system 2, at bus 2 follows a similar behaviour as explained in Case I. Thus, the first transient observed by both the points A and B would be the transmitted wave at bus 2 of the current surge coming from system 2. The observed the polarity of this wave at the two points would obviously be opposite to each other due to opposite directions of current measurement. This transmitted wave will also be short-circuited at bus 1.

## II. Analysis of Wave-front polarities for a R-L circuit

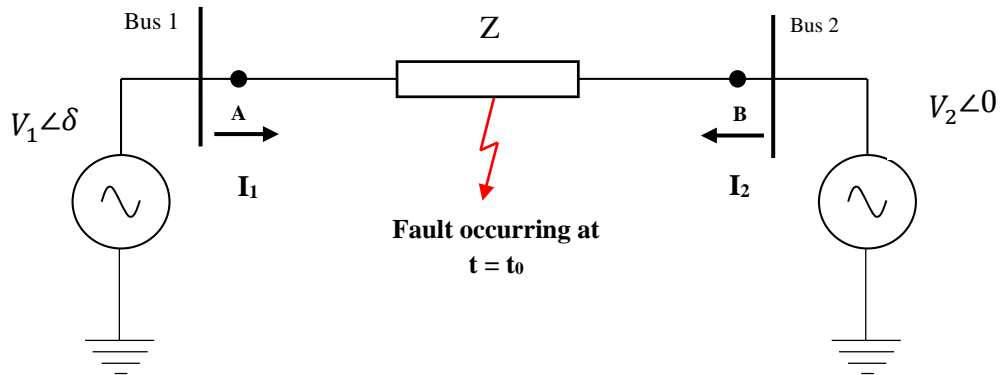


Figure (g): Pre-Fault Circuit

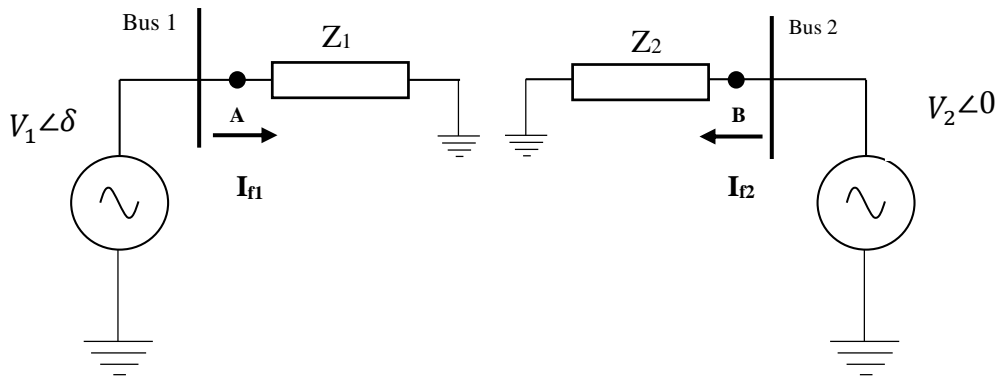


Figure (h): Post-Fault circuits

Let's consider a system, where two ideal AC voltage sources of frequency  $f$ , with a phase angle difference of  $\delta$ , are connected to a R-L impedance. The magnitude of this impedance is  $Z$ . A solid fault occurring at  $t = t_0$  divides the system into two circuits, each with a source and an impedance, as shown in the above figure. The magnitude of these two impedance sections are  $Z_1$  and  $Z_2$ , respectively. Let's take,

$$Z_1 = \sqrt{R_1^2 + (\omega \cdot L_1)^2}, \quad \text{and} \quad Z_2 = \sqrt{R_2^2 + (\omega \cdot L_2)^2}$$

; Where  $\omega = 2\pi f$ . Then the impedance angle  $\phi$  is given by,

$$\phi = \tan^{-1}\left(\frac{\omega \cdot L_1}{R_1}\right) = \tan^{-1}\left(\frac{\omega \cdot L_2}{R_2}\right)$$

The instantaneous, steady state current prior to the fault, can be written as (current going from bus 1 to bus2 is taken as positive),

$$I_1 = -I_2 = \frac{V_1}{Z_1 + Z_2} \sin(\omega t + \delta - \phi) - \frac{V_2}{Z_1 + Z_2} \sin(\omega t - \phi)$$

From the transient analysis of the two circuits, it can be proven that the fault currents of the two circuits are given by,

$$I_{f1} = \left\{ I_0 + \frac{V_1}{Z_1} \sin(\phi - \alpha - \delta) \right\} e^{-\frac{R_1}{L_1}(t-t_0)} + \frac{V_1}{Z_1} \sin(\omega t + \delta - \phi)$$

; Where  $I_0$  is the steady state current at  $t = t_0$  and  $\alpha = \omega t_0$  ( $\alpha$  is also the inception angle of the fault)

$$I_{f1} = \left\{ \frac{V_1}{Z_1 + Z_2} \sin(\alpha + \delta - \phi) - \frac{V_2}{Z_1 + Z_2} \sin(\alpha - \phi) + \frac{V_1}{Z_1} \sin(\phi - \alpha - \delta) \right\} e^{-\frac{R_1}{L_1}(t-t_0)} + \frac{V_1}{Z_1} \sin(\omega t + \delta - \phi)$$

Similarly,

$$I_{f2} = \left\{ -I_0 + \frac{V_2}{Z_2} \sin(\phi - \alpha) \right\} e^{-\frac{R_2}{L_2}(t-t_0)} + \frac{V_2}{Z_2} \sin(\omega t - \phi)$$

$$I_{f2} = \left\{ -\frac{V_1}{Z_1 + Z_2} \sin(\alpha + \delta - \phi) + \frac{V_2}{Z_1 + Z_2} \sin(\alpha - \phi) + \frac{V_2}{Z_2} \sin(\phi - \alpha) \right\} e^{-\frac{R_2}{L_2}(t-t_0)}$$

$$+ \frac{V_2}{Z_2} \sin(\omega t - \phi)$$

It can be said that the polarity of the wave front depend on the relative trajectory of the fault current with respect to the pre-fault current, immediately after the fault. In other words, if  $\frac{d}{dt}$  of the fault current at  $t = t_0$  is greater than that of the pre-fault current, then the wave front polarity is positive and vice versa. Therefore, solving the two equations  $\frac{dI_1}{dt}_{t=t_0} = \frac{dI_{f1}}{dt}_{t=t_0}$  and  $-\frac{dI_1}{dt}_{t=t_0} = \frac{dI_{f2}}{dt}_{t=t_0}$  for  $\alpha$ , would yield the two inception angles, where the switching of the polarities of the wave-fronts occur. It can be proven that the solutions given for  $\alpha$  by both the equations are the same and can be expressed as,

$$\alpha = \tan^{-1} \left( -\frac{\sin(\delta)}{k + \cos(\delta)} \right), \quad \text{Where } k = \frac{V_2 \cdot Z_1}{V_1 \cdot Z_2}$$

From this result, it is proven that the wave-front polarities observed at either end are identical (when the currents out of the busbars are measures as positive), for all faults internal to the two current measurements. For an actual transmission line, the equations become much more complicated, but it is observed that the general behavior of the wave-front polarities remain unchanged. A more comprehensive proof can be provided by representing the transmission line as a pi-section.